DISTRIBUTED CONTROL OF POWER SYSTEMS WITH DEMAND PARTICIPATION

by

Mutlu Yilmaz

Submitted in partial fulfillment of the
requirements for the degree of
Doctor of Philosophy

at

Dalhousie University
Halifax, Nova Scotia
September 2017

To loving memory of my grandfather, Mustafa Yilmaz and my aunt, Ayse Dirman

Table of Contents

List of Tables

List of Figures

Abstract

In this dissertation work, we present our research on decentralized and centralized control strategies in power systems using convex optimization methods. We have analyzed nonlinear models of power systems. These models include an exact representation of frequency and terminal voltage through which we are able to cope with the uncertain terms and unknown design parameters of a power system stabilizer.

Decentralized control lies in two aspects. First, the control approach to the problem is aimed at solving the voltage regulation problem of the power system. We suggest a method to solve the stabilization problem, which includes uncertain time-varying parameters using a state feedback controller. The main objective of the decentralized control scheme is to control the terminal voltage of synchronous generators using a decentralized voltage controller. Our model has been expanded with a stabilizer to obtain the output feedback controller. We have optimized the design parameters, which depend on the uncertainty intervals, within the feasibility region of uncertain parameters. We have implemented a bisection procedure to determine the value of design parameters. Second, we used an observer-based control for a decentralized stabilization of a multimachine power system. We have verified the contraction region for a multimachine power system. We have also performed numerous simulations of power system models to prove the stability properties of the extended Kalman filter based on contraction theory.

Finally, this work analyzes the optimal power flow problem by integrating renewable sources with demand participation in electric grids. The demand participation has been achieved by demand-side resources with renewables to curtail the actual loads. With penetrations of renewable energy in a power system, the problem has been solved by a semidefinite programming method. In addition, this method is presented for contingency scenarios, such as generation unit failures and transmission lines failures. These scenarios have been used to determine the effect of shedding load, dropping or tripping generation, or tripping transmission lines in the power system.

List of Abbreviations and Symbols Used

Abbreviations

AC	Alternating Current
AVR	Automatic Voltage Regulator
AVRs	Automatic Voltage Regulators
DAEs	Differential-Algebraic Equations
DERs	Distributed Energy Resources
EKF	Extended Kalman Filter
EMF	Electromotive Force
IEEE	Institute of Electrical and Electronics Engineers
LMI	Linear Matrix Inequality
LMIs	Linear Matrix Inequalities
LP	Linear Programming
LPV	Linear Parameter Varying
NLP	Nonlinear Programming
OPF	Optimal Power Flow
PSS	Power System Stabilizer
PSSs	Power System Stabilizers
RESs	Renewable Energy Resources
SDP	Semidefinite Programming
SMIB	Single-Machine Infinite Bus
VPP	Virtual Power Plant

Notations

$\in$	belongs to
$\forall$	for all
:	such that
$\equiv$	equivalent
$\approx$	approximately equal
$\ll$	much greater than
$\mathbb{C}$	Field of complex numbers
$\mathbb{R}$ or $\mathbb{R}$	Field of real numbers
$\mathbb{R}^n$ or $\mathbb{S}^n$	Space of n-dimensional real vectors
$\mathbb{R}^{n\times m}(\mathbb{C}^{n\times m})$	Space of $n \times m$ real (complex) matrices
$\mathbb{R}^+$	Nonnegative real numbers
$[\cdot, \cdot]$	Closed interval
$\lvert \cdot \rvert$	Euclidean vector norm
$\lVert \cdot \rVert$	Euclidean matrix norm (spectral norm)
$\det(\cdot)$	Determinant of a matrix
$\mathrm{Tr}(\cdot)$	Trace of a matrix
$\mathrm{Re}(\cdot)$	Reel part of a complex number
$\mathrm{Im}(\cdot)$	Imaginary part of a complex number
I	Identity matrix
$I_{n\times n}$	$n \times n$ identity matrix
A^{T}	Transpose of matrix A
A^{-1}	Inverse of matrix A
A^*	Conjugate transpose of matrix A
$\mathrm{diag}(A_1, \ldots, A_m)$	Block diagonal matrix with blocks $A_1, \ldots, A_m$.
$A > 0$ or $A \succ 0$	A is (symmetric) positive definite
$A \succeq 0$	A is (symmetric) positive semidefinite
$A < 0$ or $A \prec 0$	A is (symmetric) negative definite
$A \preceq 0$	A is (symmetric) negative semidefinite
$\square$	End of theorems, lemmas, facts, and proof

Acknowledgements

I would like to thank all the people who helped this Ph.D. study possible by their valuable advice, support, and endless patience.

First of all, I am thankful to my supervisor Prof. M. E. El-Hawary for providing me a Ph.D. opportunity at Dalhousie University. By his guidance, I am enlightened by his wealth of knowledge and expertise. This thesis would never been accomplished without his continuous support, invaluable comments and tireless efforts on teaching. It has been an honor and a great pleasure to be his student.

I am thankful to my advisor Dr. Bulent Bilir for providing me the opportunity to conduct research in the field of power systems at Bahcesehir University. I am grateful to him, for his enthusiasm with my study that triggered me to be a researcher and an engineer.

In addition, I would like to express my gratitude to my friends F. Kemal Bayat and Cihan Tunc. I appreciated that they shared their opinions, knowledge and suggestions concerning my Ph.D dissertation. Moreover, I warmly thank to my friends Firat Murat Senel, Levent Ceviker, and Duygu Cakir for their continued moral support and encouragement.

Last but not least, of course, I would like to give special thanks to my parents and my younger brother Baris Yilmaz for their endless love and support during my education life. I cannot find the power to succeed without their love. It was impossible to make my dreams come true. Finally, I would also like to thank my uncle Selim Yilmaz and my cousin Dr. Nese Yilmaz for their support and attention throughout this work.

Chapter 1

Introduction

1.1 Background

Modern power systems are known as the largest dynamical nonlinear network systems in the world. The interconnected power network that is now widely referred to as "the grid" has a linear supply that electric power is transferred from generating units to distribution systems via transmission systems [1],[2]. The inputs of the system are mainly defined as injections and withdrawals at the buses, and these buses deal with the supply of electricity generation to meet the demand. Injections and withdrawals of electricity cannot flow across a specified path within a transmission line, but rather, power flows move freely across all lines in a manner that is inversely proportional to line's impedance. In addition, power flows that are on transmission and distribution systems which pass through the power network are subject to network constraints by physical limitations and environmental factors. From the electricity market perspective, energy transactions are required to ensure the constant balance between electricity supply and demand between producers and consumers [3],[4]. Here energy transactions such as injections and withdrawals on the system must be stable. These transactions to complex power flows through the transmission system are not achieved easily because of the possible nonlinear behavior of power systems. Maintaining the balance of power flows is extremely critical for the secure grid operations and energy delivery.

The growing uncertainty and complexity in power grids have brought many concerns regarding the control and coordination, reliability, and security of modern power systems [5]. These challenges are due to a number of factors, including large scale transmission, distribution systems and production facilities in combination of intermittent producers; the nonlinearity in the components of interconnection and the participation of all control devices in the systems; the dynamic interactions such as

between generators and loads, combined with the fact that electricity flows freely within the system; the uncertainty in the load behaviors such as the great variation of loads in the short term; the major failures of grid elements such as generation units and the transmission grids (lines, transformers, substations); the computational complexity and different timescale and types of power system components installed [6]. Moreover, electric power systems are continuously influenced by disturbances, i.e., contingencies. Contingency involves unpredictable equipment failures or outages occurring in real-time, such as the failures of a generator, transmission line, circuit breaker, switch, other electrical components, or some combination of events which leads to a cascading outage [7]. These disturbances result in an unexpected loss of components of the interconnection; for example, the forced outages of the major generators may cause a change in the power network. As a result, a power system then suffers due to frequency and voltage changes, or operational changes to cope with the uncertain generator outputs and the curtailment of power transactions or loads. Furthermore, load disturbances are sudden variations of load demands. Obviously, electric power systems are responsible for the load variation in conditions of aggregate variation [8]. The load variations in the power system are considerably predictable; the system always modifies its generation or consumption schedule to meet the peak load and correct the load imbalances because of sudden changes in load behaviors. The optimal configuration of the power network may remain unchanged when subjected to a load disturbance [9].

These primary problems in power grids have forced power systems engineers to enhance the control methodologies and design, as well as design protection schemes to improve the reliability and efficiency of grids using extensive simulation tools [10],[11]. However, the electricity industry consists of a large electric power system and facilitates the integration of diverse energy resources into power pools [12],[13]. The diversity of resources depends heavily on the intermittent energy generation from nondispatchable sources, such as wind- and solar-based production facilities. For the power system to become more reliable and resilient, it is important to choose which control and optimization schemes as well as which (smart) control devices. Therefore, the control, coordination, planning of modern power grids results in the much greater diversity of generation required for advanced monitoring, control, and communication

techniques [14],[15],[16]. Illustrating this concept, a large electric power system and its control are based on a hierarchical structure [17],[18]. The hierarchical structure usually has several subsystems each operated by different equipment and/or utilities (at local and regional levels) coupled via tie-lines. The basic hierarchical control of power grids is exerted at specific levels [19]. Firstly, the local control is usually entirely localized by primary controllers that respond to the local output variable changes. The main function of local control is to react to fast and small deviations in supply and demand mismatches around the scheduled demand, thus restoring voltage and frequency to the desired value. At this level, the local power generation units are operating on their local measurements to find a balance between supply and demand, and increasing the stability of the local system, which is not adversely affected by the large interconnected grid. In order to meet these objectives, each generating unit has a local feedback control loop; thus, frequency and voltage regulation is implied by a local control. The automatic voltage regulator (AVR)/exciter and turbine/governor systems provide either primarily level or task oriented control schemes. The control loops of the generating units mainly provide control of the generator power output and terminal voltage, and the controllers are thus mainly responsible for frequency and voltage stabilization [20].

Next, the regional level (or secondary level) control operates a control area that includes a certain number of generating and control units. Each control area is confined to measurements in its own utility service; it is responsible for retaining the control and coordination over wide regional areas, thus ensuring reliability and continuous matching of supply and demand for the span of regional operations [17]. The control area has power generation units to follow the native load in its operating region and the agreed-upon power transaction between neighboring areas. At the regional level, the frequency and voltage deviations are eliminated at a certain operating region over a midterm-time scale. However, the regional control has a slower time scale than primary or local control [21]. On the other hand, depending on further developments of the existing power system which incorporate information and communication technology today. Modern power grids can be seen differently in a heirarchically structured level, depending on further developments of the existing power system [22].

The aim of the modern power grid is to comprise the electrical and cyber information systems in between any location of the supply and the demand. Therefore, today's power grids are supplemented by modern information, communications and automation systems [23]. The information structure of Supervisory Control and Data Acquisition (SCADA) systems of the power grid has highly hierarchical architecture and therefore falls under several layers, namely the supervisory, network, communication, control, and physical layer [24],[25]. The basic principles of modernizing grids are the following: to improve system reliability and efficiency, alleviate transmission congestion; build new generating facilities such as conventional generation resources, renewable energy resources (RESs) and demand-side management programs, and design a highly secure grid that allows to avert cascading failures of grid elements. Modern power grids also have the purpose of ensuring the design of defense strategies against potential cyber threats, attacks and random unanticipated events [26],[27]. As previously mentioned, there are several purposes that need to be addressed, using the following definitions. First, reliability is defined as the degree of performance of elements of the electricity industry; reliable operations must ensure that electricity is supplied to consumers within accepted standards and meets their desired level of reliability [28]. Thus, efficient and reliable operation of the electric system requires that there is sufficient excess generating capacity available to respond to contingency events for protecting reliability while also ensuring the real-time balancing of supply and demand. Second, electricity consumption may change significantly by time of day. In addition, security is an important task for power systems and refers to the ability of the power system to make arrangements for possible disturbance situations such as electric short circuits and unpredictable loss of grid elements, or a failure spread across a wide area or the entire power grid [29]. Furthermore, the issue of efficient dispatch and feasibility are additional objectives for the grid operations. Efficient dispatch means that the generators within the power grid are efficiently dispatched in real-time to meet actual loads at least cost, while all relevant generator operating limits and transmission constraints are taken into account. It worth noting that the total supply of generation is generally slightly larger than load demand; otherwise, the system is fragile or unclear. Thus, the reliability goal is to achieve total supply equal to or slightly above the demand [30]. Finally, power transactions on the system

must be feasible or optimal. Because of the nonlinear combination of power flows, power transactions over the transmission grids must be appropriately coordinated, or the scheduling of power transactions may be unfeasible [31].

RESs play an crucial role in distributed energy resources (DERs). The generation capacity of non-synchronous, usually stochastic, and variable generation sources, such as wind or solar-based producers with dynamic energy storage resources, contributes to a significant increase in modern power grids [32]. A key objective of the electricity industry is to extend existing generation facilities by increasing the penetration level of RESs that serve the load within reasonable cost in the long-term, and incorporating incentives for investment in RESs while continuing to invest in the existing power system. However, the integration of RESs comes with difficult challenges for current power grids. Today, there is a large effort to integrate a balanced mixture of renewable generation into electric grids. In general, one of the primary challenges is to achieve the penetration of large-scale or high-variability resources and to operate the entire power network collectively with respect to the presence of reliability and security requirements of the power grid. On the other hand, the integration of distributed RESs into the existing power grids is believed to be able to increase the actual reliability and efficiency of the system. Therefore, the electromechanical stability is required to increase reliability and efficiency using the alternative energy sources [33]. From this perspective, conventional resources, such as synchronous generators and RESs, have different dynamic characteristics. First, RESs are not natural synchronous sources locked to the nominal frequency value of the system. Second, RESs can be coupled to system with power-electronics components that have indirect grid connections [34]. In addition, the real power capacity of these individual resources is smaller, so large-scale integration is required. In real-time, these variable resources do not necessarily run for a time-frame of seconds and minutes to produce energy. Instead, dispatchable and fast-response generation resources must provide the required generation to correct the scarcity of actual supply, resulting in uncertainty and variability of nondispatchable resources. However, the incumbent generators connecting to RESs have a negative impact on system inertial response [35]. Note that the inertia of the system determines the sensitivity of system frequency due to the supply/demand balance in the grid. However, the expansion of the grid following

these variable resources adopting the high level of wind and solar generation causes a lack of stability and control over power systems. The overall stability of the system becomes more challenging with the integration of large amounts of RESs in the distribution system [36]. Furthermore, the control schemes of distributed generation have evaluated both decentralized and centralized methods. Distributed control consists of the individual distributed resources and its technologies and components in the distribution system. The control action is made in a decentralized manner and operated by its own independent control action. It mainly depends on the presence of demand response, and accommodates price-responsive demand offers or bids and demand resources to be more prone to dispatchable demand [37],[38]. Hence, it tends to reduce the peak load, provide reactive power and voltage support, and enhance power quality. In today's power grid, contrary to the more general trend, demand resources are used for grid control. Then, a centralized control scheme allows the incorporation of system level control and coordination in the distribution system. The optimal mix of new generation resources in the grid are needed to ensure optimal system operation and reliability of the distribution system. As a result, decentralized and centralized control plays a important role in utilizing RESs, which have significantly challenged the stable operation of power systems.

The general problems can be classified into frequency and voltage control problems [19]. The regulation of frequency and voltage are some of the main challenges in large electric power systems. The power system is operated at the nominal operating frequency across the entire interconnected system at any timescale. Frequency regulation is a fundamental problem that depends on the concept of autonomous decentralized control to each area or region. For this purpose, regulation in the electric industry provides the variation of loads following the power supply to enforce instantaneous production and consumption balancing (and to keep the system frequency fixed) [39],[40]. The overall frequency of system remains near-ideal nominal frequency, while depending on the load balance between generation capacity and aggregate demand in the system. Thus, generation units are used in real-time operation for load following. In this case the system frequency must be observed continuously. Smart control devices must automatically shut down or decrease load when the system frequency drops below the nominal frequency, and increase their consumption when the

frequency rises [26]. Note that when the supply exceeds the demand, the system frequency rises, and vice versa. Hence, each control area is responsible for comparing real time load against the supply and ensuring frequency stability. In addition, each control area is only responsible for its own unwanted energy deviations, or imbalances, and restores its own power balance in the operation of the system. In principle, control areas can suppress this small amount of frequency deviation. This is because generating units equipped with turbine/governor are better to stabilize frequency in response to small deviations in frequency. Finally, because of the scarcity of supply and the large fluctuations of demand; in addition, the large integration of RESs, and especially the high penetration of stochastic production in the power system, results in the occurrence of constant imbalances in practice [41],[42].

The voltage regulation at the regional level depends on the measurements of control areas. Regional levels pose problems to operate with the various generation sources and devices. The integration of renewable production into the grid entails the additional uncertainty and variability in the operation of the system. Thus, the voltage control is required to fully consolidated operations and these operations consist more centralized control methods. The voltage control for centralized system has much experience with reactive power management such as optimal power flow (OPF) [43]. The voltage control scheme needs to generate reactive power using reactive power sources such as capacitors, batteries, and generators to improve grid quality. It is of supreme importance to balance reactive power supply and demand to correct the system voltages. These sources must be adjusted daily to maintain voltages that operates within the security limits of the system. However, many generators that have AVR are able to support to the reactive power for variation of system voltages beyond the acceptable limits. In addition, the loss of reactive support or low voltage causes voltage collapse or system instability [44]. If reactive power consumption is high, it tends to stress power flow and depress transmission voltage, and might eventually produce nonconvergence. As indicated above, there are a number of issues that must be resolved, including the large integration of of RESs into the power grid, and sustaining voltage for higher demand periods. The existing grid capacities must therefore be enhanced as efficiently as possible with DERs.

The large portions of DERs in power grids produces voltage control problems in the system [45]. Moreover, the renewables using power-electronic devices imposes a heavy burden on reactive power demands.

1.2 Statement of Problem

An important feature of modern power systems is that the inclusion of conventional and renewable resources are interconnected to the end customers by means of an electric power grid. The modern power grids are prone to the generation of electricity from renewable resources. The incorporating of more RESs into the grid requires a coordinated control to optimize or maximize their electric usage in the existing power network. The large amounts of renewable resources that are required to integrate the electricity market face a number of new barriers in addition to the existing ones, especially barriers associated with their design, operation and control [12]. The main problem is that RESs have an intermittent, time-dependent, and dispersed nature that is an additional source of uncertainty for power grid operations. However, electricity generation from all options of RESs is directly influenced by increasing weather-based effectiveness or weather fluctuations. Thus, the high variability and uncertainty of renewable generation pose major challenges for the current power grid [32]. Intelligent and efficient management of both conventional and renewable-based electricity generation sources that are inherent in the electricity market requires decentralized (distributed) and centralized optimization procedures. We consider that a synchronous generator driven by steam, water, or gas turbine movers is a dominant supplier. The RESs integrate into the power grid as a large (perhaps, passive) supplier. The tasks of deployment and reliable integration of RESs support the facilitating of distributed generation technology. When the installed capacity of DERs with RESs increases, their comprehensive integration into the current grid is a difficult task. Following this, it is possible to manage these resources, such as the demand-side resources. Therefore, demand response plays a large role in achieving greater integration to maintain a balancing between supply and demand in electric power grids. The stability of power system relies on the real-time balancing between the generation and consumption of electricity. In order to achieve this, the demand

response is an important feature of electricity markets; it also enables random renewable generation which helps reduce peak load and adapt elastic demand to cover the drastic fluctuations or sudden changes in electricity generation [30]. To achieve this, the intermittent resources are dispatched through the power grid as a negative demand. In addition, ensuring the supply/demand balance in a constrained physical and cyber environment causes a unique challenge for the reliable and secure operation of power systems. On the other hand, the integration of RESs leads to design problems at the power plant. A power system normally operates at a stable operating point in the steady state. RESs cause greater volatility in the operating (equilibrium) point of power grids, and consequently, the increase of renewable generation penetration (especially, wind generation), which has a significant impact on the power grid stability and control [11]. The existing control methods are based on the characteristics of turbine-driven synchronous generators. Also, the traditional decentralized control methods may capture the dynamic behavior of synchronous generators. In order to maintain the centralized control structure, the distinct dynamic properties of renewables embeds into the control and the optimization procedure checks whether if the resulting power flows are feasible.

The electric grid has no geographic boundaries; rather, it is delineated by a complex combination of nonlinear power-flow equations. The power-flow equations represents the physical constraints on the highly complex network. To establish the OPF with RESs, distributed renewable-based energy resources are injected at related buses. Then, the physical and environmental constraints of the grid engages in the optimization scheme, and thus the optimal distributed power generation at each bus is obtained. The optimization scheme can be recast as convex optimization. In particular, in the special case where the cone is selected as the cone of positive semidefinite matrices, the optimization framework is called a semidefinite optimization which can be seen here as an OPF problem. The OPF problem is known to be NP-hard in general. The convex relaxation in the form of semidefinite programming is able to find a global optimal solution [46].

Distributed or decentralized control is a fundamental method in the control and estimation of multiple generators interconnected through a large-scale interconnected system. Decentralized control of power systems may provide efficient network control when the information and communication between subsystems or agents are constrained. The most important feature of decentralized control is its ability to handle the complexity of the power systems. This control method is used for stability analysis, frequency, and terminal voltage control of multimachine power systems. Maintaining a steady frequency and voltage are two major control problems for most of today's power systems [17]. In this case, the terminal voltage (and frequency) regulation are assumed to be done by local control action (within a control area), or are regulated by the larger network. The main objective is to keep the terminal voltage and frequency as close to their nominal value as possible. The terminal voltage and frequency are regulated primarily by decentralized excitation control. In fact, the purpose of regulating the terminal voltage and frequency is to correct the occurrence of mismatches between supply and demand due to demand fluctuations. Therefore, decentralized control algorithms for voltage and frequency regulation are achieved by introducing decentralized controllers. On the other hand, the formulating of a control problem depends on an uncertain model, implying that the effectiveness of such a control strategy is based on performance requirements over a wide operating envelope, and that disturbances are a challenging task [6]. In this respect, the given system must be an accurate representation of the original one to be properly incorporated into the analysis, and thus the controller, which is designed based on this model. In power systems, the building of models must be able to capture the design specifications of the system dynamics under model nonlinearities. The power system is subject to parametric uncertainties in its model. These parameter values may be bound to vary significantly with time and/or because of exogenous disturbances.

In general, the power system has high-order dynamics or large dimensions. A nonlinear state-space model often contains states that cannot be directly measured, or where all state variables are measurable. In many cases, the dynamical model of power systems cannot capture both the terminal voltage and frequency of synchronous machines. Consequently, the terminal voltage described by a differential equation may be used to denote the state of the system. The terminal voltage and frequency

are locally controlled by the decentralized voltage controller [47]. Consider voltage controller dynamics given by a nonlinear function of (ω, P_e); the system equation to model is then:

$$\dot{V}_t(t) = h_1(t)\omega(t) + \frac{h_2(t)}{T'}P_e(t) + \frac{h_2(t)}{T'}u_f. \tag{1.1}$$

The power system state $V_t(t)$ which is measurable state is controlled by u_f with the presence of disturbances and noises. The terms $h_1(t)$ and $h_2(t)$ are assumed to be uncertain parameters but are bounded by the operating conditions. The allowable intervals of these parameters are found by the known range of the operating region. Now the decentralized control problem is to enlarge the region of attraction and maintain stability for an allowable range of parametric uncertainties in electric power systems. The decentralized control obviously depends on the local components and its measurements in any given machine. The control must also be robust in order to guarantee the stability robustness for the whole operating region and all allowable uncertainties. Given system (1.1) when the uncertainties $h_1(t)$ and $h_2(t)$ affect the model, our objective in the following control law

$$u_f = -k_1\omega(t) - k_2P_e(t) - k_3V_t(t), \tag{1.2}$$

where $\{k_1, k_2, k_3\}$ represent linear gains respect to the bounds on $h_1(t)$ and $h_2(t)$. It is worth noting that the basic Lyapunov theory is the basic theoretical tool for stability and robustness analysis and the corresponding control strategy for the nonlinear dynamical systems. In view of this connection, the stability analysis with respect to Lyapunov techniques employs the concept of quadratic stability. The problems of parametric uncertain systems are handled by using the framework of quadratic stability, and then obtained in terms of matrix inequalities. As a consequence, both state feedback and dynamic output feedback controllers are designed for the known range of parametric uncertainties.

Contraction theory is introduced as a powerful concept to treat the stability properties of nonlinear dynamical systems. The difference between the Lyapunov and contraction stability analysis is that stabilization in the sense of Lyapunov occurs at the minima of a generally defined a given function (particular) of any solution, while contraction theory proceeds to a differential approach and the stability of trajectories of a dynamical system with respect to one another. In addition, the convergence of

solutions is determined to be independent of initial conditions [48]. With this new form of stability, contraction analysis assesses the incremental behavior of trajectories that tend to coalesce. As its natural extension, this theory can be applied to the observer-based problems and designs. To apply the contraction theory to derive the controller and observer designs for the multimachine power systems, the observer control problem is proposed [49]. Thus, the problem of a nonlinear state observer is also constructed in a decentralized manner. This leads to the observer for a given power system model. The observer design with the extended Kalman filter (EKF) achieves the decentralized control of multimachine power systems. The basis of the contraction theory arguments is then established for the stability properties of the EKF [50].

1.3 Objectives

In writing this dissertation, our objective is to improve the integration of renewable generation, while increasing the stability of a power grid, and to present the appropriate decentralized control methods for enhancing system-wide performance of a large electric power system. For this purpose, we first establish an optimal power flow program for achieving the demand-side participation at selected buses and examine the equilibrium distributed power generation across the grid using the convex optimization problem. Renewable resources are located at these buses which allows them to produce a random renewable generation. The renewable integration at the load buses is realized by an iterative algorithm, and the level of renewable penetration in the grid is increased by examining the feasible solutions of the optimal power-flow problem. Therefore, the power injection at load buses rises with an increasing penetration level of distributed renewable generation. Here, the demand participation is utilized by demand-side resources that can curtail the actual loads of the rest of the electric grid. Moreover, we also test the feasibility conditions for global optimality of the optimal power flow problem with demand participation under the various contingency scenarios.

Another objective is to resolve the decentralized control problem of power system. Following this objective, we aim to design a decentralized voltage and frequency control scheme and analyze its stability properties for a multimachine power system.

To do this, an efficient power system model to measure the terminal voltage and frequency is presented. According to this model, the synchronous machine states are described by second-order dynamics. We neglect the other states to obtain a minimal realization by defining the measurable states (namely, terminal voltage and frequency). Thus, obtaining the system dynamics is solved by using the concept of quadratic stabilization via the state feedback control scheme. We also state a method to analyze the inherent system nonlinearity due to the uncertain parameters in the model. Then, the acceptable bounds of uncertain parameters is determined according to the secure operating region of the system. As a consequence, the uncertainties caused by operating point variations are canceled by using the decentralized controller. Furthermore, we aim to solve the voltage (and frequency) regulation problem with output feedback. A decentralized output feedback controller is designed by using a power system stabilizer. The dynamics model accommodates the additional states as well as design parameters. These unknown design parameters that belong to a power system stabilizer are computed via bisection algorithm. The design parameters are optimized based on the uncertain parameters and their allowable bounds of the system, and the resulting controller stabilizes the power plant. To this end, an convex optimization problem for the design of state and output feedback controllers is solved.

This work aims to extend decentralized control design for the multimachine power system. We provide observer-based control in a decentralized fashion through a contraction theory-based analysis of the stability. The decentralized stabilization of the multimachine power system is implemented by a deterministic observer. We then propose the stability properties of the deterministic extended Kalman filter based on contraction theory. The main objective for using contraction theory is that contraction properties are specified under the multimachine power system. We also introduce a contraction metric. We thus prove that the multimachine power system model is contracting in a diagonal metric.

1.4 Methodology

The fundamental methodology in this dissertation consists of decentralized and centralized optimization strategies. Decentralized control for each individual machine contained in an area lies in two aspects: first the decentralized control approach proposes to solve the voltage regulation problem for given power system models. Here, the control problem is described as stabilizing the power system using the state feedback controller. The power system models have time-varying parameters. Parameter changes are particularly important, as uncertain parameters are bound to change with time affected by external disturbances. Therefore, stabilization of the power system model subject to uncertain (and time-varying) parameters is achieved [51]. The desired dynamical behavior of a power system varies in the parameter range of interest. The security operating region of power systems is used to determine the operating range in which the controller is used. Secondly, the voltage regulation problem is expanded with power system stabilizer (PSS) to obtain a stabilizing controller for the admissible set of uncertain parameters when full state information is not available. As a consequence, we use the Lyapunov stability theory to verify the stability of the closed-loop system corresponding to the resulting (stabilizing) controller [52]. The voltage regulation problem is thus determined by a global (local) admissible state-feedback controller, and a global (local) output-feedback controller for given requirements in the presence of uncertainties in the power system models. The designing controllers are based on linear matrix inequalities (LMIs). This control problem is addressed by means of convex optimization techniques and, at the same time, is recast as a set of LMIs and the control gain matrices are then obtained directly from LMIs optimization formulation using very efficient interior-point method algorithms [53]. By using the proposed LMIs conditions, we can verify the feasibility of the LMIs, while guaranteeing the stability of each machine or multimachine power systems.

Another methodology used in this dissertation is the observer-based scheme for decentralized stabilization of power systems, which solves the voltage regulation problem [54]. The considered observer proposes a state estimation procedure by introducing a state observer when the states are entirely available from measurements. Using the proposed Kalman filter state estimation procedure, we obtain the Kalman gain

and the calculation of the updated covariance of the state estimation error [55]. We then introduce contraction theory as a tool to study the stability properties of power systems. Contraction theory copes with the system stability by the differences between solutions with respect to different initial conditions. In contraction theory, stability is described incrementally between two arbitrary trajectories. The concept of contraction theory presents an alternative way for stability analysis of highly nonlinear systems. It is clear that contraction theory-based analysis deals with the incremental stability properties of deterministic systems. Contraction-based incremental stability is a more specific analysis techniques based on an exponential convergence of the (non)linear system [56]. Thus, the contraction properties of the EKF is used to analyze the deterministic observer for the stabilization of multimachine power system [57]. In order to adopt the contraction theory to the analysis of the power system model, we provide a deterministic nonlinear observer which is obtained by running the EKF to design of decentralized control in the power system, and the solutions are derived for the case where full state information is available to the controller for synchronous machines.

In this dissertation, the centralized control scheme is adequately formulated as the optimal power flow, and constitutes the most fundamental optimization problem for power systems [58],[59]. The OPF problem requires the optimal solution of a set of nonlinear equations, such as power-flow equations. Indeed, OPF is a method to compute the power-flow problem. Analysis of the power flow equations forms the cornerstone of the power systems so that the required task is achieved [60]. These equations allows us to see the physical capability of a power network to transfer electricity from the supply side to the demand side. Power-flow equations are widely used for each type of problem, and thus the main goal of the classical power-flow problem is to determine the unknown complex voltages at all buses. Following this, our special interest in this work is the choice of convex programming for which the resulting optimization problem is called a semidefinite optimization, or semidefinite programming (SDP) [61]. We present an implementation for the primal-dual interior-point based SDP solutions of the OPF problem; in other words, we construct a semidefinite programming relaxation of the power-flow equations [62],[63]. Under the rank condition, the SDP solution finds a global optimal solution to the OPF problem

in polynomial time, and also ensures that the local solutions are also global. The OPF via SDP also provides solutions for discrete decision variables of a power grid, including phase shifters and distributed generation, and additional constraints for more realistic case studies [64],[65],[66]. On the other hand, we expect to maintain the remaining convexity of the optimization problem. The convexity of power-flow solutions associated with the optimization problems often need to be represented via economic dispatch or OPF applications [67]. Therefore, the OPF problem is typically nonconvex as a consequence of the nonlinear nature of the power-flow equations. Thus, the set of power flow injections is nonconvex due to its computational nature. The nonlinear form of the power-flow equations in polar coordinates which involve voltage magnitudes and angles that the feasible set expressed in active power, reactive power, voltage magnitude, and angle, cannot be convex. Moreover, the power-flow equations in rectangular coordinates involving the real and imaginary parts of the bus voltages are also nonconvex. We can conclude that the nonconvexity conditions of the power-flow equations mainly depend on the rank condition, and the result in an optimization model can be intractable. The bus voltages determined from a SDP relaxation of the OPF is guaranteed to be the globally optimal solution if the rank condition is achieved [68]. Finally, the SDP is implemented to achieve the optimal solution, or an approximation of the solutions, of many realistic problems that have computational complexity [69].

As we mentioned before, the ability of a power system to integrate renewable generation mainly depends on the diversity of electricity generation resources. The growing penetration of renewable power production into power systems needs a higher degree of grid flexibility. This considerable flexibility tends to operate conventional generation at various production levels in absorbing the uncertainty and variability of renewable generation. Therefore, the facilitation of renewable integration by demand response is of particular importance in today's power grid [70]. Roughly speaking, a power system designed with demand response refers the active participation of consumers can provide efficient operation of an electricity market. The demand response action aims at assessing the benefit of the demand flexibility of desired customers by shifting or reducing their demand for high-cost or high-demand periods [37].

In general, electricity has traditionally faced flat electricity costs, but the true production costs of electricity vary over time. The demand provided by response programs enables electricity consumers to participate in such dynamic or real-time pricing and facilitate the various forms of demand-side response [71],[72]. In addition, the demand response can provide a reduction in the operating costs. The involvement of end-use consumers in demand response enables real-time pricing by shifting power consumption. As a result, the demand response programs and technologies provide to determine time-based market prices through this action and communicate electricity prices to the consumers who face challenges in receiving deterministic real-time prices. The demand-response management can restrain prices for customers receiving low prices with high renewable power production or stochastic production. On the other hand, the demand response is also used to balance between supply and demand throughout the power system. In this work, the power grid is basically designed to support the penetration of renewable resources, such as demand-side suppliers. This way, we build an optimization problem for renewable power production as a demand-side supplier. The renewable power production is precisely known. Then we aim to solve the OPF problem by defining a realization of the random renewable power production involved in the optimization problem by means of a SDP relaxation. An efficient iterative algorithm is used to penetrate renewable power gradually. The resulting optimization model is solved by using the SDP. The global optimal solution is achieved by solving the optimization problem for each incremental change of renewable production [73]. The optimal solution is then implemented to some contingency scenarios.

1.5 Relevant Literature

Over the years, much effort has gone into the mathematical modeling and control design of power systems. The main references to control theory and stability analysis for power systems are given in [74],[75],[20]. We now present an overview of the relevant literature in the area of decentralized control of large-scale complex systems. The main supposition of decentralized control schemes is that they only deal with locally available state information on the model [76],[77]. Thus, this approach

is viewed as a completely independent analysis of the control system, which takes into account online information about the states of the system. Hence, it has satisfactory performance with little or no communication between subsystems, such as weakly coupled subsystems [78],[79]. The ideas behind a robust decentralized control scheme is one of the fundamental requirements for the control of large-scale power systems. In general, the design of the robust decentralized controller for enhancing the transient stability of nonlinear power systems is discussed in [80],[81],[82],[83]. The proposed methods also include the decentralized turbine/governor control schemes. In addition, the classical control strategies of robust decentralized exciter design in power systems are developed in [84],[85],[86],[87]. Contrary to the direct-feedback linearization techinique, a new decentralized control scheme has been successfully applied in both the exciter control and turbine/governer control for the robust decentralized stabilization of large power systems based on LMIs [88],[89]. Here we focus our attention primarily on motivations of the proposed decentralized control and optimization method for some basic problems of power systems. The aim here is to introduce the frequency regulation design related to the problem of automatic generation control (AGC). In case of frequency regulation, the major coordination method is known as AGC. The earliest contributions to generation-based frequency control are expressed in [90],[91],[92],[93]. Lately, some control algorithms are implemented for the frequency control problems [94],[95],[96]. The frequency control in power systems can be divided into two levels, which are called primary control and secondary control [97],[98],[99]. The primary frequency control is well defined in [100],[101]. In addition, the purpose of AGC is to regulate frequency to its nominal value and maintain power transfer between the control areas by changing the output of generators. This is called load frequency control (LFC). Load-frequency control is major function of AGC. An overview and a comprehensive bibliography on LFC is given in [102]. Then, the earliest optimal control concepts for generation control are proposed in [103],[104],[105],[106]. Recently, the research papers about the AGC and its applications can be found in [107],[108],[109]. Furthermore, the robust control design for the LFC problem in multi-area power systems has been extensively studied in [110],[111],[112],[113]. In [114] and [115], the robust decentralized control design methodologies for LFC are studied in particular. The main objective of these papers

is to propose new control schemes for the LFC problem of multi-area power systems.

Voltage regulation is an important property for power network stability [116],[117]. The main objective is to regulate the voltage to meet its nominal value under different load conditions: traditional or disturbed. The topic of voltage regulation is studied using LQ-optimal techniques [118] and robust control techniques [119],[120]. The problem here consists in designing voltage controller that ensures transient stability over the whole operating region. This robust voltage controller has an AVR and PSS to enhance power system stability and performance under varying operating conditions [121],[122]. In [123], a control action to network stability analysis for long-term dynamics of load systems is shown. In these papers, different operation modes are proposed for secondary voltage control methods to investigate emergency action in preventing voltage instability and system breakdown is proposed [124],[125],[126]. Recently, a decentralized excitation control scheme has been proposed for voltage regulation of multimachine power systems [127].

The ideas of nonlinear stability and robust control has been a hot topic of research over the past twenty-five years. We refer the reader to [128],[129],[130],[131],[132],[133]. In this context, the mathematical theories especially designed for analysis and synthesis of an robust control of dynamic systems are discussed. Thus, the proposed control must be robust with respect to unknown cases [134],[135]. The main issues applied in robust (also optimal) control theory regard the development of conditions which guarantee the system stability in the presence of various classes of uncertainties. Then, the design of controller for the nonlinear system is presented when the close-loop system is stable and admissible. In addition, it is well known that robust H_∞ control, optimization and filtering have attracted considerable research interest [136],[137],[138],[139],[140],[141]. Since H_∞ control methods deal with the uncertain model case, it is more realistic. The authors of these books share a basic knowledge in H_∞ control theory for uncertain linear systems with nonlinear uncertainties [142],[143],[144],[145]. A decentralized fixed-structure H_∞ optimization is shown in [146]. Robust stability and robust stabilization conditions for the singular systems are also studied [147]. On the other hand, the stability robustness with respect to a wide class of nonlinear uncertainties is investigated, such as regarding input-output and state space uncertainties [148]. The uncertain cases are

due to the inaccurate modeling or measurement errors between the mathematical model and real system [149]. The class of state space uncertainties contain parametric uncertainties and norm-bounded uncertainties [150],[151],[152]. Moreover, in studies of the problems of robust stability analysis and robust stabilization with respect to parameter uncertainties, strong forms of stability methods such as quadratic stability are introduced [153],[154],[155]. In [156] and [157], necessary and sufficient conditions for quadratic stability and quadratic stabilization are expressed in detail. General methodologies that provide the successful design of state feedback and output feedback for stabilization of nonlinear systems in the presence of linear time-varying parameters are described in [52]. In particular, the problem of robust stability of systems dealing with parametric uncertainties is described in [158],[159],[160]. The stabilizing feedback controller is represented by the corresponding bilinear matrix inequalities (BMIs) or LMIs. If the LMIs optimization is found to be feasible, then one may guarantee that all possible trajectories of the proposed systems are bounded. The main properties of LMIs optimization are given in [161],[162],[163]. The problem of state feedback conrol for nonlinear quadratic systems is described in these papers [164],[165]. Based on these concepts, a dynamic output control scheme using the LMIs framework is given in [166],[162]. On the other hand, a robust output-feedback controller design via BMIs optimization is proposed in [167]. The static output feedback problem is one of the main problems in control theory. An LMIs-based method for designing static output feedback is developed in [168],[169]. In recent years, the BMIs-based technique has been widely used to solve the static output feedback problem [170],[171]. However, the BMIs-based optimization problem is not convex and known to be NP-hard [69].

The observer problem with possible observer design is proposed in this dissertation. The observer design for nonlinear systems is presented in [172],[173],[174]. The nonlinearity can be formed from direct measurements, and thus can be transformed into a linear system by a change of states and output injection [175]. In [176], the observer-based control for a class of uncertain linear systems is discussed, and the disturbance of observer-based control for nonlinear systems is also given in [177]. One of the fundamental obsever designs for deterministic linear systems is used in [178],[179]. With reference to the seminal works of Luenberger, the nonlinear

observer based on a slight modification of the extended Luenberger observer is developed in [180]. In addition to this, Kalman observer is first introduced in [55]. Then the well-known Kalman observer is designed for nonlinear systems, and called the extended Kalman filter [181],[49]. The Kalman filter algorithm is an efficient state estimator. It is widely used in estimation problems due to its optimality, tractability and robustness [57],[182]. In our work, the convergence properties of the EKF are presented using contraction theory [48],[50]. Contraction theory is a nonlinear control system tool for investigation of asymptotic properties of nonlinear dynamical systems [56],[183], and is based on an incremental stability that is an exact differential analysis of convergence [184]. Using this theory, the stochastic incremental stability approach [185], which is an observer-based control for stochastic nonlinear systems with incremental stability [186], and contraction-based nonlinear model predictive control [187] are presented. Moreover, the well-known unscented Kalman filter [188] with contraction-based analysis is given in [189]. In [190], the concept of partial contraction for nonlinear systems is discussed. Contraction theory has also been applied to stability analysis and synchronization of systems [191],[192]. The analysis of robust stability of uncertain systems with polynomial or rational dynamics through the use of convex optimization and sum of squares programming [193] and the stabilizing output-feedback controller design using contraction metric and convex optimization can be found in [194]. Applications of contraction theory are also used in many scientific disciplines such as nonlinear chemical processes [195], chaotic systems [196], biology [197], power systems [198], and neuroscience [199].

Historically, the supply structure of the power grid was dominated by centralized control of power generation units. However, the current centralized power system and its operational paradigm is restructured, and the distribution network participating in electricity markets has become a passive supplier. Decentralized power sources connect to the distribution system, which is intended to fully displace a large amount of power production by large conventional power sources. This new operating paradigm has the advantage of allowing the massive deployment of renewables to penetrate the electricity market which, in turn, allows for a reduction in the per-unit cost of renewable energy. Despite these advantages, new challenges for centralized electricity system have reported due to the growing percentage of DERs

with power-electronic technologies in existing power network [200],[201]. The main problem is that RESs are widely dispersed, and tend to be intermittent and unpredictable. In addition, the growing level of penetration renewable generation causes a voltage instability problem which is mainly related to reactive power imbalance [36]. RES-generated power, in particular wind power, is variable and uncertain. Consequently, its large-scale integration into a power system poses a large challenge for power system operators [202], [203]. As we mentioned before, the large amount of renewable integration reduces the power system's inertia. Several studies have explained that the impact of this lack of the system inertia is due to a large amount of wind generation on grid frequency regulation [204],[205]. In such a case, a large number of participants with energy storage units and price responsive loads may have a (in)direct impact on the power grid protection and control [206]. In [33], the effects of the integration of distributed generation on the electricity network are studied. As a result of the intermittent nature of nondispatchable production units, their output cannot be controlled, or can only partly be controlled, and power production is stochastic. Integration of renewables requires a higher degree of power system flexibility to be able to follow load fluctuations [207]. This way, the variations of electricity generated from RESs can be passively absorbed by customers, which are provided by demand response. Demand response schemes are responsible for achieving the demand-side flexibility that allows covering the variability of uncertain sources such as wind energy, and photovoltaics [208]. For more details, we refer again to the literature [12],[32]. Several aspects of electricity markets from the perspective of the demand-side menagement are considered in [209]. In [210], load management programs are presented for residential appliances; in addition, a price prediction scheme for real-time dynamic pricing is given in [211]. In another paper, some methods based on a dynamic programming alghoritm are implemented for the dispatch of direct load control [212], the dispatch of air conditioner direct load control [213], and profit-based load management [214]. In [215], an efficient approach for the dispatch of direct load control with the aim of reducing system operational costs is studied. The penetration of wind power production facilities in electric energy systems with load following requirements is studied in [216],[217]. The concept of a virtual power plant (VPP) composed of an intermittent source, flexable loads, storage systems, and

dispatchable generating units is introduced in [218],[219]. The main objective of a VPP is to coordinate the production and consumption in both the day-ahead and the balancing markets seeking to maximize their performance [220],[12].

Creating computer simulations of various scenarios of operation to achieve the demand-side response is one of the main purposes of our work. These simulations are performed by a semidefinite programming relaxation of the power flow equations using the OPF problem. The OPF problem is well reviewed [221],[222],[223] as a process of determining the optimal dispatch of active and reactive powers of distributed generator units. There is a large body of literature related to the OPF problem; see the following surveys [58],[59],[224]. Many special cases for the using of the OPF problem are considered in the literature. The effects of distribution networks with the OPF-based approach are discussed in [43],[225],[226]. Similar applications are studied for distributed generations in a network or an area [227],[228],[229]. Some work on basis of probabilistic OPF can be found in [230],[231],[232]. Additional applications of the OPF are developed by the use of genetic algorithms [233], a unified power flow controller [234], an evolutionary programming algorithm [235], and a fuzzy model [236]. The solutions of the OPF problem using the probabilistic and stochastic methods for RESs are presented in [237],[238],[239]. Also, the optimal control of RESs with energy storage systems is introduced in [240],[241],[242]. Then, the OPF is used to determine the optimal allocation of demand-side resources in [243]. On the other hand, many different solution schemes are proposed to the OPF problem. In general, based on the optimization techniques applied the OPF methods, they can be classified into two main categories: namely, linear programming (LP) based methods and nonlinear programming (NLP) based methods. The LP based OPF is implemented by proving a LP based algorithm for the solution of a general OPF problem [244]. Using an LP based approach to follow the primal-dual interior point methods for an OPF problem with polar coordinates is studied in [245]. Interior point algorithms using both the polar and rectangular coordinates are shown in [246]. Following these, the solution of the OPF dispatching problem by a primal-dual interior point method is obtained in [247],[248]. Next, some aproaches using the interior point methods are considred for the optimal reactive power flow problem [249] and the trust region approach with interior-point OPF algorithm [250],[251]. Some methodologies are

aimed at solving an optimal power flow problem with integrated security constraints in [252],[253],[254]. More recently, the family of interior-point methods for linear optimization were extended to solve SDP problems, which in turn solve convex optimization problems allowing self-concordant barrier functions [255]. Considerable progress has been achieved in the understanding of the basic concepts in convex programming, which is related to semidefinite programming for the OPF problem, as well as algorithmic solution schemes for conic programs. In particular, some recent advances in the convex relaxation of the OPF problem are discussed in [256],[257]. The OPF problem can be seen as the SDP optimization problem, which is the dual solution of the OPF problem [68],[258],[46]. Nonzero duality gap solutions for the OPF problem are also given in [259],[260], and a framework for exploiting sparsity in primal-dual interior-point based SDP solutions of the OPF problem is introduced. Moreover, an approach with chordal conversion techniques is used for reducing the complexity of semidefinite relaxations of OPF problems [261]. The OPF problem for DERs [262],[263],[65] and radial networks [67] is solved using SDP. In addition, an implementation of the OPF problem for direct current networks [264],[265] using a second-order cone programming relaxation is considered in [266]. Transient stability analysis using constrained programing for the OPF problem is presented in [267],[268],[269]. In this direction, another work [270] involves the security-constrained OPF. The condition that power flow optimization is based on a set of coupled OPF using a variety of variables and constraints, and constraints over these variables. Thus, the problem is described as the security-constraint OPF problem. What makes the security-constraint OPF problem different from the OPF problem is that independent system operators tend to determine an operating point that satisfies the supply/demand and network constraints not only under normal operation, but also under-prespecified contingencies corresponding to the outage of an arbitrary number of lines and generators. For more involved security-constrained OPF, we refer to [61] and the references therein. In addition, another class of conic optimization problems is the class of second-order cone problems. This conic programming problem, whose constraint cone is a product of semidefinite cones and second-order cones, is to find a global solution in a polynomial time for the OPF problem, and it has been used for various applications in power systems; see [271],[272],[273] and the references therein. In [64], the paper has dealt

with a second-order cone program relaxation is to determine the optimal solution of a general OPF problem with virtual phase shifters. They reformulate certain SDP with the OPF problem as a second-order cone program.

1.6 Dissertation Outline

The dissertation comprises six chapters. The rest of dissertation is structured as follows.

In Chapter 2, we develop some models of power systems based on the swing equation and the simplifying assumptions. First, the second-order model and the fifth-order model are used for the state feedback and the output feedback problems, respectively. The power system models are intended to be an representation of terminal voltage and frequency of generators. The models include uncertain time-varying parameters and unknown design parameters. In addition, we develop a classical model of power systems based on network equations. This model is used for the observer-based control in multimachine power system.

In Chapter 3 discuss some fundamental mathematical concepts and definitions necessary for the Lyapunov-based control of power systems. Then, we solve the voltage regulation problem in a decentralized manner. Finally, a decentralized controller with both state feedback and dynamic output feedback controllers is developed. By using the convex matrix inequality optimization problem, the quadratic stability of the closed-loop system is established. We present our numerical results for the IEEE test system.

In Chapter 4 is fully devoted to contraction theory-based analysis of stability. We discuss the contraction region and contraction metric that define power system models. The stability of nonlinear power system is proved by studying the properties of its Jacobian matrix. This concept introduced here is to use observer-based control for the multimachine power system. The decentralized control of the multimachine power system is provided by a deterministic EKF observer. We obtain our simulation results for multimachine power system cases.

In Chapter 5, we solve the optimal power flow problem with using a semidefinite programming optimization. Demand participation is used to facilitate the integration

of renewable resources. We develop an algorithm for achieving renewable energy integration. In addition, we also express the SDP-based OPF problem with contingency analyses. The results are performed for the IEEE test system.

Finally, in Chapter 6, we discuss our contributions to decentralized voltage control and observer design of power systems. Also, we discuss our demand-side participation concept for achieving renewable energy integration in power grids.

Chapter 2

Conventional Generation Modeling for Power System Control and Stability

2.1 Introduction

The mathematical model of an electrical network is a fundamental motive for power system analysis. In studying power system control and stability, mathematical knowledge of the system is predetermined. The mathematical models reflect the accurate behavior of electric power systems. The fully-accurate modeling of large power systems will, in general, be complicated and difficult to handle. However, a simpler or more abstract model is not able to capture the overall system dynamics, despite the fact that lower-dimensional models can be much easier to implement. Moreover, it can be unwise to work on the basis of a highly-detailed model in view of possible changes in power system dynamics that may take place in the course of time. In this case, the accurate model has high dimension and represents the dynamical behavior of a power system over a broad range of operating conditions with its time scales.

Electric power systems are highly nonlinear and complex systems that are constituted by a variety of utilities in different geographic locations, in which they can be reliably served under different conditions. Their dynamic behaviors are therefore influenced by nonlinearity. The scale, as well as the degree of nonlinearity and uncertainty, depend heavily how much other devices contribute to. The complexity of power generation, distribution and consumption using modern information, communication, and electronic devices are the main reasons for control, coordination, and stability problems of power systems. As nonlinear systems, there have not yet been adequate closed-form solutions for power system models. From the viewpoint of electrical theory, a nonlinear and high dimension system is representable as a classical multimachine model. This chapter provides various multimachine models under simplified assumptions.

Similar to large-scale dynamic systems, we study the modeling and control of large electric power systems which have properties similar to the computational aspects of large dynamic systems. In this way, the hierarchic structures can be adopted as a solution for the large dynamic systems. Similarly, the large power systems are based on hierarchic structures to achieve reliable operation of the power grid. From this hierarchical perspective, modern power systems that are constituted of a number of interconnected subsystems are made of a well-known layered structure [21]. The layered-architecture of large power systems are dependent on each other due to conceptual or computational reasons. In this section, we describe the physical model (or layer) of the power system which is depicted as a power plant to be controlled, and is often described by dynamic equations in accordance with the laws of physics. Following this, the separate analysis of subsystems provides the separating stabilization and the operating objectives. In order to stabilize the system, the proposed control scheme is a decentralized one, since each subsystem is stabilized by a local feedback loop [274].

In this work, we consider an individual subsystem to be a conventional generation unit consisting of a synchronous machine equipped with an exciter and turbine/governor, which is called called a generator-turbine/governor set. As previously mentioned, the local characteristics of each generation unit is modeled in a decentralized way, such that the unit is affected by its own performance and the dynamic behavior of its components. Each generator-turbine/governer set has a local feedback loop. That is, the stability of each subsystem is maintained by eliminating the mutual interactions of neighboring systems. This may occur at the level of the regional system or at each subsystem level. Since a certain region may include many conventional generation units that are coupled with tie-line, and as a result power flows through that region. In the proposed decentralized scheme, we design the local controllers via the existence of both state feedback and output feedback controllers to stabilize each individual subsystem. In this chapter, these local controllers are mainly responsible for frequency and voltage stabilization. The local frequency control is intended to keep scheduled load and scheduled generation in balance. The voltage control achieves voltage regulation, but it is only based on local measurements.

We measure the performance of a subsystem with respect to controlling system frequency and voltage. Using a decentralized approach, the control and coordination on a system-wide basis may be provided.

In our formulation of power system models, we specify the system of differential equations which represents valuable information about the dynamical behavior of power systems. Differential equations are the most useful and widely applied tools in describing models of dynamic systems. Mathematically, the problem of fitting can often be modeled by a set of ordinary differential equations (ODEs), partial differential equations (PDEs), or/and delayed differential equations (DDEs). However, the problem can naturally be extended to models described by differential-algebraic equations (DAEs). In fact, the nonlinear differential equations are highly constrained by the characteristics of algebraic equations power system models. In the literature, various approaches have been proposed to solve DAEs. Following [275], one can solve all equations simultaneously by using the trapezoidal integration method. In this case, the whole set of system equations is considered. Therefore, the system matrix is quite sparse and the solution may be computed by using sparse solution techniques. Alternatively, the other approach allows the computation of subsystems independently by eliminating some Jacobian elements from the system matrix. In the latter case, the power system model can also be described by difference equations. Consequently, these nonlinear equations can be solved independently for each component of power systems. The local dynamics of generator units that are subject to adding network constraints are represented as algebraically coupled DAEs of the following form:

$$\dot{x}(t) = f(x, y, u, t), \tag{2.1}$$

$$0 = g(x, y, u, t), \tag{2.2}$$

where x is the state vector which contains the local and dynamic state variables of a conventional generator unit, the vector y contains all of the algebraic variables, u is the input to the system, and t is the time in seconds. As indicated above, algebraic constraints on the electric network are the algebraic power-flow equations. The local dynamics of the generator unit and the network couplings may require modification of the power system model formulation by by introducing new variables.

2.2 Modeling Procedure

Basically, electric power systems may consider as synchronous generation units, and electric loads interconnected through a transmission lines, i.e., a transmission network. Power systems are comprised of a large number of multimachines multimachines that accommodate nonlinearities in the interconnections among the neighboring synchronous machines. In this case, all the synchronous machines run in parallel and at the synchronous speed when used under normal operating conditions. The stator fields and rotor fields of the machines are synchronized in the machine, which means that their rotational speeds must be almost exactly equal for successful operation of the system. To maintain electromechanical stability of the system, the stator voltages and currents of all the machines have the same frequency and the rotor mechanical speed of each machine is exactly proportional to this frequency, in proportion the number of generator windings on the synchronous machine. Therefore, the rotors of all interconnected synchronous machines in the system must remain in synchronism; see [276] for details.

In this section, we first discuss the basic equation governing the electromechanical dynamics of power systems. This equation is often referred to as the classic swing equation. The swing equation, which is based on Newton's second law, governs the rotor dynamics of a synchronous machine. Clearly, the swing equation governs speed (and frequency) of synchronous machine in a power system. In relating the dynamic performance of the machine to the power network, the swing equation can be formulated by the units of power instead of the units of torque. Power is a preferred unit, since it is more suitable than torque to measure. Roughly speaking, power equals the product of torque and speed, thus power becomes almost exactly proportional to torque. As seen in this relationship, the electrical power output is almost exactly equal to the power in accordance with magnetic fields within the machine. Finally, the well-known swing equation in the second-order differential equation is

$$M\ddot{\delta} + D\dot{\delta} = P_m - P_e, \tag{2.3}$$

where M denotes the normalized inertia constant, $M = 2H/\omega_0$ in seconds-squared per electrical radian, the inertia constant H has units of seconds, ω_0 is synchronous

speed which is equivalent to $2\pi f_0$ in electrical radians per second, and f_0 is the rated frequency in Hertz. In addition, D is the damping constant in per unit, δ is the rotor angle of the machine in electrical radians, P_m is the mechanical input power from the prime-mover, and P_e is the electrical power output absorbed by the network from the generator. Note that P_e must balance the power absorbed by the rest of network at the generator bus and is related to the other network variables through the standard power-flow equations. The power quantities P_m and P_e are in per unit.

In the following analysis, the model does not include such a detailed representation of the synchronous machine. In this work, the power system models are considered under various simplifying assumptions and explanations.

1. Each synchronous machine is assumed to be equipped with the same type of exciter control and turbine/governor.

2. In Eq. (2.3), it is assumed that P_m is constant for all machines during the time interval of interest.

3. Loads are not considered and/or represented as constant impedance while comprising the local state variables from each conventional generation unit.

4. The subscript indexes d and q show in the coordinate system of direct and quadrature axis.

5. Subtransient parameters can be neglected.

6. Sum of the reactance for a one-machine, infinite-bus power system is considered as

$$X_{ds} = X_d + X_T + X_L \tag{2.4}$$

$$X'_{ds} = X'_d + X_T + X_L \tag{2.5}$$

   where X_d and X'_d are direct axis reactance and direct axis transient reactance of the machine in per unit, respectively. X_T and X_L are transformer and transmission line reactance in per unit, respectively.

7. The constant voltage behind transient reactance model the machine is valid.

8. The rotor angle of the machine coincides with the voltage behind the transient reactance angle.

9. The transformer voltages are neglected and the armature resistance, which is very small, is neglected for the excitation system.

2.3 The Models

2.3.1 SMIB System

In this subsection, we shall present a *single-machine infinite-bus* (SMIB) power system model. A SMIB involves a power system consisting of a synchronous machine which is connected via a transmission line to an infinite bus. However, an infinite bus represents a voltage source with constant phase, magnitude, and frequency, and it is not affected by the amount of current that flows into the transmission lines. It also may be defined as a machine having zero impedance and infinite inertia. A major bus of a large power system may often be chosen as an infinite bus. The internal voltage of the machine is represented by the phasor $E\angle\delta$ where δ is the phase angle and is also the initial rotor angle of the machine with respect to a synchronously rotating reference frame. For each machine of the system, the constant magnitude E is denoted the internal voltage of the machine, and the voltage $V\angle 0$ is called the voltage of the infinite bus. The initial rotor angle, by the internal voltage leading to the infinite bus voltage, coincides with rotor angle of the synchronous machine. The internal voltages and rotor angles for each synchronous machine are calculated using the generated active and reactive powers, voltage magnitudes, and angles. To do this, we first perform a power-flow analysis to determine system voltages, angles, and active and reactive power generation. In addition, transmission line includes the reactance X which is the equivalent reactance of the transmission network, including the transient reactance of the machine and the resistance R which represents the equivalent resistance of the transmission network. Thus, power flows freely along all available transmission lines from the generators to the loads by dividing among all connected lines flowing in the electric network, in inverse proportion to the impedance Z on each line. The electric network can be assumed to be losses, so all lines including the resistance can

be neglected.

2.3.2 Local Dynamics

The main objective of this section is to introduce a power system model for measuring voltage (and frequency) in a decentralized way. The model is supposed to be an exact representation of the power system and includes the main power system indicators such as frequency and voltage. Then we investigate some strategies that are robust with respect to deviations between the proposed model and reality. The model is motivated by earlier study of a generator model with these same components in [51],[116]. The model that we study is flexible enough to incorporate locally available information associated with the generator unit(s). Note that in contrast to the papers [51],[116], we consider the salient-pole case [277]. Throughout this subsection, we consider a multimachine power system with ith generator in the system. The state-space representation for such a system is described by the following equations

$$\dot{\delta}_i(t) = \omega_i(t), \tag{2.6}$$

$$\dot{\omega}_i(t) = M^{-1}\left(-D_i\omega_i - \Delta P_{ei}\right), \tag{2.7}$$

where

$$P_{ei}(t) = \frac{E'_{qi}V_s \sin\,\delta_i(t)}{X'_{ds}}, \tag{2.8}$$

and $\omega_i(t)$ is departure of machine speed from synchronous speed ω_0 in electrical radians per second, $\Delta P_{ei}(t) = P^0_{mi} - P_{ei}(t)$. E'_{qi} denotes the transient EMF of the ith machine in per unit, and V_s is the infinite-bus voltage in per unit. Correspondingly, the generator reactive power can be shown as

$$Q_{ei}(t) = \frac{E'_{qi}V_s \cos\,\delta_i(t)}{X'_{ds}} - \frac{V_s}{X'_{ds}}. \tag{2.9}$$

Note that $\delta_i(t)$ and $\omega_i(t)$ are measurable state variables. Next, we extend the model for the state variables of steam valving control. The differential equation for ith machine belongs to a simple nonreheat turbine that can be expressed in the forms

$$\dot{P}_{mi}(t) = \frac{1}{T_{Mi}}\left[-P_{mi}(t) + X_i(t)\right], \tag{2.10}$$

where T_{M_i} is the turbine time constant and X_i is the stream valve opening for ith machine in per unit. In addition, the governor-hydraulic model for ith machine can be formulated as a first-order differential equation [74],[278]

$$\dot{X}_i(t) = \frac{1}{T_{Ei}}\left[-X_i(t) - \frac{1}{R_i}\omega_i(t) + P_{mi}^0\right], \tag{2.11}$$

where $P_{mi}^0 = P_{mi}(t)$, and P_{mi}^0 is the mechanical power at the initial steady state. T_{Ei} is the governor time constant and R_i is the regulation constant in per unit.

The exciter model addresses how to measure generator terminal voltage using the concept of terminal voltage regulation, which is the main function of exciter control. The electrical power delivered by the ith machine is related by the definition

$$P_{ei}(t) \equiv E'_{qi}(t)I_{qi}(t), \tag{2.12}$$

where

$$E'_{qi}(t) = E_{qi}(t) + (X_{di} - X'_{di})I_{di}(t), \tag{2.13}$$

and $E_{qi}(t)$ is the EMF of the ith machine. Here I_{di} and I_{qi} are defined as

$$I_{di}(t) = \frac{E'_{qi}(t) - V_s\cos\,\delta_i(t)}{X'_{ds}}, \tag{2.14}$$

$$I_{qi}(t) = \frac{V_s\,\sin\,\delta_i(t)}{X'_{ds}}, \tag{2.15}$$

where the expressions of $I_{di}(t)$ and $I_{qi}(t)$ are the armature windings currents of the ith machine. Note that $I_{di}(t)$ and $I_{qi}(t)$ cannot be measured directly but they can be obtained from measurable variables. In addition, $E_{qi}(t)$, $E'_{qi}(t)$, $I_{di}(t)$, $I_{qi}(t)$, and V_s are in per unit. Then, $P_{ei}(t)$ is differentiable and measurable from Eq. (2.12), we write

$$\dot{P}_{ei}(t) = \dot{E}'_{qi}(t)I_{qi}(t) + E'_{qi}(t)\dot{I}_{qi}(t) \tag{2.16}$$

with

$$\dot{E}'_{qi}(t) = \frac{1}{T'_{doi}}\Big[-\frac{E'_{qi}(t)X_{ds}}{X'_{ds}} + \frac{(X_{di} - X'_{di})V_s\,\cos\,\delta_i(t)}{X'_{ds}} + E_{fdi}(t)\Big], \tag{2.17}$$

$$\dot{I}_{qi}(t) = \frac{V_s\,\cos\,\delta_i(t)}{X'_{ds}}, \tag{2.18}$$

where T'_{do} is direct axis transient open circuit time constant in seconds and E_{fi} is the field voltage of ith machine in per unit.

Then substituting Eq. (2.17) and Eq. (2.18) into (2.16), we obtain

$$\dot{P}_{ei}(t) = \left\{ \frac{1}{T'_{doi}} \Big[- \frac{E'_{qi}(t) X_{ds}}{X'_{ds}} + \frac{(X_d - X'_d) V_s \cos \delta_i(t)}{X'_{ds}} + E_{fdi}(t) \Big] \right\} I_{qi}(t) + E'_{qi}(t) \left\{ (\frac{V_s \cos \delta_i(t)}{X'_{ds}}) \dot{\delta}_i(t) \right\} \tag{2.19}$$

or equivalently,

$$\dot{P}_{ei}(t) = \left\{ \frac{(X_d - X'_d) V_s \cos \delta_i(t) - E'_{qi}(t) X_{ds}}{X'_{ds} T'_{d0}} \times \frac{V_s \sin \delta_i(t)}{X'_{ds}} + \frac{E_{fdi}(t) \times V_s \sin \delta_i(t)}{X'_{ds} T'_{d0}} \right\} + \left\{ \frac{E'_{qi}(t) V_s \cos \delta_i(t)}{X'_{ds}} \right\} \omega_i(t). \tag{2.20}$$

We recall that the Eq. (2.12) and E'_q is the unmeasured value and can be eliminated from the Eq. (2.20)

$$\dot{P}_{ei}(t) = - \frac{P_{ei}(t) X_{ds}}{X'_{ds} T'_{d0}} + \frac{(X_d - X'_d) V_s^2 \sin 2\delta_i(t)}{2 X'^2_{ds} T'_{d0}} + \frac{E_{fdi}(t) V_s \sin \delta_i(t)}{X'_{ds} T'_{d0}} + \left\{ Q_{ei}(t) + \frac{V_s^2}{X'_{ds}} \right\} \omega_i(t). \tag{2.21}$$

Each side of the above equation is multiplied by $\frac{X'_{ds}}{X_{ds}}$ and the equation can be written as follows;

$$\dot{P}_{ei}(t) = - \frac{P_{ei}(t)}{T'_{d0}} + \frac{1}{T'_{d0}} \left\{ \frac{(X_d - X'_d) V_s^2 \sin 2\delta_i(t)}{2 X_{ds} X'_{ds}} + \frac{E_{fdi}(t) V_s \sin \delta_i(t)}{X_{ds}} + \frac{X'_{ds}}{X_{ds}} T'_{d0} \left(Q_{ei}(t) + \frac{V_s^2}{X'_{ds}} \right) \omega_i(t) \right\}. \tag{2.22}$$

Here the control input is defined as

$$u_{1i} = \frac{(X_d - X'_d) V_s^2 \sin 2\delta_i(t)}{2 X_{ds} X'_{ds}} + \frac{E_{fdi}(t) V_s \sin \delta_i(t)}{X_{ds}} + \frac{X'_{ds}}{X_{ds}} T'_{d0} \left(Q_{ei}(t) + \frac{V_s^2}{X'_{ds}} \right) \omega_i(t). \tag{2.23}$$

Thus, $P_{ei}(t)$ is used as alternative state instead of $E'_{di}(t)$ and $E'_{qi}(t)$. Note that the reactive power $Q_{ei}(t)$ can be measured and calculated explicitly. Finally, the derivative of $P_{ei}(t)$ is formulated as

$$\dot{P}_{ei}(t) = - \frac{1}{T'_{doi}} P_{ei}(t) + \frac{1}{T'_{doi}} u_{1i}. \tag{2.24}$$

Next, we will formalize the generator terminal voltage $V_t(t)$ as a state variable. The main idea here is that the expression of $V_t(t)$ is written in terms of $\delta_i(t)$ and $P_{ei}(t)$. The algebraic equation of the ith generator terminal voltage is

$$V_{ti}^2(t) = V_{di}^2 + V_{qi}^2, \tag{2.25}$$

where

$$V_{di} = X_{qi} I_{qi}(t), \tag{2.26}$$

$$V_{qi} = -X'_{di} I_{di}(t) + E'_{qi}(t), \tag{2.27}$$

which results in

$$V_{ti}(t) = \left\{ E'^2_{qi}(t) - 2E'_{qi}(t) X'_{di} I_{di}(t) + X'^2_{di} I^2_{di}(t) + X^2_{qi} I^2_{qi}(t) \right\}^{\frac{1}{2}}. \tag{2.28}$$

Then, we can eliminate $I_{di}(t)$ and $I_{qi}(t)$ from Eq. (2.28). To do this, recalling Eq (2.14) and Eq. (2.15), we obtain

$$V_{ti}(t) = \left\{ E'^2_{qi}(t) - 2E'_{qi}(t) X'_{di} \left(\frac{E'_{qi}(t) - V_s \cos \delta_i(t)}{X'_{ds}} \right) + X'^2_{di} \left(\frac{E'_{qi}(t) - V_s \cos \delta_i(t)}{X'_{ds}} \right)^2 + X'^2_{qi} \left(\frac{V_s \sin \delta_i(t)}{X'_{ds}} \right)^2 \right\}^{\frac{1}{2}}. \tag{2.29}$$

By defining $X'_{ds} = X_s + X'_{di}$, Eq. (2.29) becomes

$$V_{ti}(t) = \frac{1}{X'_{ds}} \Big\{ E'^2_{qi}(t) X_s^2 + 2E'_{qi}(t) X'_{di} X_s V_s \cos \delta_i(t) + X'^2_{di} V_s^2 \cos^2 \delta_i(t) + X'^2_{qi} V_s^2 \sin^2 \delta_i(t) \Big\}^{\frac{1}{2}}. \tag{2.30}$$

In above equation, $E'_q(t)$ is not measurable. We rewrite the terminal voltage of the ith machine in terms of the $P_e(t)$ by using Eq. (2.8), and the following result is thus obtained.

$$V_{ti}(t) = \left\{ \frac{P^2_{ei}(t) X_s^2}{V_s^2 \sin^2 \delta_i(t)} + \frac{2X'_{di} X_s P_{ei}(t) \cot \delta_i(t)}{X'_{ds}} + \frac{X'^2_{di} V_s^2 \cos^2 \delta_i(t)}{X'^2_{ds}} + \frac{X'^2_{qi} V_s^2 \sin^2 \delta_i(t)}{X'^2_{ds}} \right\}^{\frac{1}{2}}. \tag{2.31}$$

Differentiating (2.31) yields:

$$\dot{V}_{ti}(t) = h_{1i}(t)\dot{\delta}_i(t) + h_{2i}(t)\dot{P}_{ei}(t), \tag{2.32}$$

where

$$\begin{aligned} h_{1i}(t) = &-\frac{P_{ei}^2(t)X_s^2 \cot \delta_i(t)}{V_{ti}(t)V_s^2 \sin^2\delta_i(t)} - \frac{P_{ei}(t)X'_{di}X_s}{V_{ti}(t)X'_{ds} \sin^2\delta_i(t)} \\ &- \frac{X'^2_{di}V_s^2 \sin 2\delta(t)}{2V_{ti}(t)X'^2_{ds}} + \frac{X'^2_{qi}V_s^2 \sin 2\delta(t)}{2V_{ti}(t)X'^2_{ds}}, \\ h_{2i}(t) = &\frac{P_{ei}(t)X_s^2}{V_{ti}(t)V_s^2 \sin^2\delta_i(t)} + \frac{X'_{di}X_s \cot \delta_i(t)}{V_{ti}(t)X'_{ds}}. \end{aligned} \tag{2.33}$$

Expressions $h_1(t)$ and $h_2(t)$ are assumed to be uncertain parameters which are only known in their uncertainty interval. The nonlinearity of the power system model is modeled in terms of two time–varying parameter vectors, $h_1(t)$ and $h_2(t)$. For the case of two uncertain parameters, the terminal voltage $V_t(t)$ contains all nonlinear terms that are uncertain parameters that are considered in only a function of measurements, whose time behaviour is unknown. Thus, we have four points $(h_1, h_2) = (\underline{h}_1, \overline{h}_1, \underline{h}_2, \overline{h}_2)$ for two uncertain parameters which are possibly time-dependent. To find the uncertainty interval for the parameters (h_1, h_2), we use the security operating constraints for the power system model. In doing so, we provide the bounds of the uncertainty range where the system remains stable with respect to allowable operating conditions of the system. In addition, the control input is not assumed to be constant since we have an uncertain parameter $h_{2i}(t)$ in the input vector.

Remark 1. *Saliency of the synchronous machines is not neglected from the parameters $h_1(t)$ and $h_2(t)$.*

The main goal is to choose the terminal voltage as a state variable, since this provides measurement of the synchronous machine of terminal voltage directly. Finally, we introduce the decentralized feedback control input u_{1i} into (2.32), obtaining

$$\dot{V}_{ti}(t) = h_{1i}(t)\omega_i(t) - \frac{h_{2i}(t)}{T'_{doi}}P_{ei}(t) + \frac{h_{2i}(t)}{T'_{doi}}u_{1i}. \tag{2.34}$$

Notice that, the control input u_{1i} is defined with $Q_{ei}(t)$ in Eq. (2.23). Alternatively, u_{1i}

can be written in terms of δ_i. That is:

$$u_{1i} = \frac{V_s}{X_{ds}} \sin(\delta_i(t)) \left[E_{fdi} + T'_{d0}(X_{di} - X'_{di}) \frac{V_s}{X'_{ds}} \omega_i(t) \sin(\delta_i(t)) \right] + T'_{d0} \omega_i(t) \cot(\delta_i(t)). \tag{2.35}$$

2.4 Network Model

Decentralized control and coordination in generators is required to effectively and reliably coordinate of power systems. However, both generation and load require access to an interconnected network of transmission lines. The transmission network consists of high voltage transmission lines, transformers, phase shifters and other utilities that enable the transfer of electricity production from generators to loads. The complete power system model for dynamic stability control depends on the integration of more components to the network configuration, as well as their interactions in the system. Thus, the transmission network plays an important role in interactions. In order to obtain a more realistic power system, the synchronous machine, AVR/exciter, and turbine/governor equations are combined by the network equations. In addition the local dynamics of generators and load deviations are subject to transmission network constraints.

Let the electrical network consist of n-buses power system with $\mathcal{N} = \{1, 2, \ldots, n\}$ connected by the set of transmission lines $\mathcal{L} \subseteq \mathcal{N} \times \mathcal{N}$. The system has generator buses $\mathcal{G} \subseteq \mathcal{N}$, in other words, these buses represent synchronous machines. $\mathcal{N} - \mathcal{G}$ represents the load buses. Now, we can view the network mathematical model by the nodal equation that is the relationship between node current and voltage in the linear network. Hence, the nodal equation of an electrical network can be generally described by $\mathbf{I} = \mathbf{YV}$ and it can shown in a matrix form

$$\begin{bmatrix} I_1 \\ I_2 \\ \vdots \\ I_n \end{bmatrix} = \begin{bmatrix} Y_{11} & Y_{12} & \cdots & Y_{1n} \\ Y_{21} & Y_{22} & \cdots & Y_{2n} \\ \vdots & \vdots & \ddots & \vdots \\ Y_{n1} & y_{n2} & \cdots & Y_{nn} \end{bmatrix} \begin{bmatrix} V_1 \\ V_2 \\ \vdots \\ V_n \end{bmatrix}, \tag{2.36}$$

where $\mathbf{I} = \begin{bmatrix} I_1 & I_2 & \ldots & I_n \end{bmatrix}^{\mathrm{T}}$ is current vector and I_k is the nodal current injected to

the bus; V_k is the complex voltage at bus $k \in \mathcal{N}$, which is measured from the reference node; the diagonal element Y_{kk} is the self admittance or the input admittance at node k for every $k \in \mathcal{N}$, and the off-diagonal element Y_{kj} $(k, j \in \mathcal{N}, k \neq j)$ is the mutual admittance or the transfer admittance between nodes k and l. Note that the self admittance for a node is the sum of all the admittances connected to that node; the mutual admittance between two given nodes is the negative of the admittance connected between the given nodes. Here,

$$\mathbf{Y}_{kk} = Y_{kk}\angle\theta_{kk} = G_{kk} + jB_{kk}, \tag{2.37}$$

$$\mathbf{Y}_{kj} = Y_{kj}\angle\theta_{kj} = G_{kj} + jB_{kj}, \tag{2.38}$$

where $G_{kk} = Y_{kk}\cos\theta_{kk}$ is the short-circuit conductance; $G_{kj} = Y_{kj}\cos\theta_{kj}$ is the mutual conductance; and $B_{kj} = Y_{kj}\sin\theta_{kj}$ is the mutual susceptance. Thus, when formulating the network equations, the nodal admittance matrix of the power grid $\mathbf{Y} = \mathbf{G} + \mathbf{jB}$ is used, in which $n \times n$ complex-value matrix is defined. We can also use the trigonometric identities:

$$G\cos\delta + B\sin\delta = Y\sin(\delta + \theta), \tag{2.39a}$$

$$G\sin\delta - B\cos\delta = -Y\cos(\delta + \theta). \tag{2.39b}$$

Let $\mathbf{P} + \mathbf{jQ}$ be the complex (or apparent) power of all the buses. The power balance equations can be written as

$$\mathbf{P} + \mathbf{jQ} = \mathrm{diag}\{\mathbf{V}\mathbf{V}^*\mathbf{Y}^*\}. \tag{2.40}$$

The above equation can be divided into a real and an imaginary part. Thus, the active power injection at bus k is described by

$$P_k = \mathbf{Re}\{V_k I_k^*\}, \quad k \in \mathcal{N} \tag{2.41}$$

and the reactive power injection at bus k:

$$Q_k = \mathbf{Im}\{V_k I_k^*\}, \quad k \in \mathcal{N}. \tag{2.42}$$

Here, V_k is the voltage phasor for every $k \in \mathcal{N}$. Substitution of Eq. (2.41) into the

Eq. (2.45) gives

$$P_k = \mathbf{Re}\left\{\sum_{j=1}^{n} V_k V_j Y_{kj} \angle(\delta_k - \delta_j - \theta_{kj})\right\}, \quad k \in \mathcal{N}$$
$$= \sum_{j=1}^{n} V_k V_j Y_{kj} \cos(\delta_k - \delta_j - \theta_{kj}). \tag{2.43}$$

Following this, we can also write

$$P_k = V_k^2 Y_{kk} \cos\theta_{kk} + \sum_{\substack{j=1 \\ j\neq k}}^{m} V_k V_j Y_{kj} \cos(\delta_k - \delta_j - \theta_{kj}), \quad k \in \mathcal{N} \tag{2.44}$$
$$= V_k^2 G_{kk} + \sum_{\substack{j=1 \\ j\neq k}}^{n} V_k V_j Y_{kj} \cos(\delta_k - \delta_j - \theta_{kj}). \tag{2.45}$$

The formulation of electrical active power injection at bus k is also presented in terms of the line susceptances and conductances. Now, one can write

$$P_k + jQ_k = \sum_{j=1}^{n} V_k V_j (G_{kj} - jB_{kj}) \left[\cos(\delta_k - \delta_j) + j\sin(\delta_k - \delta_j)\right] \quad k \in \mathcal{N} \tag{2.46}$$

Again, this can be stated as the active power injection:

$$P_k = \sum_{j=1}^{n} V_k V_j [G_{kj}\cos(\delta_k - \delta_j) + B_{kj}\sin(\delta_k - \delta_j)], \quad k \in \mathcal{N} \tag{2.47}$$

or

$$P_k = V_k^2 G_{kk} + \sum_{\substack{j=1 \\ j\neq k}}^{n} V_k V_j Y_{kj} \left[\sin\theta_{kj}\sin(\delta_k - \delta_j) + \cos\theta_{kj}\cos(\delta_k - \delta_j)\right], \tag{2.48}$$
$$= V_k^2 G_{kk} + \sum_{\substack{j=1 \\ j\neq k}}^{n} V_k V_j [B_{kj}\sin(\delta_k - \delta_j) + G_{kj}\cos(\delta_k - \delta_j)], \quad k \in \mathcal{N}. \tag{2.49}$$

Also,

$$Q_k = \sum_{j=1}^{n} V_k V_j [G_{kj}\sin(\delta_k - \delta_j) - B_{kj}\cos(\delta_k - \delta_j], \quad k \in \mathcal{N} \tag{2.50}$$

or

$$Q_k = -V_k^2 B_{kk} - \sum_{\substack{j=1 \\ j\neq k}}^{n} V_k V_j [B_{kj}\cos(\delta_k - \delta_j) - G_{kj}\sin(\delta_k - \delta_k)], \quad k \in \mathcal{N}. \tag{2.51}$$

Obviously, the electrical real power delivered to the power network by the ith machine is a function of the angle differences $(\delta_k - \delta_j)$ between the ith machine and the machines connected to that machine.

The electrical real and reactive power, P_k and Q_k, come from the nonlinear AC power-flow equation. The flows in power grid are defined by nonlinear AC power-flow equations. The goal of the classical power-flow problem is to determine the unknown complex voltages at all buses. The power-flow problem is usually computed approximately through linearization the process or in an asymptotic sense via the standard Newton-Raphson method. The values of all unknown variables are fully determined with a sufficiently close initial guess. The power network has generator and load buses. The active powers and voltage magnitudes are known at generator buses, and active and reactive powers are known at load buses. Thus, the network equations can be expressed for both generator and load buses, and the resulting equations are nonlinear. The network equations for generator buses are given by

$$0 = -\left[\frac{E_i V_i}{X_i}\sin(\delta_i - \theta_i)\right] + \sum_{j=1}^{n} V_k V_j [G_{kj}\cos(\delta_k - \delta_j) + B_{kj}\sin(\delta_k - \delta_j)], \tag{2.52}$$

$$0 = -\left[\frac{E_i V_i}{X_i}\cos(\delta_i - \theta_i) - \frac{V_i^2}{X_i}\right] + \sum_{j=1}^{n} V_k V_j [G_{kj}\sin(\delta_k - \delta_j) - B_{kj}\cos(\delta_k - \delta_j)] \tag{2.53}$$

for ith synchronous machine and $i, k \in \mathcal{G}$.

The power balance equations for load bus at bus $k \in \mathcal{N} - \mathcal{G}$ are given by

$$0 = P_{D_k} + \sum_{j=1}^{n} V_k V_j [G_{kj}\cos(\delta_k - \delta_j) + B_{kj}\sin(\delta_k - \delta_j)], \tag{2.54}$$

$$0 = Q_{D_k} + \sum_{j=1}^{n} V_k V_j [G_{kj}\sin(\delta_k - \delta_j) - B_{kj}\cos(\delta_k - \delta_j)] \tag{2.55}$$

2.5 Contributions on Models

State-space models are used to represent the dynamical models such as classical models of power systems. Thus, a power system model is characterized using the state-space form for the analysis of the system behavior. In this section, we develop some state-space models consisting of synchronous machines interconnected via the transmission network. For every $i \in \mathcal{G}$, let $P_{ci} = P_{mi} - E_{qi}'^2(t)G_{ii}$. Then the swing dynamics of the ith machine becomes

$$M_i \frac{d^2\delta_i}{dt^2} + D_i \frac{d\delta_i}{dt} = P_{ci} - \sum_{\substack{j=1 \\ j\neq k}}^{n} E'_{qi}E'_{qj}[G_{ij}\cos(\delta_i - \delta_j) + B_{ij}\sin(\delta_i - \delta_j)]. \tag{2.56}$$

Note that the asynchronous damping constant D_{ij} is neglected from the above equation. In this way, we convert n second-order differential equations into $3n$ first-order differential equations. We now can rewrite (2.56) as follows:

$$\begin{aligned} \dot{\delta}_i(t) &= \omega_i(t), \quad i \in \mathcal{G} \\ M_i\dot{\omega}_i(t) &= P_{ci} - D_i\omega_i(t) - \sum_{\substack{j=1 \\ j\neq i}}^{n} E'_{qi}E'_{qj}\alpha_{ij}, \quad i \in \mathcal{G} \end{aligned}$$

and with excitation,

$$T'_{d0_i}\dot{E}'_{qi}(t) = -(1 - \Delta X_{d_i}B_{ii})E'_{qi} - \Delta X_{d_i}\sum_{\substack{j=1 \\ j\neq i}}^{n} E'_{qj}\beta_{ij} + E_{fd_i}, \quad i \in \mathcal{G}$$

where $\Delta X_{d_i} = X_{d_i} - X'_{d_i}$ and $E_{fd_i} = E^0_{fd_i} + u_i$. Using the Eq. (2.39), we get

$$\alpha_{ij} = G_{ij}\cos(\delta_i - \delta_j) + B_{ij}\sin(\delta_i - \delta_j), \tag{2.57}$$

$$\beta_{ij} = G_{ij}\sin(\delta_i - \delta_j) - B_{ij}\cos(\delta_i - \delta_j). \tag{2.58}$$

Defining the following constants

$$\begin{aligned} v_{ij} &= G_{ij}^2 + B_{ij}^2\,, & \theta_{ij} &= \arctan\left(\frac{G_{ij}}{B_{ij}}\right), \\ a_i &= \frac{1}{T'_{d0_i}}\left(1 - B_{ii}\Delta X_{d_i}\right)\,, & b_i &= \frac{\Delta X_{d_i}}{T'_{d0_i}}\sqrt{v_{ij}}\,. \end{aligned} \tag{2.59}$$

Using these new definitions, we define the state-space model with the state variables $\left(\delta_i, \omega_i, E'_{qi}\right)$,

$$\begin{aligned}
\dot{\delta}_i(t) &= \omega_i(t), \quad i \in \mathcal{G} \\
\dot{\omega}_i(t) &= P_{ci} M_i^{-1} - \frac{D_i}{M_i}\omega_i(t) - M_i^{-1} \sum_{\substack{j=1 \\ j\neq i}}^{n} E'_{qi} E'_{qj} \sqrt{v_{ij}} \sin\left(\delta_i - \delta j + \theta_{ij}\right), \quad i \in \mathcal{G} \\
\dot{E}'_{qi}(t) &= -a_i E'_{qi} - b_i \sum_{\substack{j=1 \\ j\neq i}}^{n} E'_{qj} \cos\left(\delta_i - \delta_j + \theta_{ij}\right) + E_{fi}, \quad i \in \mathcal{G}
\end{aligned} \tag{2.60}$$

where $E_{fi} = \frac{E_{fd_i}}{T'_{d_{0i}}}$ is the constant parameter for all machines ($i \in \mathcal{G}$). For every $i \in \mathcal{G}$, $a_i, b_i > 0$, $\theta_{ij} = \theta_{ji}$.

On the other hand, the dynamics of a synchronous machine are not in strict feedback form, thus $P_{ei}(t)$ is a state variable instead of unmeasurable state $E'_{qi}(t)$. However, measurement of the terminal voltage $V_{ti}(t)$ is the main issue in this chapter. As we have seen before, the terminal voltage $V_{ti}(t)$ is a nonlinear function of $\delta_i(t)$, $P_{ei}(t)$ that is assumed to be unknown and time-varying, and depends on the derivatives of $\delta_i(t)$ and $P_{ei}(t)$. To regulate the terminal voltage directly, we have so far used the terminal voltage equation given in (2.34), which is represented in terms of $\delta_i(t)$ and $P_{ei}(t)$. Thus, the dynamics of terminal voltage lead to a highly nonlinear equation. Next, we set the system dynamics with three measurable states:

$$\begin{aligned}
\dot{\omega}_i(t) &= -\frac{D_i}{M_i}\omega_i(t) - \frac{1}{M_i}P_{ei}(t) \quad i \in \mathcal{G}, , \\
\dot{P}_{ei}(t) &= -\frac{1}{T'_{doi}}P_{ei}(t) + \frac{1}{T'_{doi}}u_{1i} \quad i \in \mathcal{G}, \\
\dot{V}_{ti}(t) &= h_{1i}(t)\omega_i(t) - \frac{h_{2i}(t)}{T'_{doi}}P_{ei}(t) + \frac{h_{2i}(t)}{T'_{doi}}u_{1i} \quad i \in \mathcal{G}.
\end{aligned}$$

Finally, the active power output is measured at every bus of the power network, thus $P_{ei}(t)$ can be removed from the above model, and is introduced as a new input of the system [279]. The dynamic model can be written by the following state V_{ti}:

$$\dot{V}_{ti}(t) = h_{1i}(t)\omega_i(t) + h_{2i}(t)u_{fi} \quad i \in \mathcal{G}, \tag{2.61}$$

where $u_{fi} = \dot{P}_{ei}(t)$ is assumed to be a decentralized feedback input. The state $V_{ti}(t)$ is subject to the uncertain parameters $h_1(t)$ and $h_2(t)$ and can be controlled by the new input u_{fi}. The closed-form solution of (2.61) is derived for the case where full state information is available. In the case where full state information is available, the decentralized voltage controller is linear in the state and in the disturbance.

The state-space model with the new input can be represented as

$$\dot{x}(t) = Ax(t) + Bu_f, \tag{2.62}$$

where the system state vector $x = [\omega \ V_t]^{\mathrm{T}}$.

2.5.1 Power System Stabilizers

Power system stabilizers are widely used in power systems [280]. The PSSs serve to add an auxiliary signal to AVRs which is input of the excitation system of a generator. In general, PSSs are used for damping enhancement in power systems oscillation, and to damp out the low-frequency oscillations of the machine through the excitation system. As a result, PSSs in operation improve power system dynamic stability, and also improve the system-wide performance of power systems with other control devices.

A PSS design is proposed for a decentralized output feedback problem. Additional state variables are applied to the power system model. As a result, the control action is provided by the certain states of the model. As a starting point for the design [281], we provide the standard representation of PSSs which include a third order transfer function. The dynamic model consisting of a constant gain, a washout filter, and a lead-lag filter as follows

$$G_i(s) = K_{S_i} \frac{sT_{wi}}{1 + sT_{wi}} \frac{(1 + sT_{1i})(1 + sT_{3i})}{(1 + sT_{2i})(1 + sT_{4i})} \quad i \in \mathcal{G}, \tag{2.63}$$

where T_{1i}, T_{2i}, T_{3i}, T_{4i} and T_{wi} are the time constants, and in addition, K_{S_i} is the stabilizer gain. In this case, the value of the washout time constant T_w is not critical for phase shift or gain at the oscillating frequency. Thus it is accepted to be unaffected. Then, for mathematical simplicity, we can write the expression of $G_i(s)$ as

$$G_i(s) = K_i + \frac{\beta_{2i}s^2 + \beta_{1i}s + \beta_{0i}}{s^3 + \alpha_{2i}s^2 + \alpha_{1i}s + \alpha_{0i}} \quad i \in \mathcal{G}, \tag{2.64}$$

where $K_i = K_{S_i}\frac{T_{1i}T_{3i}}{T_{2i}T_{4i}}$ and the coefficients $\{\beta_{0i}, \beta_{1i}, \beta_{2i}\}$ and $\{\alpha_{0i}, \alpha_{1i}, \alpha_{2i}\}$ are explicit functions of the time constants. Let $\xi = [\xi_1, \xi_2, \xi_3]^{\mathrm{T}}$ be PSS state. Then we write an appropriate dynamic model for a PSS as

$$\begin{aligned}
\dot{\xi}_{1i} &= -\alpha_{2i}\xi_{1i} + \xi_{2i} + \beta_{2i}\omega_i(t) + u_{1i} \quad i \in \mathcal{G}, \\
\dot{\xi}_{2i} &= -\alpha_{1i}\xi_{1i} + \xi_{3i} + \beta_{1i}\omega_i(t) + u_{2i} \quad i \in \mathcal{G}, \\
\dot{\xi}_{3i} &= -\alpha_{0i}\xi_{1i} + \beta_{0i}\omega_i(t) + u_{3i} \quad i \in \mathcal{G}.
\end{aligned} \tag{2.65}$$

The PSS input is given by

$$u_{pi} = K_i\omega_i(t) + \xi_i \quad i \in \mathcal{G}. \tag{2.66}$$

Moreover, additional inputs are assumed for the states of PSSs such as $[u_{1i}, u_{2i}, u_{3i}]^{\mathrm{T}}$. Following the state-space approach (2.65), these additional inputs are an auxiliary step in the both control and design principle. For this purpose, we may write a feedback strategy in the following PSS path:

$$\begin{bmatrix} u_{1i} & u_{2i} & u_{3i} \end{bmatrix}^{\mathrm{T}} = \begin{bmatrix} \eta_{1i} & \eta_{2i} & \eta_{3i} \end{bmatrix}^{\mathrm{T}} \xi_{1i}. \tag{2.67}$$

Notice that only states (ω_i, V_{ti}) are available for input u_{fi}. Furthermore, the states of a PSS are only observable variables and it is assume that they may not be measurable. The input u_{pi} is assumed to be a continuous function of the states (ω_i, V_{ti}). Using the PSS input u_{pi}, we model the power system as the fifth-order system:

$$\begin{aligned}
\dot{\omega}_i(t) &= -\frac{D}{M}\omega_i(t) - \frac{1}{M_i}P_{ei}(t), \\
\dot{V}_{ti}(t) &= h_{1i}(t)K_i\omega_i(t) + h_{2i}(t)u_{fi} + \xi_1, \\
\dot{\xi}_{1i} &= -(\alpha_{2i} - \eta_1)\xi_{1i} + \xi_{2i} + \beta_{2i}(t)\omega_i(t), \\
\dot{\xi}_{2i} &= -(\alpha_{1i} - \eta_2)\xi_{1i} + \xi_{3i} + \beta_{1i}(t)\omega_i(t), \\
\dot{\xi}_{3i} &= -(\alpha_{0i} - \eta_3)\xi_{1i} + \beta_{0i}(t)\omega_i(t),
\end{aligned} \tag{2.68}$$

where

$$\alpha_{2i} - \eta_1 = \frac{1}{T_{2i}} + \frac{1}{T_{4i}} + \frac{1}{T_{wi}}, \tag{2.69}$$

$$\alpha_{1i} - \eta_2 = \frac{1}{T_{2i}T_{4i}} + \frac{1}{T_{4i}T_{wi}} + \frac{1}{T_{2i}T_{wi}}, \tag{2.70}$$

$$\alpha_{0i} - \eta_3 = \frac{1}{T_{2i}T_{4i}T_{wi}}. \tag{2.71}$$

Remark 2. *In this work, the coefficients* $\{\alpha_{2i}, \alpha_{1i}, \alpha_{0i}\}$ *are assumed to be constant. On the other hand, the coefficients* $\{\beta_{2i}(t), \beta_{1i}(t), \beta_{0i}(t)\}$ *are required to be adjusted for the changing of uncertain parameters* $h_{1i}(t)$ *and* $h_{2i}(t)$*. Thus, a control or optimization scheme is needed to regulate the states of the fifth-order dynamics and these coefficients will change accordingly.*

Finally, the closed-form solution is derived for the case where partial state information is available to the fifth-order system.

2.6 Conclusion

In this chapter, a general state-variable forms of mathematical modeling of a multimachine power system are presented. We aim to establish some models for designing the controllers that are to obtain appropriate measures for modern power systems. In (2.60), we firstly develop a classic model involving network equations for the observer-based analysis of power systems. A first contribution of this chapter is to propose a model in (2.61) for the voltage regulation problem of power systems, which takes into account the known allowable bounds of parametric uncertainties of the state equations of the system. These parametric uncertainties are deterministic and obtained depending on the system operating conditions. Then, the dynamics of a single generator are described with two major states: the frequency and terminal voltage of a synchronous machine. The nonlinearity of the model is only affected by these uncertain time-varying parameters, and hence, the state V_{ti} is used to eliminate everything else using these uncertain parameters. The aim of the model is to neglect other states of the synchronous machine, thus the system voltage and frequency are also affected by the input as electrical output power of the generator. The voltage

regulation problem is represented as a stabilizing controller problem using decentralized feedback. The control action provides a stabilization for the rest of the system by locally stabilizing each machine. The second-order system makes it possible to derive decentralized control for the closed-loop full-state measurement structure in a general setting with operating constraints of the power system and the requirements in the presence of parametric uncertainties on control action. This can further be simplified to the case of the state feedback problem.

A second contribution of this chapter is to enhance the model (2.61) with a power system stabilizer. The goal of the enhanced model is to solve the output feedback problem. In (2.65), using the states of the power system stabilizer, we propose a high-order model for a decentralized control-based output feedback controller. The design parameters of PSSs are controlled by uncertain parameters, which in this case are optimized using Bisection iterative algorithms.

Chapter 3

Voltage Control of Power Systems via Convex Optimization

3.1 Introduction

Voltage control is one of the main issues of power systems. The need to provide new voltage control methodologies is recognized by power system researchers, see [282]. The resulting increase in electrical demands, number of generation facilities with intermittent generation units, loading of transmission grids, high power transfers, and the loss of generation or transmission facilities in the power systems, all pose voltage control problems for power systems. The complexity of electric grids has greatly increased the concern for maintaining the voltages (and frequency) within a secure range pertaining to all system electrical equipment, and addressing the need to design security measures for modern power grids [283]. In most cases, the voltage control strategies are organized in both centralized and decentralized manners.

The main objective of this chapter is to control the terminal voltage (and frequency) of synchronous generators. The control action is characterized in a decentralized way. The main idea here is that it is not possible to eliminate many feedback loops from the controller design for a large electric power system since the cost of this process is expected to be much more expensive than the decentralized method. This difficulty motivated us to suppose that the system is composed of (non)interacting subsystems that are controlled independently on the system's local control action. This method is a modeling and solving control strategy for large power systems. In order to achieve this control strategy, the modeling process requires the measurement of terminal voltage and frequency of synchronous generators. However, the system frequency is a key system variable. That is, the system operates at a unique frequency in the entire interconnected system. As a consequence, all the local controllers of the synchronous generators are implemented to regulate the system frequency due to the

limitations of power flow through transmission lines. In the voltage control problem, the local variables on the controller and the power-flow equations often interact weakly; these weak interactions are neglected. As a result, the voltage control scheme achieves the measurement of voltage between suitable operating ranges. The system uncertainties are modeled by the nonlinear terms of the terminal voltage. In other words, the dynamics of terminal voltage contain the nonlinear terms that are the only function of the online measurements. The terminal voltage equation depends on parametric uncertainties for which their exact values are unknown or *a priori* known constants. This allows effective measurement of the terminal voltage.

For the solution process of the decentralized scheme, we design a decentralized controller with both state feedback and dynamic output feedback controllers to stabilize each individual generator. System modeling, viewed as two different dynamic models, is the fundamental motivation for the design of these decentralized controllers for power systems. In this chapter, we suggest a solution strategy to solve the decentralized voltage control problem that is subject to uncertain parameters using the case of full and partial state measurements. To achieve this, we adopt the following procedure. We first build a control scheme associated with the relevant models with uncertain (time-dependent) terms. By defining a set of scheduling variables from the knowledge of power system dynamics and/or based on the most recent power flow results [284], we determine the upper and lower bounds of these uncertain terms. Note that we do not need to know their equilibrium values. The model is decomposed into the points chosen from within the operating range of the system considered. Thus the power system model is rewritten using these points or sets. Actually, each set represents the known combination of the upper and lower bounds of the power system model. If these uncertain terms drift over time between these *a priori* known constants, we make sure that the proposed control behavior remains within acceptable bounds. The controller is then designed for each generator such that the stability of the system is guaranteed. Based on the stability conditions, stabilizing controllers are designed as a convex optimization problem characterized by linear matrix inequalities. Finally, the corresponding feedback gain of the voltage controller is constructed based on a feasible solution of the LMIs optimization problem.

3.2 Stability

The purpose of this section is to present basic definitions and theorems for our stability analysis. Lyapunov theory is applied for the fundamental stability analysis. We begin with a formal definition of stability [285],[286],[287]. The concept of stability may be defined as the solutions of differential equations which, given a reference solution $x^*(t, t_0^*, x_0^*)$ of

$$\dot{x}(t) = f(t, x) \tag{3.1}$$

with $x_0^* = (t, t_0^*, x_0^*)$ for $x, x_0^* \in \mathbb{R}^n$, where x, a scalar function of time t, is the state variable, $0 \leq t_0 \leq t,\ t, t_0 \in \mathbb{R}$, and $f(\cdot, \cdot)$, is a known vector function, can be obtained if the value of t and the function x are given. We consider that the system (3.1) satisfies the standard conditions for the existence and uniqueness of solutions. Then, using the system (3.1) given in any other time t_0, we can compute the future of the state $x(t)$ at time $t \geq t_0$ that starts from the initial state $x(t_0)$ if t_0 is understood. The stability relative to any given solution starts from $x(t, t_0, x_0)$, then flows to $x^*(t, t_0^*, x_0^*)$, letting $t_0^* \approx t_0$ and $x_0^* \approx x_0$, the given solution remains close to $x^*(t, t_0^*, x_0^*)$ for latter times. Indeed, the solution of (3.1) is often expressed as $x(t, t_0, x_0)$, which exists for all initial conditions (t_0, x_0) and involves a function $x(t)$ which is the solution of the system (3.1). Here, we need to know $x(t)$ for all initial times t_0. In addition, we can say that there is at least one solution $x(t)$ of the system (3.1) that lies in (t_0, x_0).

Fact 3.2.1. *For the system* (3.1)*, there exists a unique solution defined on some (bounded) interval of the form* $[0, +\infty)$*. The unique solution can be determined at initial time* t_0 *that starts from* x_0 *for the system* (3.1)*, and we obtain* $x(t_0) = x_0$ *defined in the interval* $[t_0, +\infty)$ *for all* $x_0 \in \mathbb{R}^n$*.*

Therefore, the state at time t_0 appears to be a parameter of the infinite-dimensional system (3.1). However, this accommodates the property of solution continuity in the initial conditions that are sufficient for it. The case of a continuous $x(t)$ in the initial conditions corresponds to sufficient conditions for a perturbed solution to remain close to an unperturbed solution defined in a finite interval of time. However, a small change in the initial conditions causes small changes in the system. It is worth noting that it is always possible to go back in time and determine x_0 from $x(t)$.

Assumption 3.2.1. *Recall that in system* (3.1)*, we assume that*

$$f(t,0) \equiv 0, \tag{3.2}$$

where f is continuous and $f(t,\cdot)$ is locally Lipschitz, uniformly in t. It is said that $x = 0$ is the equilibrium point of the system (3.1) *which is at the origin of the state space.*

Remark 3. *If the equilibrium point is not the origin, a new origin is constructed in $\mathbb{R}^n$ as the equilibrium of interest.*

From these explanations, we arrive at the following formal definition of stability in context of Lyapunov stability theory. Lyapunov deals only with the stability relative to any given solution, a candidate function of any solution, with respect to a particular reference solution. Stability in the sense of Lyapunov is described under the functions of perturbed and unperturbed motions. Lyapunov gives a description for stability motion for ordinary differential equations, thus stability of motion for a physical dynamic system acts to keep its motion near a certain trajectory with respect to a perturbation that refers to a small change in the initial condition, see [130].

Definition 3.2.1 (**Lyapunov stability**)**.** *For a system described by* (3.1)*, the equilibrium point $x = 0$ (or the origin is a stable equilibrium) is said to be stable if, for any given $\epsilon > 0$ and $t_0 \geq 0$, there exists $\delta > 0$ such that $\|x(t_0)\| < \delta$ implies $\|x(t)\| < \epsilon$ for all $t \geq t_0$. It is stable if for any given $t_0 \geq 0$, there exists φ such that $\|x\,(t, t_0, x_0)\,\| < \varphi(\|t_0\|)$ for all $t \geq t_0$. It is said to be uniformly stable if it is stable, and δ is independent of t_0. It is said to be unstable if it is not stable.*

In the above, $\|\cdot\|$ represents the vector 2-norm. The number δ is the function of ϵ and t_0, that is $\delta = \delta(t_0, \epsilon)$. Lyapunov stability contains mild requirements that rely on linearization about the equilibrium points. However, stability is defined at the time t_0. On the other hand, the Lyapunov theorem admits positive define and negative define (Lyapunov) functions which are only defined locally. Therefore, we can conclude the following definition.

Definition 3.2.2. *A continuous function $W : \mathbb{R}^n \to \mathbb{R}^+$ is said to be locally positive definite if $W(0) = 0$ and $W(x) > 0$ for small $\|x\| \neq 0$. A continuous function $W : \mathbb{R}^n \to \mathbb{R}$ is said to be globally positive define (or positive define) if $W(0) = 0$ and*

$W(x) > 0$ for all $x \neq 0$. For a continuous differentiable function $V : \mathbb{R}^+ \times \mathbb{R}^n \to \mathbb{R}^+$ in (3.1)*, which absolutely depends on time, and suppose that $V(t, x)$ positive define if $V(t, 0) = 0$ for all $t \geq 0$, and $V(t, x) \geq W(x)$ for all $t \geq 0$, $x \in \mathbb{R}^n$ where $W(x)$ is positive define function, in addition, $V(t, x)$ also corresponds to Lyapunov function for finite-dimensional systems.*

3.2.1 Asymptotic Stability

We extend the concept of stability in the sense of Lyapunov to include asymptotic stability. Primary interest in this subsection will be the asymptotic stability and exponential stability in this subsection, see [288],[285] for details.

Definition 3.2.3 (**Asymptotic Stability**)**.** *For a system described by* (3.1)*, the trivial solution $x = 0$ is said to be asymptotically stable in the sense of definition 3.2.1 if it is stable, and for any given $t > t_0$ and $\epsilon > 0$, there exists $\delta > 0$ such that $\|x_0\| \leq \delta$ implies $\lim_{t\to\infty} x(t, t_0, x_0) = 0$.*

The definition of asymptotic stability as defined in above may be written by a more precise statement such as $\|x_0\| < \delta$ which implies that for any $\eta > 0$, there exists $T(\eta) > 0$ such that

$$\|x_0\| < \delta \quad \Longrightarrow \quad \|x\left(t, t_0, x_0\right)\| < \eta \qquad \forall t > t_0 + T. \tag{3.3}$$

From this, we arrive at the following definitions.

Definition 3.2.4. *] Let Definition 3.2.1 hold. We shall say that the origin of* (3.1) *is said to be asymptotically stable if it is stable, and for any given $\eta > 0$, $t_0 \geq 0$, there exists a $\delta > 0$; there exists, in addition, a number $T > 0$, such that $\|x_0\| < \delta$ implies $\|x\left(t, t_0, x_0\right)\| < \eta$ for all $t > t_0 + T$. It is uniformly asymptotically stable if it is uniformly stable δ and T does not depend on t_0.*

In the above, δ is a function of t_0, and T depends on t_0, x_0, and η, that is $\delta = \delta(t_0)$ and $T = T(t_0, x_0, \eta)$. From the above proposed definitions of asymptotic stability, the definition of attractivity is defined as follows:

Definition 3.2.5. *Consider the system* (3.1)*, which is said to be (locally) attractive for all $t > t_0$ if there exists $\eta > 0$, and for any given x_0 satisfying $\|x_0\| < \eta$ such*

that $\lim_{t\to\infty} x(t, t_0, x_0) = 0$ *that is uniformly with respect to* t_0, x_0. *It is attractive if it is globally attractive for all* $\mathbb{R}^n$.

Therefore,

$$\|x_0\| < \delta \quad \Longrightarrow \quad \lim_{t\to\infty} x(t, t_0, x_0) = 0. \tag{3.4}$$

We conclude that $x = 0$ is uniformly locally attractive, and there exists δ independent of t_0 for which Eq. (3.4) holds. Furthermore, it is required that the convergence in Eq. (3.4) is uniform. In the description that follows, Definitions 3.2.3 and 3.2.4 are local, since they describe neighborhoods of the equilibrium point. We shall say that an equilibrium point $x = 0$ is globally stable if it is stable for all initial conditions $x_0 \in \mathbb{R}^n$. Thus, global asymptotic stability is a concept which guarantees the asymptotic stability for all initial conditions or all initial states in the state space in $\mathbb{R}^n$. Furthermore, global stability is highly desirable, so we want to achieve it. We now focus on the definitions of (local) asymptotic stability and indicate where it is extended to global notions of stability. Therefore, with this and local definitions, we provide the following theorem [285],[130],[131].

Definition 3.2.6 (**Global asymptotic stability**). *For a system described by* (3.1), *we take the equilibrium state to be the origin which is globally asymptotically stable if it is stable in the sense of definitions 3.2.1 and 3.2.5 for any given* $\delta > 0$, $\eta > 0$, *and* $t \geq 0$ *and there exists* $\|x_0\| < \delta$ *implies* $\|x(t, t_0, x_0)\| < \eta$ *for all* $t > t_0 + T$. *It is said to be globally (uniformly) asymptotically stable if it is (uniformly) asymptotically stable, and* δ *can be chosen to be arbitrary large.*

The concept of uniform stability can apply to time-varying linear systems, as well as to nonlinear systems. We now need the following definition [52].

Definition 3.2.7 (**Uniform stability**). *The equilibrium point* $x = 0$, *is called a uniformly stable equilibrium point of* (3.1) *if for any given* $\epsilon > 0$, *there exist* $\delta(\epsilon) > 0$ *such that* $\|x_0\| < \delta$ $\|x(t, t_0, x_0)\| \leq \epsilon$ *for all* $t > t_0$ *and for all* $t_0 \geq 0$. *It is uniformly locally attractive; there exists* δ *independent of* t_0.

In other words, δ in the above definition can be chosen independently of t_0. However, the concept of stability for time-invariant systems implies uniform stability and,

for time-varying systems, asymptotic stability is equivalent to uniform asymptotic stability. Thus, if the equilibrium point of the system (3.1) is stable then it is uniformly stable. In addition, if it is asymptotically stable then it is said to be uniformly asymptotically stable.

It is important to stress that the definitions of asymptotic stability cannot pose as the speed of convergence of trajectories to the origin. Hence, the following definition holds [130].

Definition 3.2.8. *The equilibrium point $x = 0$ of system* (3.1) *is said to be (locally) exponentially stable if there exists positive scalars k and α such that $\|x(t, t_0, x_0)\| \leq k\|x_0\|e^{-\alpha(t-t_0)}$ for all $t > t_0$ and for all $t_0 \geq 0$.*

Here, the constant α is (an estimate of) the rate of convergence.

We can conclude that the properties of uniform asymptotic stability are equivalent to exponential stability for linear time-varying systems. In addition, exponential stability and uniform asymptotic stability imply uniform stability and asymptotic stability and correspond to Lyapunov stability. On the other hand, uniform asymptotic stability does not ensure exponential stability. Thus, the system (3.1) can be uniformly asymptotically stable but not exponentially stable. We finally note that the definition of asymptotic stability does not contain Lyapunov stability, and the definition of exponential stability does not contain uniform stability.

3.2.2 Quadratic Stability

Quadratic stability analyzes the stability robustness for any (possibly infinite) time-variation of the uncertain parameters where the stability is defined between the allowable bounds of the uncertain parameters. Quadratic stability implies that the quadratic Lyapunov functions depend on the uncertainties or perturbation terms. Quadratic stability obviously guarantees robust stability when dealing with systems that have parametric uncertainty, but on the other hand, the converse is not true. In this case, it is often convenient to search for a quadratic Lyapunov function which is independent of the uncertain parameters. In addition, the solutions are constructed by the LMIs and computed using on convex optimization, see [52],[155],[147]. Then, we introduce the following definition.

Definition 3.2.9 (**Quadratic Stability**). *Consider an uncertain linear system described by*

$$\dot{x}(t) = A(\rho)x(t), \quad \rho \in \Omega. \tag{3.5}$$

The system in (3.5) *is said to be quadratically stable, if there exists a positive definite matrix* $P \in \mathbb{R}^{n\times n}$ *such that for all* $p \in \Omega$

$$A(\rho)^{\mathrm{T}}P + PA(\rho) < 0. \tag{3.6}$$

From this definition, it is also possible to write the dual form of the quadratic stability of the system (3.5) as follows

$$A(\rho)^{\mathrm{T}}Q + QA(\rho) < 0, \tag{3.7}$$

where Q is a positive define matrix and can be obtained from pre- and post-multiply inequalities (3.6) by P^{-1} that is $P^{-1} = Q$.

Due to the uncertain parameters that are time-varying, the system matrix $A(\rho)$ obtained from Hurwitz stability criterion can no longer guarantee exponential stability. Thus, we further need to expand Lyapunov functions, such as a parameter-dependent Lyapunov function. Then, the system (3.5) has a positively defined solution. A quadratic Lyapunov function can be formed from the solution P,

$$V(t, x) = x(t)^{\mathrm{T}}Px(t) \tag{3.8}$$

such that asymptotic stability of the uncertain system in (3.5) for all $\rho \in \Omega$ can be proven by applying the Lyapunov approaches. In other words, the analytical expression (3.8) indicates that for any asymptotically stable system, we can always find the stability condition that is referred to as a quadratic stability condition. Obviously, the system (3.5) is quadracilally stable if there exists a quadratic Lyapunov function which is used to ensure stability. Thus, the concept of quadratic stability implies asymptotic stability of the uncertain system in (3.5). One reason to the quadratic Lyapunov functions in the literature is to simplify analysis and synthesis of uncertain systems. We also enlarge the concept of quadratic stability and quadratic stabilizability to the form of time-varying parameter uncertainties.

For a Lyapunov function which depends on uncertain parameters, it is also possible to construct a quadratic Lyapunov function $V(t,x)$, and therefore, we may further write

$$V(t,x) = x(t)^{\mathrm{T}} P x(t) > 0, \tag{3.9}$$

which achieves

$$\dot{V}(t,x) = x(t)^{\mathrm{T}}(A(\rho)^{\mathrm{T}} P + P A(\rho))x(t) < 0. \tag{3.10}$$

It is more convenient to use quadratic functions, such as a parameter-dependent Lyapunov function

$$V(t,x) = x(t)^{\mathrm{T}} P(t) x(t), \tag{3.11}$$

since the uncertainty in a system may cause changes in the location of the equilibrium point. Therefore, the use of parameter-dependent Lyapunov functions is to prove stability for a range of allowable uncertainty. A parameter-dependent Lyapunov function $P(t)$ is more general than a fixed Lyapunov function, and indeed less conservative in all situations.

3.3 Stabilization

In this section, we deal with the stabilization problem for the systems subjected to uncertain time-dependent parameters. The design of controllers is proposed such that the closed-loop system is stable. Then, the design of both state feedback and dynamic output feedback controllers is investigated. The stabilization process aims to obtain a considered feedback controller that stabilizes the closed-loop system, with the main feedback schemes being state and output feedback. To prove the stability of the proposed control schemes, the concept of quadratic stability is considered and thus the uncertain system with parameter uncertainties is handled. Algorithms are provided for computing the convex optimization problem. Finally, the stabilizing controller matrices are obtained using the corresponding feasible solution of the LMIs.

3.3.1 State Feedback Control

The aim of this subsection is to present the design problem of a state feedback controller using the concept of quadratic stabilization [157]. We consider the uncertain

system with parametric uncertainties described by

$$\dot{x}(t) = A(\rho)x(t) + B(\rho)u(t), \quad t \geq 0 \tag{3.12}$$

where $x(t) \in \mathbb{R}^n$ is the state vector and $u(t) \in \mathbb{R}^m$ is the input vector. In this case, we assume that all state variables are mesurable (available). For the system in (3.12), we assume a linear feedback control law:

$$u(t) = Kx(t), \qquad K \in \mathbb{R}^{m\times n}, \tag{3.13}$$

where K is an appropriate gain matrix. Applying this controller in (3.12), a solution of the closed-loop system is therefore given by:

$$\dot{x}(t) = (A(\rho) + B(\rho)K)x(t). \tag{3.14}$$

We conclude that the state feedback controller matrix K found in this manner stabilizes the system (3.14) locally. Clearly, the chosen controller matrix K determines a dynamic behavior of the state vector $x(t)$. Then, we have the following quadratic stabilization result [159],[160].

Definition 3.3.1. *The uncertain continuous system in* (3.12) *is said to be quadratically stabilizable via linear state feedback if there exists the matrix K such that the eigenvalues of the closed-loop matrix $A + BK$ all belong to a region*

$$\mathcal{D} = \{z \in \mathbb{C} : d_0 + d_1(z + z^\star) + d_2 z z^\star < 0\}$$

of the complex plane, where d_0, d_1, $d_2 \in \mathbb{R}$ are given scalars. Typical choices are $d_0 = d_2 = 0$, $d_1 = 1$ for the left half of the complex plane (continuous-time stability) and $d_2 = -d_0 = 1$, $d_1 = 0$ for the unit disk center (discreet-time stability). Therefore we conclude that the closed-loop system is quadratically stable.

To investigate the problem of state feedback for the linear parameter-varying system (3.12) with given matrices $A(\rho)$, $B(\rho)$, and $C(\rho)$, we find the stabilizing state feedback matrix K such that all that eigenvalues of $A(\rho) + B(\rho)K$ belong to the stability region $\mathcal{D}$, and are strictly negative. Here $A(\rho)$ and $B(\rho)$ are allowed to be time-varying, and its eigenvalues are in the region $\mathcal{D}$ for all uncertainties $\rho \in R$. In view of this, the main result of this section is the following theorem.

Theorem 3.3.1. *The uncertain continuous system in* (3.12) *is said to be quadratically stable if and only if there exists a positive define matrix* $P \succ 0$ *and a matrix* L *such that*

$$A(\rho)P + PA^{\mathrm{T}}(\rho) + B(\rho)L + L^{\mathrm{T}}B^{\mathrm{T}}(\rho) \prec 0, \quad \forall \rho \in R, \tag{3.15}$$

where $P \in \mathbb{R}^{n\times n}$ *and* $L \in \mathbb{R}^{m\times n}$ *is any matrix. In the following, there exists a stabilizing control state feedback* $u(t) = Kx(t)$ *with stabilizing linear feedback gain matrix* $K = LP^{-1}$.

Proof. See [52] for a detailed proof. □

Therefore this controller stabilizes the system (3.12).

3.3.2 Output Feedback Control

In this subsection, we deal with the design of dynamic output feedback in which all state variables are not available for feedback [147]. Similar to the system in (3.12), the system is defined as

$$\begin{aligned} \dot{x}(t) &= A(\rho)x(t) + B(\rho)u(t), \\ y(t) &= Cx(t), \end{aligned} \tag{3.16}$$

where $y(t) \in \mathbb{R}^p$ is the system output. For the system (3.16) with parametric uncertainties, we propose dynamic output feedback controllers. The following dynamic output feedback controller for a continuous time model is represented:

$$\begin{aligned} \dot{\xi}(t) &= A_c\xi(t) + B_c y(t), \\ u(t) &= C_c\xi(t) + D_c y(t), \end{aligned} \tag{3.17}$$

where $\xi(t) \in \mathbb{R}^{n_c}$ is the internal state of the controller, and A_c, B_c, C_c, and D_c, are the controller matrices. All controller matrices are real constant matrices with compatible dimensions and $A_c \in \mathbb{R}^{n_c\times n_c}$. Following this, the controller is completely determined by the selection of the matrix as a compact form:

$$K = \left[\begin{array}{c|c} A_c & B_c \\ \hline C_c & D_c \end{array}\right]. \tag{3.18}$$

Our aim is to design a dynamic output feedback controller with the following structure:

$$u(t) = Ky(t). \tag{3.19}$$

We call K the dynamic controller matrix. The controller K has a fixed-structure to be determined, and its order n_c is prescribed by the user depending on design requirements. It is also worth noting that we assume the full order controller, which is the given order of the controller, and is greater or equal to the order of the actual system, which is a restrictive condition for high-order cases. For simplicity, we deal with controllers of the same order as the actual system. Then, applying the stabilizing controller (3.17) to an uncertain system (3.16) results in a closed-loop system:

$$\eta(t) = A_c\eta(t), \tag{3.20}$$

where

$$\eta(t) = \begin{bmatrix} x(t) \\ \xi(t) \end{bmatrix}. \tag{3.21}$$

We may conclude that there exists a dynamic output feedback controller in the form of (3.17) that guarantees the stability of the resulting closed-loop system (3.20). By following this line, one can show the closed-loop realization:

$$A_c(\rho) = \begin{bmatrix} A(\rho) + B(\rho)D_c(\rho)C(\rho) & B(\rho)C_c(\rho) \\ B_c(\rho)C(\rho) & A_c(\rho) \end{bmatrix}. \tag{3.22}$$

Applying the Lypunov stability theory in [289], it can be seen that the matrix $A_c(\rho)$ is asymptotically stable if and only if there exists a positive define matrix $P > 0$, $P = P^{\mathrm{T}}$ of dimension $n \times n$ such that

$$A_c^{\mathrm{T}}(\rho)P + PA_c(\rho) < 0. \tag{3.23}$$

In order to solve the dynamic controller design problem, we have the following lemma [161] and [290], which is used to present the output feedback stabilization results.

Lemma 3.3.2. *Given symmetric matrices $X \in \mathbb{R}^{n\times n}$ and $Y \in \mathbb{R}^{n\times n}$, there exist symmetric matrices $T \in \mathbb{R}^{n\times n}$ and $Z \in \mathbb{R}^{n\times n}$, and two nonsingular matrices $M \in \mathbb{R}^{n\times n}$ and $N \in \mathbb{R}^{n\times n}$. Consider the problem of finding the matrices X and Y. Suppose that the change of controller variables is implicitly described in terms of the (unknown) Lyapunov matrix P. Let matrices P and its inverse be partitioned as*

$$P = \begin{pmatrix} Y & M \\ M^T & T \end{pmatrix}, \qquad P^{-1} = \begin{pmatrix} X & N \\ N^T & Z \end{pmatrix}, \tag{3.24}$$

and, together, these satisfy $PP^{-1} = I$. The inequality is thus:

$$\begin{pmatrix} X & I \\ I & Y \end{pmatrix} \succ 0. \tag{3.25}$$

Proof. More details on the proof can be found in [147]. □

Now, using the linearization of LMIs [291], the following theorem is a consequence of the previous lemma.

Theorem 3.3.3. *Consider the uncertain system described by* (3.16)*. There exists a dynamic output state feedback controller in the form of* (3.17) *and which results in a closed-loop system* (3.20)*. The system is quadratically stable if and only if there exist matrices X, Y and continuous matrix-valued function $\hat{B}_c$ and $\hat{C}_c$ such that*

$$A(\rho)X + XA^{\mathrm{T}}(\rho) + B(\rho)\hat{C}_c(\rho) + \hat{C}_c^{\mathrm{T}}(\rho)B^{\mathrm{T}}(\rho) \prec 0, \tag{3.26a}$$

$$YA(\rho) + A^{\mathrm{T}}(\rho)Y + \hat{B}_c(\rho)C(\rho) + C^{\mathrm{T}}(\rho)\hat{B}_c^{\mathrm{T}}(\rho) \prec 0. \tag{3.26b}$$

If (3.26) *holds, then we can always find matrices X, Y, $\hat{B}_c$ and $\hat{C}_c$ that satisfy* (3.26)*, and both M and N are nonsingular. The corresponding dynamic output feedback controller in* (3.17) *can be chosen with the following parameters:*

$$\begin{aligned} A_c = M^{-1}\Big(&\hat{A}_c(\rho) - YB(\rho)C_c(\rho)N^{\mathrm{T}} - MB_c(\rho)C(\rho)X \\ &- Y\big(A(\rho) + B(\rho)D_c(\rho)C(\rho)\big)X\Big)N^{-\mathrm{T}}, \end{aligned} \tag{3.27}$$

$$B_c = M^{-1}\big(\hat{B}_c(\rho) - YB(\rho)D_c(\rho)\big), \tag{3.28}$$

$$C_c = \big(\hat{C}_c(\rho) - D_c(\rho)C(\rho)Y\big)N^{-\mathrm{T}}. \tag{3.29}$$

Proof. The proof can be found in [52]. □

Here, $\hat{A}_c$, $\hat{B}_c$ and $\hat{C}_c$ are the new controller variables which can be written as

$$\begin{aligned}\hat{A}_c &= MA_c(\rho)N^{\mathrm{T}} + MB_c(\rho)C(\rho)X + YB(\rho)C_c(\rho)N^{\mathrm{T}} \\ &\quad + Y\big(A(\rho) + B(\rho)D_c(\rho)C(\rho)\big)X, \qquad (3.30)\\ \hat{B}_c &= MB_c(\rho) + YB(\rho)D_c(\rho), \qquad (3.31)\\ \hat{C}_c &= C_c(\rho)N^T + D_c(\rho)C(\rho)X. \qquad (3.32)\end{aligned}$$

Therefore, suppose that there exist some positive define matrices $X \succ 0$, $Y \succ 0$, and the inequality in (3.25) together with (3.26) provides strict LMIs, ensuring that the system in (3.16) is quadratically stable. Finally, the dynamic output feedback problem can be solved by finding a feasible solution to the following optimization problem:

$$\begin{aligned} X &\succ 0, && (3.33a)\\ Y &\succ 0, && (3.33b)\\ A(\rho)X + XA^{\mathrm{T}}(\rho) + B(\rho)\hat{C}_c(\rho) + \hat{C}_c^{\mathrm{T}}(\rho)B^{\mathrm{T}}(\rho) &\prec 0, && (3.33c)\\ YA(\rho) + A^{\mathrm{T}}(\rho)Y + \hat{B}_c(\rho)C(\rho) + C^{\mathrm{T}}(\rho)\hat{B}_c^{\mathrm{T}}(\rho) &\prec 0, && (3.33d)\\ \begin{pmatrix} X & I \\ I & Y \end{pmatrix} &\succ 0. && (3.33e)\end{aligned}$$

In this case, M and N can be chosen to be full row rank, that is

$$MN^{\mathrm{T}} = I - XY. \qquad (3.34)$$

It is noted that the condition in (3.25) is a strict matrix inequality. To overcome this difficulty, the inequality constraint that defines the variable should be formulated such a way that the variable has a positive sign $\epsilon \succ 0$

$$\begin{pmatrix} X & \epsilon I \\ \epsilon I & Y \end{pmatrix} \succ 0. \qquad (3.35)$$

3.4 Uncertainty Analysis with Convex Programming

3.4.1 General Case of Uncertain Parameters

Let us assume that the uncertain system under consideration can be described by a state-space representation of the following form:

$$\dot{x}(t) = A(\rho)x(t) + B(\rho)u(t), \quad \text{for } t \geq 0, \tag{3.36a}$$

$$y(t) = C(\rho)x(t) + D(\rho)u(t) \tag{3.36b}$$

where $A(\rho) \in \mathbb{R}^{n\times n}$, $B(\rho) \in \mathbb{R}^{n\times m}$, $C(\rho) \in \mathbb{R}^{p\times n}$ are the system matrices. Here, the real matrices $A(\rho)$, $B(\rho)$, $C(\rho)$, and $D(\rho)$ are not precisely known but are bounded, and their unknown variations depend on time. In this case, they are assumed to belong to a convex bounded uncertainty polytope domain defined by

$$\begin{aligned}\Omega &= \Bigg\{ \big[A(\rho), B(\rho), C(\rho), D(\rho)\big] \\ &= \sum_{i=1}^{r} \rho_i \big[A_i,\ B_i,\ C_i,\ D_i\big]; \quad \sum_{i=1}^{r} \rho_i = 1; \quad \rho \geq 0 \Bigg\}.\end{aligned} \tag{3.37}$$

With this, we define the system with uncertain parameters described in state-space as

$$\dot{x} = \underbrace{\left\{ A_0 + \sum_{i=1}^{r} \rho_i A_1 \right\}}_{A(\rho)} x + \underbrace{\left\{ B_0 + \sum_{i=1}^{r} \rho_i B_1 \right\}}_{B(\rho)} u, \quad y = \underbrace{\left\{ C_0 + \sum_{i=1}^{r} \rho_i C_1 \right\}}_{C(\rho)} x, \tag{3.38}$$

where r is the number of uncertain parameters and the vector of parametric uncertainties is $\rho = (\rho_1 \dots \rho_r)^{\mathrm{T}} \in \mathcal{R} \subset \Omega$. We consider that the set $\mathcal{R}$ is a hyber-box such that

$$\mathcal{R} : [\underline{\rho}_1, \overline{\rho}_1] \times [\underline{\rho}_2, \overline{\rho}_2] \times \cdots \times [\underline{\rho}_r, \overline{\rho}_r] \tag{3.39}$$

Then, $\Omega = \{\rho : \underline{\rho}_i \leq \rho_i(t) \leq \overline{\rho}_i;\ \underline{\rho}_i, \overline{\rho}_i \in \mathbb{R};\ i = 1, \dots, r\}$ is a set of admissible uncertainties. Similarly, we only have information regarding the minimum and maximum values of parametric uncertainties, that is $\Omega = \{\rho : \rho_i \in [\underline{\rho}_i, \overline{\rho}_i]\}$, which allow us to define a collection of 2^r vertices of the admissible value of the parameter ρ. The bounds of $\underline{\rho}_i$ and $\overline{\rho}_i$ are known *a priori*, thus the uncertain parameter $\rho_i(t)$ is to be assumed to drift over time between given prior bounds, and possibly time-varying parameters.

These parameters are affected by the uncertainties in the system (possibly state and input dependent).

Remark 4. *In this chapter, we assumed that uncertain parameters are time-varying. $A(\rho)$, $B(\rho)$, and $C(\rho)$ may be converted into constant matrices by the bounded values of uncertain parameters as $\underline{\rho}_i \leq \rho_i(t) \leq \overline{\rho}_i$. On the other hand, the bounded time derivatives or variations on the uncertain parameters are neglected.*

When the time-varying parameter uncertainties appear in the system, the negativity of the real part of the eigenvalues may no longer be sufficient to guarantee the Hurwitz stability criterion. Hence, it is known that the stability analysis succeeds using the Lyapunov methods, which leads to the quadratic stability that implies the exponential stability of the system for all allowable parameter bounds.

3.4.2 Basic Computations

The purpose of this subsection is to present the operating regions of the power system model. Recall that the highly nonlinear equation of the terminal voltage is described by

$$\dot{V}_{ti}(t) = h_{1i}(t)\dot{\delta}(t) + h_{2i}(t)u_{fi} \quad i \in \mathcal{G}. \tag{3.40}$$

Here, the notation ρ is replaced by h when no confusion arises. It can be seen that the dynamic state equation of terminal voltage is modeled in terms of the uncertain parameters (h_{1i}, h_{2i}), where the solution for this problem is provided under the assumption that the pairs (h_{1i}, h_{2i}) can stabilize the system. So, these chosen parameters vary from one operating point to another, thus the system as a whole can be stabilized. For that reason, we first introduce the rotor angle, electrical power, and terminal voltage constraints

$$\delta_i \in \left[\underline{\delta_i}, \overline{\delta_i}\right], \tag{3.41a}$$

$$P_{ei} \in \left[\underline{P}_{ei}, \overline{P}_{ei}\right], \tag{3.41b}$$

$$V_{ti} \in \left[\underline{V}_{ti}, \overline{V}_{ti}\right]. \tag{3.41c}$$

In our analysis, the operating range of the electrical power outputs (p.u) and the terminal voltages (p.u) for all generators can be chosen as

$$0.05 \leq P_{ei}(t) \leq 1.2, \tag{3.42a}$$

$$0.95 \leq V_{ti}(t) \leq 1.05. \tag{3.42b}$$

Following this, the operating range of rotor angle (degree) is assumed to be suitable between

$$40^{\circ} \leq \delta_i(t) \leq 130^{\circ}. \tag{3.42c}$$

It is worth mentioning here that the large rotor interval and increasing number of uncertain parameters may cause significant computational cost. Consequently, to calculate the stabilizing solution Eq. (3.40), one can restrict to the analysis using these operating points.

Remark 5. *The operating points between* $10^{\circ} < \delta_i(t) < 40^{\circ}$ *and* $130^{\circ} < \delta_i(t) < 170^{\circ}$ *can be accepted as the extreme operating intervals for a synchronous machine and are omitted for this work.*

The main difficulty here is to measure the uncertain parameters online. Thus, we need *a priori* knowledge of these parameters regarding the bounds of uncertain parameter vectors $(\underline{h}_{1i}, \overline{h}_{1i}, \underline{h}_{2i}, \overline{h}_{2i})$ for every $i \in \mathcal{G}$. To do this, defining the certain operating range of $(\delta_i(t),\, P_{ei}(t),\, V_{ti}(t))$ as shown above and assuming the measurement of $(\delta_i(t),\, P_{ei}(t),\, V_{ti}(t))$, we apply a gridding technique to find all grid points between these intervals via incremental value 0.1 for $P_{ei}(t)$, $V_{ti}(t)$, and 0.5 for $\delta_i(t)$. See our previous work for further detail [292]. Therefore, we can grid the uncertain parameters along these points. Furthermore, these time-varying parameters of the system are specified separately using these grid points as

$$h_{1i}(t) = \underbrace{-\frac{P_e^2(t)X_s^2\cot\delta(t)}{V_t(t)V_s^2\sin^2\delta(t)}}_{h_{11}} \underbrace{-\frac{P_e(t)X_d'X_s}{V_t(t)X_{ds}'\sin^2\delta(t)}}_{h_{12}}$$
$$\underbrace{-\frac{X_{di}'^2V_s^2\sin 2\delta(t)}{2V_{ti}(t)X_{ds}'^2}}_{h_{13}} + \underbrace{\frac{X_{qi}'^2V_s^2\sin 2\delta(t)}{2V_{ti}(t)X_{ds}'^2}}_{h_{14}}, \tag{3.43a}$$

$$h_{2i}(t) = \underbrace{\frac{P_e(t)X_s^2}{V_t(t)V_s^2\sin^2\delta(t)}}_{h_{21}} + \underbrace{\frac{X_d'X_s\cot\delta(t)}{V_t(t)X_{ds}'}}_{h_{22}}. \tag{3.43b}$$

As a consequence, we get

$$h_{\Sigma 1i} = h_{11i} + h_{12i} + h_{13i} + h_{14i}, \tag{3.44a}$$

$$h_{\Sigma 2i} = h_{21i} + h_{22i}. \tag{3.44b}$$

Then, using the MATLAB `min` and `max` commands, we finally obtain the upper and lower operating ranges of uncertain parameters for the given the operating ranges:

$$\underline{h}_1 = \texttt{min}(\texttt{min}(\texttt{min}(h_{\Sigma 1i}))), \tag{3.45a}$$

$$\overline{h}_1 = \texttt{max}(\texttt{max}(\texttt{max}(h_{\Sigma 1i}))), \tag{3.45b}$$

$$\underline{h}_2 = \texttt{min}(\texttt{min}(\texttt{min}(h_{\Sigma 2i}))), \tag{3.45c}$$

$$\overline{h}_2 = \texttt{max}(\texttt{max}(\texttt{max}(h_{\Sigma 2i}))). \tag{3.45d}$$

The region of the parameter's space is perceived as the upper and lower operating range of uncertain parameters in the dynamic state equation (3.40), and also the power system model.

We conclude that the state (3.40) is assumed to be available for control design. In addition, the physical power plant to be controlled is admitted to have an unknown nonlinearity from the given uncertain parameters, which may be known imprecisely. For our problem, for the uncertain parameters $h_{1i}(t)$ and $h_{2i}(t)$ with the allowable intervals $(\underline{h}_{1i}, \overline{h}_{1i}, \underline{h}_2, \overline{h}_{2i})$ such that for all h_{1i} and h_{2i} that satisfy $\underline{h}_{1i} < h_{1i}(t) < \overline{h}_{1i}$ and $\underline{h}_{2i} < h_{2i}(t) < \overline{h}_{2i}$, the system is stable. We determine bounds on uncertainty ranges where the power system remains in stability regions, then we construct a feasible solution to a set of LMIs that guarantees quadratic stability of the system

for the time-varying parameters of the suggested feedbacks. At this point, one may guarantee that all possible trajectories of the power system models are bounded. The associated algorithms for the constructive treatment of the controller design problem are also presented.

3.4.3 Case Study: 39-Bus System

Throughout this section, we use the IEEE 39-bus test system to illustrate decentralized voltage control with the state feedback and output controllers. We assumed that the operating ranges in (3.42) are the same for all generators. To obtain the synchronous machine measurements, the single-line diagram of a 39-bus system is given in Fig. 3.1. The voltage magnitudes and phase angles can be calculated using power-flow analysis [293],[284]. The rest of the system parameters can be found in [74].

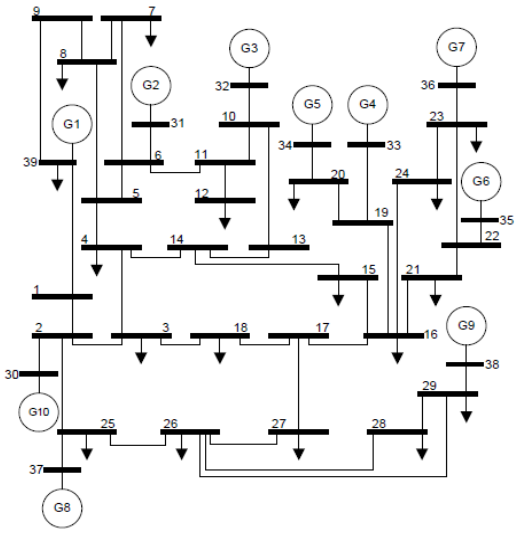

Figure 3.1: Single-line diagram of the 39-bus system

The inertia coefficients, the damping constants, initial voltage magnitude, and the angle of the 39-bus test system are listed in Table 3.1.

Table 3.1: The list of the generators data

Bus	Gen	M	D	V (pu)	θ (deg)
30	G10	4	5	1.050	−7.37
31	G2	3	4	0.982	0.00
32	G3	2.5	4	0.984	−0.18
33	G4	4	6	0.997	−0.19
34	G5	2	3.5	1.012	−1.63
35	G6	3.5	3	1.049	1.77
36	G7	3	7.5	1.064	4.46
37	G8	2.5	4	1.028	−1.58
38	G9	2	6.5	1.027	3.89
39	G1	6	5	1.030	−14.53

Taking the definitions of $h_{1i}(t)$ and $h_{2i}(t)$ in (3.43) and (3.44) into account, we define the uncertain parameters of $h_{1i}(t)$ and $h_{2i}(t)$ that are dependent on the region of the parameter space. In doing so, based on the knowledge of these parameter values, we aim to implement our controller design. Therefore, we can show the resulting values for the allowable uncertainty range of these parameters. In Table 3.2, these values are given. These parameters are not known exactly, but their instantaneous values are only available for measurements of time. The power system models have continuous dependence on these parameters, and are uniformly bounded for the uncertainty interval of these time-varying parameters.

Table 3.2: The uncertainity intervals for the model

Bus	Gen	$\underline{h}_1$	$\overline{h}_1$	$\underline{h}_2$	$\overline{h}_2$
30	G10	1.0142	1.1464	0.0101	0.0116
31	G2	0.9180	1.0851	0.0266	0.0330
32	G3	0.2614	0.3469	0.0221	0.0270
33	G4	2.1882	2.4713	0.0201	0.0246
34	G5	0.0287	0.1506	0.0438	0.0564
35	G6	0.3635	0.4470	0.0176	0.0207
36	G7	2.5375	2.8627	0.0222	0.0271
37	G8	0.2939	0.3805	0.0214	0.0257
38	G9	−0.0464	0.0118	0.0223	0.0270
39	G1	−0.0083	−0.0003	0.0032	0.0036

3.5 Main Results

In preparing the solutions for for the design of a decentralized structure, each controller utilizes its own local measurement only, and each control region utilizes measurements for its own utility only. As indicated above, we first determine operating conditions to guarantee the stability region in a given parameter space. The voltage controllers allow us to regulate the voltage (and frequency) with complete *a priori* knowledge of all parameters participating in the dynamic representation of the considered models. The design of the controller is not prescribed since it is to be found during the control process. These controllers are also analyzed for power system models that include parametric uncertainties in the the system matrix and input matrix. It is worth pointing out that the input matrix is uncertain, and all uncertainties in the system are also bounded and thus restrict our consideration to operating ranges. The stability is proven for a known range of uncertain parameters that allow us to use online information which occurs in the control process.

The main objective of this section is to find stabilizing state feedback and output feedback controllers for the power system. To do this, the quadratic stability for the voltage regulation problem of synchronous machines is proposed. This process corresponds to the decentralized solution of the convex optimization problem at each allowable interval of the system. If the solutions are feasible, then the desired stabilizing controllers that are able to operate online are constructed. Using the state and output feedback controls, we propose to obtain all stabilizing gain matrices via LMIs and encourage numerical results. The stabilizing controllers are stable and stabilize the power system. Finally, this leads us to determine whether the power system is stable for the allowable intervals of uncertain parameters without explicitly tracking how the uncertainty changes the location of the equilibrium point. Furthermore, the numerical results are performed using the YALMIP [294] and Matlab R2015b running on an Intel i3 Core CPU(@2.50Ghz) with 8 GB memory. All solutions are also given in terms of LMIs. We use version 1.3 of Sedumi to solve LMIs problems [53].

3.5.1 Solving the State Feedback Problem

In this subsection, we consider a state feedback controller design for the decentralized voltage control problem. A desired state feedback controller is constructed by solving parameter uncertainties in the proposed power system model. Thus, the quadratic stabilization problem of the power system is solved under the assumption that a full state vector is available for measurements. The state feedback controllers are designed such that the closed-loop system is asymptotically stable.

Suppose that we have two synchronous machine states and a control input, that is, $(\omega_i(t), V_{ti}(t))$ and $u_{fi}(t)$. The power system model with parametric (polytopic type) uncertainties is described:

$$\begin{bmatrix} \dot{\omega}_i(t) \\ \dot{V}_{ti}(t) \end{bmatrix} = \begin{bmatrix} -\lambda_i & 0 \\ h_{1i}(t) & 0 \end{bmatrix} \begin{bmatrix} \omega(t) \\ V_t(t) \end{bmatrix} + \begin{bmatrix} 0 \\ h_{2i}(t) \end{bmatrix} u_f(t) \quad i \in \mathcal{G}, \tag{3.46}$$

where

$$A_i(\rho) = \begin{bmatrix} -\lambda_i & 0 \\ h_{1i}(t) & 0 \end{bmatrix}, \quad B_i(\rho) = \begin{bmatrix} 0 \\ h_{2i}(t) \end{bmatrix}. \tag{3.47}$$

Here, $\lambda_i = D_i/M_i$ is a constant term. We assume that both frequency and terminal voltage are measurable for each generator. Throughout this chapter, the matrices $A_i(\rho)$ and $B_i(\rho)$ may be linearly parametrized in ρ, which is not precisely known but assumed to be constant.

In order to build up the given matrices (3.47), we need to evaluate the design parameters (3.45) that are formed by the known bounds. The matrices describing the system (3.46) are modeled around the collection of 2^r known bounds chosen in the operating range of the system considered. Consequently, the bound matrices are given in the following forms:

$$A_i^1 = \begin{bmatrix} -\lambda_i & 0 \\ \underline{h}_{1i} & 0 \end{bmatrix}, \quad B_i^1 = \begin{bmatrix} 0 \\ \underline{h}_{2i} \end{bmatrix} \quad i \in \mathcal{G}, \tag{3.48a}$$

$$A_i^2 = \begin{bmatrix} -\lambda_i & 0 \\ \underline{h}_{1i} & 0 \end{bmatrix}, \quad B_i^2 = \begin{bmatrix} 0 \\ \overline{h}_{2i} \end{bmatrix} \quad i \in \mathcal{G}, \tag{3.48b}$$

$$A_i^3 = \begin{bmatrix} -\lambda_i & 0 \\ \overline{h}_{1i} & 0 \end{bmatrix}, \quad B_i^3 = \begin{bmatrix} 0 \\ \underline{h}_{2i} \end{bmatrix} \quad i \in \mathcal{G}, \tag{3.48c}$$

$$A_i^4 = \begin{bmatrix} -\lambda_i & 0 \\ \overline{h}_{1i} & 0 \end{bmatrix}, \quad B_i^4 = \begin{bmatrix} 0 \\ \overline{h}_{2i} \end{bmatrix} \quad i \in \mathcal{G}. \tag{3.48d}$$

Next, we present the numerical results to illustrate the application of the proposed method in Theorem 3.3.1. The detailed solution is only for the 10th generator (30th Bus) of the test system. Based on the Theorem 3.3.1, the LMIs are solved such that

$$\begin{aligned} P &\succ 0, \\ A(\rho_{(k)})P + PA^{\mathrm{T}}(\rho_{(k)}) + B(\rho_{(k)})L + L^{\mathrm{T}}B^{\mathrm{T}}(\rho_{(k)}) &\prec 0 \end{aligned} \tag{3.49}$$

with $k = 1, \ldots, 2^r$. The resulting inequality (3.49) for generators can be found strictly feasible in the given bounds in (3.42). Therefore, the positive define symmetric solution with a matrix L can be found using MATLAB output in short precision as follows:

$$P = \begin{bmatrix} 0.4540 & -0.0042 \\ -0.0042 & 1.0001 \end{bmatrix} \tag{3.50}$$

with eigenvalues [0.4539 1.0001], and

$$L = \begin{bmatrix} -45.6338 & -45.7009 \end{bmatrix}. \tag{3.51}$$

The solution of state feedback controller is

$$u(t) = \begin{bmatrix} -100.9543 & -46.1238 \end{bmatrix} x(t), \tag{3.52}$$

such that the closed-loop system is stable, where

$$K = \begin{bmatrix} -100.9543 & -46.1238 \end{bmatrix}. \tag{3.53}$$

Therefore, by Theorem 3.3.1, we conclude that the system is quadratically stabilizable with a stabilizing state feedback. The resulting SDP relaxations of the generators are presented in Table 3.3. We guarantee that all numerical solutions are strictly feasible.

Table 3.3: The outcome of the SDP relaxations of the system

Generators	$40^\circ < \delta_i(t) < 130^\circ$
G1,...,G10	strict feasible

The computations of the state feedback controller for the rest of generators in the system are summarized in Table 3.4.

Table 3.4: Numerical results for all generators

Gen	Eigenvalues	Gain matrix
G1	0.6522, 1.0000	[1.2837 − 147.308]
G2	0.4275, 1.0005	[−34.9433 − 16.8236]
G3	0.3622, 1.0000	[−12.9185 − 20.3722]
G4	0.3812, 1.0012	[−108.227 − 22.6270]
G5	0.3333, 1.0000	[−1.9212 − 9.9787]
G6	0.6358, 1.0001	[−21.4955 − 26.1004]
G7	0.2370, 1.0009	[−117.165 − 20.4981]
G8	0.3622, 1.0000	[−14.8019 − 21.2262]
G9	0.1852, 0.9999	[0.7675 − 20.2743]

On the other hand, we also demonstrate the results of local area measurements of the test system. For this system, areas are randomly chosen between the closest generation units. We now present the solution of local area measuremets, including generator unit G8, G9, and G10. With these generation units, we compute the matrix P using LMI optimization

$$P = \begin{bmatrix} 0.2560 & -0.1438 \\ -0.1438 & 1.0599 \end{bmatrix} \tag{3.54}$$

with eigenvalues [0.2311 1.0849], and the matrix L

$$L = \begin{bmatrix} -21.1078 & -22.3804 \end{bmatrix}. \tag{3.55}$$

The gain matrix is described as:

$$K = \begin{bmatrix} -102.0795 & -34.9657 \end{bmatrix}. \tag{3.56}$$

The strictly feasible solutions are shown for each local area in Table 3.5.

Table 3.5: The resuts for local areas

Local Areas	Eigenvalues	Gain matrix
G2, G3	0.3643, 1.0001	$[-25.8392 \quad -18.6039]$
G4, G5	0.2518, 1.0572	$[-54.0072 \quad -18.3039]$
G6, G7	0.2829, 1.0505	$[-21.3103 \quad -29.0557]$

The local areas can be seen in Fig. 3.2.

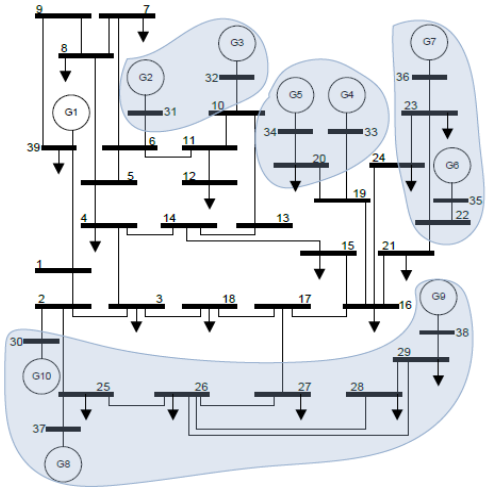

Figure 3.2: Generators in local areas

3.5.2 Solving the Output Feedback Problem

In this section, the decentralized voltage control problem is solved under the assumption that not all states are measurable. In the same way as the state feedback problem, the parametric uncertainties in the power system model are represented by the known range of uncertain parameters. Again, we solve a convex LMI problem for the output feedback problem. We consider a different method to solve the model

that does not rely on the bound matrices in (3.48). Instead, we again restrict our solutions to the known range of uncertain parameters (3.45) for the operating points of the system (3.42), and solve the corresponding output feedback problem using the linear paremeter varying (LPV) stabilization [294]. Then the numerical procedures for designing the output feedback gain matrix are introduced. The feedback gain of the desired output feedback controller is obtained with the quadratic stabilization of the power system. Numerical results on the test system clearly demonstrate the effectiveness of the suggested procedure with the proposed PSS.

As we mentioned before, a PSS is designed based on the power system model (3.46). It is assumed that the proposed PSS is linear and decentralized. Its dynamics are based on local interactions. We first write the additional dynamical equations of the power system. Here, the additional states of the PSS are assumed to be unmeasurable states. By introducing the unmeasurable states, we consider the extended model with the following state-space representation:

$$\begin{bmatrix} \dot{\omega}_i(t) \\ \dot{V}_{ti}(t) \\ \dot{\xi}_1 \\ \dot{\xi}_2 \\ \dot{\xi}_3 \end{bmatrix} = \begin{bmatrix} -\lambda_i & 0 & 0 & 0 & 0 \\ K_i * h_{1i}(t) & 0 & 1 & 0 & 0 \\ \beta_{2i} & 0 & -c_{2i} & 1 & 0 \\ \beta_{1i} & 0 & -c_{1i} & 0 & 1 \\ \beta_{0i} & 0 & -c_{0i} & 0 & 0 \end{bmatrix} \begin{bmatrix} \omega(t) \\ V_{ti}(t) \\ \xi_{1i} \\ \xi_{2i} \\ \xi_{3i} \end{bmatrix} + \begin{bmatrix} 0 \\ h_{2i}(t) \\ 0 \\ 0 \\ 0 \end{bmatrix} u_{fi}(t) \quad i \in \mathcal{G}, \quad (3.57)$$

where

$$A_i(\rho) = \begin{bmatrix} -\lambda_i & 0 & 0 & 0 & 0 \\ K_i * h_{1i}(t) & 0 & 1 & 0 & 0 \\ \beta_{2i} & 0 & -c_{2i} & 1 & 0 \\ \beta_{1i} & 0 & -c_{1i} & 0 & 1 \\ \beta_{0i} & 0 & -c_{0i} & 0 & 0 \end{bmatrix}, \quad B_i(\rho) = \begin{bmatrix} 0 \\ h_{2i}(t) \\ 0 \\ 0 \\ 0 \end{bmatrix}. \quad (3.58)$$

In the following our design, the power system model has two directly measurable states (ω_i, V_{ti}) and three observable states $(\xi_{1i}, \xi_{2i}, \xi_{3i})$. Therefore, we obtain a fifth-order system. In order to simplify the notations, the constant terms $\{c_{2i}, c_{1i}, c_{0i}\}$ are replaced by the Eqs. (2.69), (2.70), and (2.71), respectively. Then, the output matrix

of the system is

$$C = \begin{bmatrix} 1 & 0 & 0 & 0 & 0 \\ 0 & 1 & 0 & 0 & 0 \\ 0 & 0 & 1 & 0 & 0 \end{bmatrix}. \tag{3.59}$$

Clearly, from the above discussion, $\{c_{2i}, c_{1i}, c_{0i}\}$ is assumed to be constant for our design. They can be calculated using the time constants $\{T_{1i}, T_{2i}, T_{3i}, T_{4i}, T_{wi}\}$ of the PSS. On the other hand, the following parameters $\{\beta_{2i}, \beta_{1i}, \beta_{0i}\}$ depend on the system behaviors at time t, so we do not mention them explicitly. These parameters need to be optimized. We can perform the optimization method for our controller design as follows. In the case of two uncertain parameters, such as in the model (3.57), we rewrite the four points $(h_1(t), h_2(t)) = (\underline{h}_1, \overline{h}_1, \underline{h}_2, \overline{h}_2)$ which denote the bounds on the uncertainty range. It is clear that these parameters depend on the uncertain parameters as:

$$\beta_{2i}(h_{1i}(t), h_{2i}(t)) > 0,$$
$$\beta_{1i}(h_{1i}(t), h_{2i}(t)) > 0,$$
$$\beta_{0i}(h_{1i}(t), h_{2i}(t)) > 0.$$

These parameters are then optimized while the other coefficients $\{c_{2i}, c_{1i}, c_{0i}\}$ are kept constant. The optimization problem with respect to the uncertain parameters h_{1i} and h_{2i} is implemented as a computation procedure to find the design parameters of PSS. To find the design parameters $\{\beta_{2i}, \beta_{1i}, \beta_{0i}\}$, we implement a bisection algorithm into the convex program. Then, we obtain the optimal values of $\beta_{2i}(h_{1i}(t), h_{2i}(t))$, $\beta_{1i}(h_{1i}(t), h_{2i}(t))$, $\beta_{0i}(h_{1i}(t), h_{2i}(t))$. Following this procedure, these parameters multiply by a scalar coefficient, then we use the bisection algorithm to find the maximum value of parameters $\{\beta_{2i}, \beta_{1i}, \beta_{0i}\}$ for which the solution is feasible between the allowable intervals of the parameters h_{1i} and h_{2i}.

Remark 6. *β_{0i} has a small value, and is assumed to be zero for our calculations. To integrate the parameter β_{0i} into the algorithm increases the iteration number, thus computation time.*

Compared to the state feedback problem, we suppose numerical results for the 10th generator (30th Bus) of the test system. The parameters of the PSS are tabulated in Table 3.6.

Table 3.6: Table of PSS parameters

T_1	T_2	T_3	T_4	T_w	K_{PSS}
1.5	4	0.07	4.75	7.5	30

In view of Theorem 3.3.3, we first write the our problem for $k = 2^r$ vertices in (3.33)

$$X \succ 0, \tag{3.60a}$$

$$Y \succ 0, \tag{3.60b}$$

$$A(\rho_{(k)})X + XA^{\mathrm{T}}(\rho_{(k)}) + B(\rho_{(k)})\hat{C}_c(\rho_{(k)}) + \hat{C}_c^{\mathrm{T}}(\rho_{(k)})B^{\mathrm{T}}(\rho_{(k)}) \prec 0, \tag{3.60c}$$

$$YA(\rho_{(k)}) + A^{\mathrm{T}}(\rho_{(k)})Y + \hat{B}_c(\rho_{(k)})C(\rho) + C^{\mathrm{T}}(\rho_{(k)})\hat{B}_c^{\mathrm{T}}(\rho_{(k)}) \prec 0, \tag{3.60d}$$

$$\begin{pmatrix} X & I \\ I & Y \end{pmatrix} \succ 0. \tag{3.60e}$$

As a result of solving the problem (3.60), it is found that the LMIs in (3.60) are feasible, and a set of solutions is obtained as follows:

$$X = \begin{bmatrix} 6.1051 & -0.0546 & -0.0623 & -0.1073 & -0.0069 \\ -0.0546 & 13.6227 & -5.6861 & -0.9654 & -0.3024 \\ -0.0623 & -5.6861 & 25.0461 & 3.0841 & 10.0828 \\ -0.1073 & -0.9654 & 3.0841 & 12.9254 & 1.5506 \\ -0.0069 & -0.3024 & 10.0828 & 1.5506 & 20.9996 \end{bmatrix}, \tag{3.61}$$

with eigenvalues $\{6.1021 \;\; 9.3415 \;\; 12.3014 \;\; 16.0394 \;\; 34.9145\}$;

$$Y = \begin{bmatrix} 11.5944 & -0.0423 & 0.1107 & -0.0157 & -0.0106 \\ -0.0423 & 11.1418 & -1.0180 & 0.3890 & -0.1754 \\ 0.1107 & -1.0180 & 21.7098 & -4.1384 & -7.2590 \\ -0.0157 & 0.3890 & -4.1384 & 8.9233 & -4.4814 \\ -0.0106 & -0.1754 & -7.2590 & -4.4814 & 18.7323 \end{bmatrix} \tag{3.62}$$

with eigenvalues $\{4.4683 \;\; 11.0008 \;\; 11.5949 \;\; 17.3680 \;\; 27.6696\}$, and

$$\hat{B}_c = \begin{bmatrix} 6.1678 & -0.0000 & -0.0000 \\ -1.4345 & -5.4748 & 0.0000 \\ -0.0191 & -11.6568 & 7.5711 \\ -0.2334 & 1.0109 & -23.7374 \\ 0.0372 & -0.3968 & -0.1970 \end{bmatrix}, \tag{3.63}$$

$$\hat{C}_c = \begin{bmatrix} -77.9348 & -162.9619 & -332.2961 & 141.7255 & -927.6218 \end{bmatrix}. \tag{3.64}$$

To this end, we now investigate the controller matrices $\mathcal{A}_c$, $\mathcal{B}_c$, $\mathcal{C}_c$, and $\mathcal{D}_c$. We only consider the case $\mathcal{D}_c = 0$ to design the output feedback controller. Then,

$$\mathcal{B}_c = \hat{B}_c M^{-1}, \tag{3.65}$$

$$\mathcal{C}_c = \hat{C}_c N^{\mathrm{T}}, \tag{3.66}$$

$$\mathcal{A}_c(\rho) = -M^{-1}\left(A^{\mathrm{T}}(\rho) + YA(\rho)X + YB(\rho)C_c N^{\mathrm{T}} + MB_c CX\right) N^{\mathrm{T}}. \tag{3.67}$$

Therefore, we can choose a nonsingular matrix $N > 0$, which is actually taken to be a constant matrix. One can choose this matrix with appropriate weighting such as $N = 100I_5$, then $M = (I_5 - XY)\, N^{-\mathrm{T}}$. Hence, we first determine all solutions of (3.65),(3.66),(3.67):

$$\mathcal{B}_c = \begin{bmatrix} -8.8159 & 0.0771 & 0.4710 \\ 1.0533 & 6.1008 & 0.8791 \\ 0.3080 & 4.2327 & -2.1659 \\ 0.2436 & 3.0383 & 27.9704 \\ -0.0719 & -0.0315 & 4.4928 \end{bmatrix}, \tag{3.68}$$

$$\mathcal{C}_c = \begin{bmatrix} -0.7793 & -1.6296 & -3.3230 & 1.4173 & -9.2762 \end{bmatrix}. \tag{3.69}$$

To obtain the matrix $\mathcal{A}_c(\rho)$ is a more complicated process. We explain the ideas below.

Bisection Algorithm

Basically, the model (3.57) is represented by the scalar uncertainties that are affine functions with respect to the parameter-varying state transition matrix $A(\rho)$ and the

parameter-varying input matrix $B(\rho)$. In this case, we pretend that measurements of all states are not available to the controller, especially the states of the power system stabilizer. Clearly, the unknown design parameters of $\{\beta_{2i}, \beta_{1i}\}$ make the system more uncertain. It is now necessary to resolve the voltage regulation problem to obtain the PSS design parameters. Instead of tuning the stabilizer output limits, we alternatively use a bisection algorithm to calculate the maximum values of the PSS parameters $\{\beta_{2i}, \beta_{1i}\}$. The full parameterized matrix $A(\rho)$ and $B(\rho)$ seems to be

$$A(\rho) = \begin{bmatrix} \star & 0 & 0 & 0 & 0 \\ \rho & 0 & \star & 0 & 0 \\ \tau * \beta_{2i} & 0 & \star & \star & 0 \\ \tau * \beta_{1i} & 0 & \star & 0 & \star \\ 0 & 0 & \star & 0 & 0 \end{bmatrix}, \qquad B(\rho) = \begin{bmatrix} 0 \\ \rho \\ 0 \\ 0 \\ 0 \end{bmatrix}, \tag{3.70}$$

where the sign $(\star)$ represents the constant terms and τ is an unknown coefficient. As already mentioned above, we propose a convex optimization problem here. The bounded uncertain parameter(s) ρ leads to a quasi linear parameter varying representation of system (3.70) with the unknown coefficient τ acting with an objective function.

Finally, the optimization algorithm which uses the bisection procedure consists of some steps [294]. Firstly, the optimization process finds a lower bound on optimal τ, which means that any feasible τ that can be computed. Then, an upper bound on optimal τ is obtained, and the lower bound is incremented until feasibility of the iterates is maintained. In other words, the process is continued until an infeasible solution is obtained for the fixed τ. When this is the case, the τ value between lower and upper bounds is checked. If it is feasible, the lower bound is updated; otherwise, it is not, and the upper bound is updated. This process is then repeated until the bounds are sufficiently close to each other. In summary, we impose strict uncertain parameter constraints on the model and solve the associated convex feasibility problem. These uncertain parameters depend on the unknown coefficient τ on the system. If a solution exists, we find values for the scalar decision coefficient τ which satisfies the allowable parameter(s) uncertainty.

Using 3.2, we recall that the allowable intervals of two uncertain parameters are

$$1.0142 \leq h_1(t) \leq 1.1464, \tag{3.71}$$

$$0.0101 \leq h_2(t) \leq 0.0116. \tag{3.72}$$

For these intervals, $\beta_1 = 11.7609$ and $\beta_2 = 11.7814$ for the 10th generator (30th Bus) of the 39-Bus system. Neglecting the parameter β_{0i}, the solution of the rest of generators are shown in Table 3.7.

Table 3.7: The solutions of PSS design parameters

Gen	β_2	β_1
G1	60.7768	11.2633
G2	5.3825	5.2831
G3	5.4786	5.3664
G4	5.4439	5.4439
G5	5.5382	5.5272
G6	40.9422	10.4563
G7	2.3557	5.7349
G8	5.4755	5.4755
G9	5.9358	5.7430

The optimized values for couples (β_2, β_1) of each generation unit are the maximum values for which the constraints are feasible. The solutions are computed by using YALMIP with Sedumi as its computational engine to solve the problem.

On the Matrix $\mathcal{A}_c$

As we mentioned before, it is not easy to see the matrix $\mathcal{A}_c(\rho)$ immediately, because the matrix $\mathcal{A}_c(\rho)$ consists of the system matrix $A(\rho)$ and the input matrix $B(\rho)$ and it is linearly parameterized in the uncertainty, ρ is constrained to a polytope. Although their bounded values are known, the controller is obtained online or known in advance. In that case, the worst time-varying parameter realization is performed and the controller matrix $\mathcal{A}_c(\rho)$ can be computed. In addition, the matrices $A(\rho)$ and $B(\rho)$ can

be calculated for the normalized values of uncertain parameters, and the controller matrix $\mathcal{A}_c(\rho)$ is then obtained. We calculate the worst-case infinity norm of the matrix $A(\rho)$. Nevertheless, maximizing the norm of a vector over a polytope is an NP-hard optimization problem. However, we integrate an algorithm into our main program to solve this problem. According to this algorithm, the infinity norm of a matrix can be rewritten using the largest 1-norm of the rows. This needs to be composed of every row, therefore the worst-case 1-norm of each row is computed. As we will see in the sequel, the computation of worst-case 1-norm is a very difficult task. The algorithm used to calculate the worst-case 1-norm numerically is outlined in [294]. We again define a scalar decision coefficient τ. The algorithm computes the worst-case τ over the uncertain parameter(s) ρ. According to this algorithm, we describe a matrix of size $2^n \times n$ that consists of all possible combinations of summing up the elements in a row dealing $+1$ and -1. Then we take into account all upper-bound constraints for the explicit representation of the 1-norm for all rows. We also use the bounds in (3.71) to solve the problem. Doing this, the worst-case upper bound is minimized. Our focus here is on upper bounds obtained using the scalar decision coefficient σ.

In addition, we can also determine a shift of the eigenvalues of $A(\rho)$ when the worst case infinity norm is minimized. Again, we define a scalar decision coefficient ς. Introducing this unknown coefficient, one can rewrite it in the form

$$A(\rho) = A(\rho) + \varsigma I_5 \tag{3.73}$$

The solutions are obtained by using the external solver FMINCON via YALMIP. We thus have the following results for each generator.

Table 3.8: The solutions of coefficients τ, ς, $\hat{\tau}$

Bus	Gen	τ	ς	$\hat{\tau}$
G30	G10	1.5939	0.2019	1.3920
G31	G2	1.5939	0.2070	1.3869
G32	G3	1.6000	0.2430	1.3570
G33	G4	1.5939	0.0921	1.8018
G34	G5	1.7500	0.3180	1.4320
G35	G6	1.5939	0.2399	1.3540
G36	G7	2.5000	0.3127	1.9873
G37	G8	1.6000	0.2430	1.3570
G38	G9	3.2500	1.0680	2.1820
G39	G1	1.5939	0.2399	1.3540

Here, the obtained coefficients τ, ς, and $\hat{\tau}$ are the worst-case upper bound, a shift of the eigenvalues of $A(\rho)$ occurs, and the current value of $\hat{\tau}$ is minimized.

3.6 Conclusion

A first contribution of this chapter is the methodology we suggested for solving the voltage regulation problem. The power system models have uncertain time-varying parameters. Considering the terminal voltage and frequency as the state variables, the power system model is represented as the stabilizing controller problem using a decentralized calculation procedure. In addition, the model used in previous works is slightly modified to measure only the terminal voltage and frequency. The solutions to the voltage regulation problem are then obtained by the widely acceptable (and secure) operating range of the power system. The control action takes into account the known range of unknown uncertainties to determine a set of feasible solutions to the optimization problem. In this case, we use a manual implementation, which means that coefficient matrices are formed using upper and lower intervals of the system. The voltage controller consists of a closed-loop full-state measurement structure, and the quadratic stability of the closed loop is thus analyzed. The resulting

optimization problem is solved by using LMIs, and strictly feasible solutions are obtained. Therefore, quadratic stability is guaranteed for the uncertainty interval for the power system. For the power system model, the system remains quadratically stable for parameters in the allowable uncertainty range. We illustrate the results through single generating units and the units in local areas. From the numerical results, we notice that the controller is based on assumptions of the operating range of the power system. We mainly present the Lyapunov stability analysis in this chapter.

A second contribution of this chapter is to propose an appropriate model (3.57) describing the power system. When such a model is considered, the power system adapts a traditional controller such as a power system stabilizer. The model used to solve the state feedback problem is enhanced with PSS states to solve the voltage regulation problems with respect to the case of partial knowledge of state variables. Therefore, the resulting optimization problem is called a dynamic output feedback problem. The enhanced model is intended to be an exact representation of frequency and terminal voltage, which will allow us to cope with time-varying parameter uncertainties, as well as the unknown design parameters of a PSS. In fact, it is assumed that the dynamics of the enhanced model are corrupted by uncertain parameters with the PSS design parameters. With the aim of Theorem 3.3.3, we obtain quadratically stabilizing output feedback controller. Then we compute the feasibility of the problem (3.60) and find the controller matrices. Another contribution of this section is the determination of the PSS parameters in which the uncertain parameters guarantee quadratic stability for the allowable uncertainty range. In order to achieve this objective, we use the bisection procedure to find the maximum value of the unknown PSS design parameters in the model. In the section that follows, we introduce the analysis of the worst-case norm for the matrices, including time-varying parameter uncertainties. Finally, we calculate a shift of the eigenvalues of the system matrix $A(\rho)$, and all results for the test system are clearly reported.

Chapter 4

Observer-Based Control Using Contraction Theory

4.1 Introduction

In this chapter, we discuss an observer-based control methodology for the stabilization of power systems. We use a multimachine power system model and construct the proposed observer of this model. As in the previous chapter, the observer design is characterized in a decentralized way. In the proposed decentralized scheme, we design the observer via locally available measurements associated with the synchronous generator unit(s). The proposed model is first presented in this manner. Next, by the observer-controller design, a deterministic observer for the power system model is implemented [174]. This results in recontraction of the state information case among the subsystems through the feature of control theory, which allows only measurement-based subsystem states and outputs. The deterministic observer design relies on the power system model and uses the full state measurements. Thus, the observer convergence analysis is used to stabilize the power system. Furthermore, we propose a state feedback problem for designing a Kalman observer. The main objective of this chapter is to address observer-based control in state feedback design, and allow us to stabilize a multimachine power system, especially by using the stability analysis with contraction theory as a means to achieve contraction.

Contraction theory is a stability theory for nonlinear systems, and is the main stability analysis tool used in this chapter [48]. It guarantees an incremental stability for uncertain nonlinear systems, especially time-varying systems. It is used for analyzing the stability of nonlinear systems by highlighting the convergence of all trajectories between two arbitrary systems. Here, we primarily focus on a contraction-based approach, which has some advantages over the Lyapunov-based stability analysis. After establishing the attractive features of contraction theory, we analyze the decentralized stability of the multimachine power system which can be stabilized by a deterministic

observer. Then, we introduce the stability properties of the extended Kalman filter based on contraction theory, which can be represented as a deterministic observer for nonlinear power systems.

Since the fundamental works of Kalman and Bucy [55], as well as Luenberger [178], state estimation of dynamical systems has been studied in the control theory literature. State estimation is a procedure to estimate the states of a dynamical system caused by uncertainties in the model, as well as the output measurements that are caused by predicable disturbances, so that each state exhibits the natural and uncorrelated behavior of each other state [181]. Well-known state estimators for linear systems, such as the Kalman Filter and Luenberger observer, are certainly accurate [175]. The Kalman filter described with a continuous-time linear model (i.e., time-varying) is implemented on the nonlinear model. In general, model uncertainties (which are defined inconsistencies in dynamical behavior between the estimated model and the actual model) cause poor performance of the observer, and thus, cause erratic changes in the system behavior. In practice, the control signal is determined by a nonlinear map. The approximate (but sufficiently accurate) solutions can be obtained. This method is also known as the also extended Kalman filter in the literature [49]. The EKF is used in cases where accurate knowledge of the system nonlinear model is unknown, and is indeed extended from the Kalman filter, which is widely used in the framework of state estimation. However, the EKF is responsible for linearizing the system, relying on its first order approximation along the estimated (i.e., trusted) trajectories. Therefore, we shall employ convergence of the continuous-time EKF in this chapter. The basic idea of the EKF from the perspective of contraction theory is to establish necessary conditions to guarantee contraction so that exponential convergence of the deterministic EKF is proved. Finally, the proposed solution method is based on the convergence properties of the EKF and can also be used for the deterministic case, similar to Lyapunov methods. Using the contraction analysis, the linearisation-based method implies exponential convergence under certain conditions. To this end, our goal is to analyze the stability of the multimachine power system and ensure the exponential convergence of the EKF using contraction stability analysis. The primary aim of this chapter is to study the convergence behaviors of the EKF with the help of contraction theory [50]. We then propose to the use of the

observer-based control method for the multimachine power system.

Contraction theory and Lyapunov stability theory are different approaches [183]. First of all, contraction theory provides an alternative description and solution method, and is used to analyze the exponential convergence properties of nonlinear systems or different problem structures. Contrary to Lyapunov, in contraction theory it is not required to have an explicit knowledge of a specific equilibrium point, but the stability analysis depends on differential displacements of the trajectories of nonlinear systems, in which it assumed that the virtual displacements of system states (that is, infinitesimal displacements) are fixed. Thus, terms that are not mainly related to the convergent behavior of the system are eliminated by using virtual displacements. Then, if initial conditions and disturbances of any kind vanish within an exponential manner-in other words, if the nonlinear system recovers its previous trajectory exponentially when it is subjected to a perturbation-then it is called a contracting system [56]. This theory does not depend on choosing a potential energy function which leads only to stability analysis in the Lyapunov sense. However, contraction theory leads to an incremental form of stability, and also implies an exponential form of convergence [184]. As a result, the incremental stability guarantees exponential convergence through the use of the incremental version of global exponential stability. Contraction theory-based stability analysis is also described as incremental convergence between a pair of neighboring trajectories. From the incremental stability perspective, it enables the stability of trajectories with respect to one another instead of respect to same attractor. As a matter of fact, the trajectories of a system converge on one another exponentially in contrast with attraction, leading to some equilibrium point or stability with respect to origin. In the sense of contraction theory, contraction analysis is evaluated using the stability properties of some duplicated systems, such as virtual and actual (or true) systems. This analysis can be made on the virtual system in which any pair of neighboring trajectories converge on each other. Furthermore, the main attention here is focused on the observer as well as the observer convergence analysis of EKF. We then turn to a consideration of Kalman gain viewing as the linear observer gain or possibly time-varying gain, which corresponds to a particular trajectory of the EKF with an arbitrary metric. Consequently, from the contraction theory-based analysis point of view, the true state

trajectory of a system becomes combined with particular trajectories of the virtual system. The corresponding estimation error of the EKF tends to act exponentially as the true state, and can be seen as the contraction properties of the virtual system which render the incremental stability of the system. Finally, simulation results on the multimachine power system model indicate that contraction analysis accurately characterizes system behavior and provides all information on the state dynamics with our theoretical results.

4.2 Review of Contraction Theory of Nonlinear Systems

Contraction theory provides an exponential convergence of observer states to the real states of a given model. It is not required to have an explicit knowledge of a stable equilibrium, but stability analysis depends on differential displacement such as a virtual displacement on the trajectory of nonlinear systems, see [50] for details. To compute the corresponding trajectories, we consider the following nonlinear system

$$\dot{x}(t) = f(t, x), \tag{4.1}$$

and differentiate a virtual displacement operator $\delta_v x(t)$, which means an differential variation with respect to a fixed time. We get

$$\delta_v \dot{x}(t) = (\partial f/\partial x)(t, x)\delta_v x(t). \tag{4.2}$$

A virtual transformation is defined by $\delta_v z(t) = \Gamma(t, x)\delta_v x(t)$ with a square and non-singular matrix $\Gamma(t, x)$. Therefore, the distance of the virtual displacement is given as

$$\delta_v^{\mathrm{T}} z(t)\delta_v z(t) = \delta_v^{\mathrm{T}} x(t)\mathcal{M}(t, x)\delta_v x(t), \tag{4.3}$$

where $\mathcal{M}(t, x)$ is a metric for the virtual system. The metric $\mathcal{M}$ is bounded in t. Even though $\mathcal{M}$ tends to approach infinity as $t \to \infty$, the metric may be unbounded in x and t, and the system trajectory $x(t)$ may grow unboundedly. In this case, having unboundedness of $\delta_v^{\mathrm{T}} x(t)\mathcal{M}(t, x)\delta_v x(t)$ implies that $\delta_v x(t)$ converges to zero exponentially and also requires that the metric is reestablished using coordinate transformation. In addition, mathematically, $\delta_v \dot{x}(t)$ leads to a linear tangent differential form; then, we have the following well-known theorem about contraction theory [48].

Theorem 4.2.1 (**Contraction Theory**). *Consider the nonlinear deterministic system* $\dot{x}(t) = f(t,x)$. *For each time* t, x *is in* $\mathbb{R}^n$, *where* f *is a continuous and smooth nonlinear function. Let the Jacobian matrix of* f *with respect to its first variable be* $\mathcal{J}' = \partial f/\partial x$. *If there exists a transformation matrix* $\Gamma(t,x)$ *such that a uniformly positive definite metric* $\mathcal{M}(t,x) = \Gamma(t,x)^{\mathrm{T}}\Gamma(t,x)$ *and the corresponding generalized Jacobian matrix* $\mathcal{J} = (\dot{\Gamma} + \Gamma\mathcal{J}')\Gamma^{-1}$ *is uniformly negative definite, then all trajectories converge exponentially to a single trajectory, with convergence rate* $\sup_{t,x} |\lambda_{max}(\mathcal{J})| = \lambda > 0$ *where* λ_{max} *is the largest eigenvalue of the symmetric part of* $\mathcal{J}$, *hence contraction.*

Based on this theorem, contraction theory is used to investigate the stability of the system through solutions which are independent of its initial conditions and regardless of nominal motion. In the case that a stable (or specific) equilibrium point has stability does not need to be known explicitly, then the system will tend to converge back to that equilibrium without variations in initial conditions. Next, all trajectories converge to this equilibrium point, which is dedicated to global exponential convergence. Similar to the definition in the previous chapter, we have the following definition of global exponential stability [130].

Definition 4.2.1 (**Global Exponential Stability**). *The system* (4.1) *is said to be globally and exponentially stable if there exist two positive scalar* k *and* β *such that* $\|x_1(t) - x_2(t)\| \leq k\|x_1 - x_2\|e^{-\beta t}$ *for all* $x_1, x_2 \in \mathbb{R}^n$, *and all* $t \geq 0$.

We now express these two relations between Theorem 4.2.1 and Definition 4.2.1. If we assume that the system (4.1) is globally contracting with the contraction rate λ and there is a bounded, uniformly positive definite and bounded metric such that $\mathcal{M}(t,x)$, the following holds

$$\underline{\sigma}^2 I \leq \mathcal{M}(t,x) \leq \overline{\sigma}^2 I, \tag{4.4}$$

where $\underline{\sigma}$ and $\overline{\sigma}$ are two positive scalars and therefore $k = \overline{\sigma}/\underline{\sigma}$. We conclude that if the system (4.1) is globally and exponentially stable, then the system (4.1) is globally contracting. Notice that our focus is on the system (4.1) whose trajectories exponentially converge on one another, which is a stronger form than Lyapunov approaches which define stability with respect to arbitrary initial conditions, as well as attractivity of the origin for all solutions (i.e., for all initial conditions).

Global asymptotic stability in the Lyapunov sense means that the asymptotic stability holds for all initial conditions (states) in the state-space. Here, further discussion revolves around the distinction between asymptotic stability definitions and properties, as well as basic theorems on Lyapunov stability theory, and a concise and historical survey can be found in [285]. It is important to stress that the Krasovskiĭ theorem implies an asymptotic stability; in other words, Krasovskiĭ's generalized asymptotic global convergence theorem respects a constant metric which allows exponential convergence.

Along the same lines, one of the main properties of contradiction theory-based analysis, in contrast to stability in the Lyapunov sense, is that it is not known *a priori* along which trajectory the system will converge. A notation of convergence, rather than stability, can be seen here. It also follows from Theorem 4.2.1 that one can use the metric to verify convergence on a unique trajectory, irrespective of the initial conditions, and also to ensure the existence and/or uniqueness of equilibria. Therefore, we conclude the following [183],[295].

Definition 4.2.2 (**Contraction Metric**). *If a continuously differentiable (contraction) metric $\mathcal{M}(t,x) \in \mathbb{R}^{n\times n}$ is a symmetric, uniformly positive definite such that $(\mathcal{J}')^{\mathrm{T}}\mathcal{M}(t,x) + \mathcal{M}(t,x)\mathcal{J}' + \dot{\mathcal{M}}(t,x)$ is also uniformly negative definite, then it satisfies the (strong) condition*

$$(\mathcal{J}')^{\mathrm{T}}\mathcal{M}(t,x) + \mathcal{M}(t,x)\mathcal{J}' + \dot{\mathcal{M}}(t,x) < -\beta\mathcal{M}(t,x) \tag{4.5}$$

with a strictly nonnegative scalar β, and therefore the system (4.1) *is said to be exponentially contracting, has a unique finite equilibrium, and all trajectories converge to this equilibrium.*

The stability and the domain of attraction of an equilibrium point can be found using a contraction metric. In particular, a contraction metric is evaluated from a Riemannian metric which is the distance function between any two points at a given time. Contrary to a contraction metric over a Lyapunov function, the contraction condition is robust to perturbations of the given system [296],[297]. It follows immediately from Definition 4.2.2 that the exponential convergence on a single trajectory is proved if the whole state space belongs to a finite region of

contraction (4.5) such as $(\mathcal{J}')^{\mathrm{T}}\mathcal{M}(t,x) + \mathcal{M}(t,x)\mathcal{J}' + \dot{\mathcal{M}}(t,x)$ with respect to the contraction metric $\mathcal{M}(t,x)$ and convergence rate β. It also follows that the stability criteria from a contraction metric must satisfy $\mathcal{M}(t,x) > 0$ and the condition $(\mathcal{J}')^{\mathrm{T}}\mathcal{M}(t,x) + \mathcal{M}(t,x)\mathcal{J}' + \dot{\mathcal{M}}(t,x) < 0$. However, the metric $\mathcal{M}(t,x)$ with the equation (4.3) defines a Riemann space. We then get the following consequence of definition [56].

Definition 4.2.3 (**Contraction region**). *Given the system equations* (4.1)*, a region of the state space is defined as a contraction region if the* $\mathcal{J}' = \partial f/\partial x$ *is uniformly negative definite under given metric* $\mathcal{M}(t,x)$ *in that region.*

The convex contraction region has a most unique equilibrium point, since any length between two trajectories is shrinking exponentially in that region. Thus, global exponential convergence to the given trajectory is satisfied when the whole state space lies in the region of contraction for given metric $\mathcal{M}(t,x)$. In addition, the exponential convergence of $\delta_v z(t)$ to 0 also involves exponential convergence $\delta_v x(t)$ to 0 which can be contained in the region of contraction with uniformly positive definite $\mathcal{M}(t,x)$ and uniformly negative definite $\mathcal{J}$. Indeed, for a constant metric $\mathcal{M}$, this exponential convergence establishes the Krasovskiĭ theorem for global asymptotic stability (convergence) of the systems. Here, we use the constant metric to reduce the Krasovskiĭ method. Thus, to obtain necessary and sufficient conditions for asymptotic stability, the Lypunov-Krasovskiĭ method can be used. The finite dimensional system $\dot{x} = Ax(t)$ is asymptotically stable if (and only if), for any given positive definite $\mathcal{M}$ matrix, the Lyapunov equation

$$\mathcal{M}A + A^{\mathrm{T}}\mathcal{M} < 0 \tag{4.6}$$

has a positive definite solution. Indeed, a Lyapunov-like function can be constructed from the solution $\mathcal{M}$,

$$V(x) = f^{\mathrm{T}}(x)\mathcal{M}(t,x)f(x), \tag{4.7}$$

which achieves

$$\dot{V}(x) = -f^{\mathrm{T}}(x)\mathcal{M}(t,x)f(x). \tag{4.8}$$

Also,

$$\dot{V}(x) = f^{\mathrm{T}}(x)\left((\mathcal{J}')^{\mathrm{T}}\mathcal{M}(t,x) + \mathcal{M}(t,x)\mathcal{J}' + \dot{\mathcal{M}}(t,x)\right) f(x) < 0, \tag{4.9}$$

and it is said to be globally stable. Here, $\mathcal{M}(t,x)$ is a contraction metric for the system $\dot{x} = f(t,x)$ and $V(x)$ is nonnegative for all points in the state space where $f(x) \neq 0$.

An alternative to Lyapunov approaches is to generate a contraction metric. To achieve stability robustness, the main difference is the fact that a Lyapunov function expects to have a known equilibrium point. In this case, a contraction metric derives the existence of a stable equilibrium indirectly. Note that this will be convenient if the equilibrium point drifts away due to dynamics or uncertainty in the system.

In light of the results in this section, the following virtual system dynamics will be of particular interest to us. Before discussing these results, in detail in the next section, we define a virtual system of the form:

$$\dot{z}(t) = f(t,z) + K(y(t) - h(t,z)) \tag{4.10}$$

with gain K and the measurement of $y(t)$, which is continuously differentiable

$$\delta_v \dot{z}(t) = (A - KC)\delta_v z(t), \tag{4.11}$$

where $A = (\partial f/\partial z)(t,z)$ and $C = (\partial h/\partial z)(t,z)$. We assumed that $f(0,t) = 0$ for every $t \geq 0$, therefore the equilibrium is stable for $A - KC$. It is worth notice that A and $\mathcal{J}'$ can be replaced. To this end, we define an observer of the form:

$$\dot{\hat{z}}(t) = f(t,\hat{z}) + K(t)(y(t) - h(t,\hat{z})). \tag{4.12}$$

Lemma 4.2.2 (**Deterministic Contraction**). *Assume that the assumptions of Theorem 4.2.1 and Definition 4.2.2 are fulfilled. If there exists a positive scalar for $\beta > 0$, then the virtual system* (4.10) *contracts, and exponential convergence to a single trajectory can be concluded in the region which is in an identical form discussed in* (4.5). *Then,*

$$A^{\mathrm{T}}\mathcal{M}(t,z) + \mathcal{M}(t,z)A + \dot{\mathcal{M}}(t,z) \leq -\beta\mathcal{M}(t,z). \tag{4.13}$$

Proof. This lemma is proved in the following section. □

The positive definite scalar β is deterministic, and verifies the regions of uniformly negative definite $\mathcal{J}$. The observer dynamics (4.12) of the virtual system (4.10) act as a particular solution of the real system (4.1) [186],[185]. The observer dynamics (4.12) can handle the properties of the system (4.10), and this leads to a global exponentially nonlinear observer design.

The key concept of this approach is that nonlinear contraction theory can be made exact, and at the same time, deals with global properties of nonlinear systems, referring to the case when global exponential convergence (stability) is guaranteed. The rate of converge can be explicitly determined and expressed in terms of eigenvalues of a well-defined symmetric matrix. We then derive the proposed metric for contraction analysis of a power system model. By using the constant metric, corresponding constant Γ, the explicit region of exponential convergence is obtained for our controller design based on linearization about an equilibrium point. Therefore, the model is contracting with respect to the proposed metric.

4.3 Contraction Analysis of EKF

The problem considered in this section consists of determining a Kalman observer filter. We try to characterize the concept of contraction theory for the EKF that corresponds to a deterministic Kalman observer. Under the above considerations, the system can be represented by the following form:

$$\dot{x}(t) = f(t, x, u), \tag{4.14a}$$

$$y(t) = h(t, x), \tag{4.14b}$$

where $x \in \mathbb{R}^n$ is the state of the system; $u \in \mathbb{R}^m$ is the input; $y \in \mathbb{R}^p$ is the measured output; f and h are smooth, which satisfies the conditions for existence and uniqueness of the solution.

We are now ready for the definition of observer [178],[49].

Definition 4.3.1 (**Observer**). *Let us consider a system* (4.14). *The structure of observer dynamics is formally defined as*

$$\dot{x}(t) = F(t, x, y, u), \tag{4.15a}$$

$$\hat{x}(t) = H(t, x, y), \tag{4.15b}$$

such that:
(i) $\hat{x}(0) = x(0) \Rightarrow \hat{x}(t) = x(t)$ *for all* $t \geq 0$*;*
(ii) $\|\hat{x}(t) - x(t)\|$ *tends to zero as* $t \to \infty$
If (ii) holds, then for any given $x(0)$*,* $\hat{x}(0)$*, the observer is said to be global.*
If (ii) holds with exponential convergence, the observer is said to be exponential.
If (ii) holds for exponential convergence with a convergence rate, the observer is said to be tunable.

Here, $x(0)$ is the initial value of the system (4.14), $x(t)$ is a trajectory of the perturbed system (4.14), and $\hat{x}(t)$ is a observer trajectory of the same system. If we know the initial value $x(0)$ which belongs to the ball of the center $\hat{x}(0)$, then $x(t)$ can be obtained. On the other hand, if the initial $x(0)$ is unknown, $\dot{x}(t)$ can be estimated online from some erroneous $\hat{x}(0)$, therefore $x(t)$ converges exponentially to $\hat{x}(0)$ around the observer trajectory $\hat{x}(t)$, allowing us to evaluate the estimation error generated by the perturbation. However, the measured output $y(t)$ of the system (4.14) is not equal to $h(t, x)$ and one cannot assume that $\|\hat{x}(t) - x(t)\|$ tends towards zero. The Kalman filter state esmimation problem is given by the following definition [57],[49].

Definition 4.3.2 (**Extended Kalman Filter**)**.** *Given a nonlinear system of the form* (4.14)*, the following EKF observer is defined by*

$$\dot{\hat{x}}(t) = f(t, \hat{x}, u) + K(t, \hat{x})(y(t) - h(t, \hat{x})), \tag{4.16}$$

where $K(t, \hat{x})$ *is the Kalman gain for some* $K > 1$*. Using the shorthand notation* $S := C(t, \hat{x})^{\mathrm{T}} W^{-1} C(t, \hat{x})$*, we get two EKF equations with respect to the dynamics:*

$$\dot{\hat{x}}(t) = f(t, \hat{x}, u) + P(t, \hat{x}) C(t, \hat{x})^{\mathrm{T}} W^{-1}(y(t) - h(t, \hat{x})), \tag{4.17}$$

$$\dot{P}(t, \hat{x}) = A(t, \hat{x}) P(t, \hat{x}) + P(t, \hat{x}) A(t, \hat{x})^{\mathrm{T}} + V - P(t, \hat{x}) S(t) P(t, \hat{x}), \tag{4.18}$$

where $A(t, \hat{x}) = (\partial f / \partial x)(\hat{x}(t), u(t))$ *and* $C(t, \hat{x}) = (\partial h / \partial x)(\hat{x}(t))$*.* W *and* V *are the measurement noise and Gaussian noise covariance matrices, respectively, which are assumed to be constant, and satisfy* $W = W^{\mathrm{T}} > 0$*,* $V = V^{\mathrm{T}} > 0$*. Consequently, the continuous EKF gain is determined by* $K(t, \hat{x}) = P(t, \hat{x}) C(t, \hat{x})^{\mathrm{T}} W^{-1}$*.*

Assumption 4.3.1. $\hat{x}(t)$ *is the estimated state, and the differential Riccati equation (DRE)* $\dot{P}(t, \hat{x})$ *has a symmetric solution* $P(t, x)$ *on* $[0, \infty]$ *and is defined uniformly*

positive definite. There exist two time-varying scalar $\underline{\alpha}(t), \overline{\alpha}(t) > 0$ *such that* $\underline{\alpha}(t)I \leq P(t,\hat{x}) \leq \overline{\alpha}(t)I$ *for every* $t \geq 0$.

Using the Definition 4.3.2, we are interested in obtaining the estimated $\hat{x}(t)$ that results from the the EKF equations (4.17) and (4.18), which are result in the solution of the virtual system

$$\dot{z}(t) = f(t,z) + K(t,\hat{x})(y(t) - h(t,z). \tag{4.19}$$

As a consequence, we have proved that this system (with respect to the distance between two arbitrary trajectories) is equivalent to zero, and hence it follows that the convergence of the estimation error $\hat{x} - x$ decreases to zero. Furthermore, $\hat{x}(t) - x(t) \to 0$ as $t \to +\infty$. Since the estimation error tends towards zero, we then get a contradiction through the virtual system (4.19). In order to prove the contraction results, including Lemma 4.2.2, for the virtual system, we first assume a metric $\mathcal{M} = P^{-1}$ using the Assumption 4.3.1 for the virtual dynamics (4.19). One is shown as the squared length in the sense of metric:

$$\|Z(t,z)\|^2 = Z^{\mathrm{T}}(t,z)P^{-1}(t,\hat{x})Z(t,z), \tag{4.20}$$

where $Z(t,z)$ is a tangent vector at $z(t)$ and allows us to verify

$$\dot{Z}(t,z) = \left[A(t,z) - K(t,\hat{x})C(t,z)\right] Z(t,z). \tag{4.21}$$

We now show the contraction of the virtual system (4.19), see [50]. For this propose, the derivative of the metric is first given by

$$\frac{d}{dt}\left\{Z^{\mathrm{T}}(t,z)P^{-1}(t,\hat{x})Z(t,z)\right\} =$$
$$\dot{Z}^{\mathrm{T}}(t,z)P^{-1}(t,\hat{x})Z(t,z) + Z^{\mathrm{T}}(t,z)\frac{d}{dt}\left\{P^{-1}(t,\hat{x})\right\}Z(t,z) + Z^{\mathrm{T}}(t,z)P^{-1}(t,\hat{x})\dot{Z}(t,z).$$

Recall that, by (4.11), we let $\dot{Z}(t,z) = (A - KC)Z(t,z)$, then

$$Z^{\mathrm{T}}(t,z)\left[(A-KC)^{\mathrm{T}}P^{-1}(t,\hat{x}) + \frac{d}{dt}\left\{P^{-1}(t,\hat{x})\right\} + P^{-1}(t,\hat{x})(A-KC)\right]Z(t,z).$$

Finally,

$$\frac{d}{dt}\left\{Z^{\mathrm{T}}(t,z)P^{-1}(t,\hat{x})Z(t,z)\right\} =$$
$$Z^{\mathrm{T}}(t,z)P^{-1}(t,\hat{x})\left[P(t,\hat{x})(A-KC)^{\mathrm{T}} - \dot{P}(t,\hat{x}) + (A-KC)P(t,\hat{x}\right]P^{-1}(t,\hat{x})Z(t,z)$$

Next, we also need to show the $\frac{d}{dt}\{P^{-1}(t,\hat{x}\}$.

$$\dot{P}^{-1}(t,\hat{x}) = -P^{-1}(t,\hat{x})\dot{P}(t,\hat{x})P^{-1}(t,\hat{x}),$$

using the DRE (4.18) and gain matrix $K(t,\hat{x})$, we can write

$$\frac{d}{dt}\left\{Z^{\mathrm{T}}(t,z)P^{-1}(t,\hat{x})Z(t,z)\right\} =$$
$$- Z^{\mathrm{T}}(t,z)C^{\mathrm{T}}(t,\hat{x})W^{-1}C(t,\hat{x})Z(t,z) - Z^{\mathrm{T}}(t,z)P^{-1}(t,\hat{x})VP^{-1}(t,\hat{x})Z(t,z).$$

We know that $W = W^{-1} > 0$,

$$\frac{d}{dt}\left\{Z^{\mathrm{T}}(t,z)P^{-1}(t,\hat{x})Z(t,z)\right\} \leq -Z(t,z)P^{-1}(t,\hat{x})VP^{-1}(t,\hat{x})Z(t,z).$$

Again, from Asumption 4.3.1 using $\overline{\alpha}$, $\underline{\alpha}$, and $\underline{v}$, which is the smallest eigenvalue of V, then

$$\frac{d}{dt}\left\{Z^{\mathrm{T}}(t,z)P^{-1}(t,\hat{x})Z(t,z)\right\} \leq (-\underline{v}/\overline{\alpha})Z^{\mathrm{T}}(t,z)P^{-1}(t,\hat{x})Z(t,z)$$

and hence (4.19) is contracting which guarantees the $\hat{z}$ converges exponentially to the actual state x. We note that the metric introduced by (4.20) is defined as Euclidean distance and is time-varying.

According to the above results, we obtain the following Lemma [48],[50].

Lemma 4.3.1. *Consider the metric* (4.20) *running the EKF based on the dynamics* (4.17), (4.18) *and the virtual dynamics* (4.19). *Taking* $\mathcal{A}(t,\hat{x},z) = A(t,z) - A(t,\hat{x})$ *and* $\mathcal{C}(t,\hat{x},z) = C(t,z) - C(t,\hat{x})$, *we get*

$$\frac{d}{dt}\Big\{Z^{\mathrm{T}}(t,z)P^{-1}(t,\hat{x})Z(t,z)\Big\} = Z^{\mathrm{T}}(t,z)P^{-1}(t,\hat{x})\mathcal{M}(t,\hat{x},z)Z(t,z)P^{-1}(t,\hat{x})Z(t,z)$$
$$\mathcal{M} = P(t,\hat{x})\mathcal{A}^{\mathrm{T}} + \mathcal{A}P(t,\hat{x})$$
$$+ P(t,\hat{x})HP(t,\hat{x}) - P(t,\hat{x})NP(t,\hat{x}) - V, \qquad (4.22)$$

where $H = \mathcal{C}^{\mathrm{T}}W^{-1}\mathcal{C}$ *and* $N = C(t,z)^{\mathrm{T}}W^{-1}C(t,z)$.

Proof.

$$\dot{Z}(t,z) = \Big[A(t,z) - K(t,\hat{x})C(t,z)\Big]Z(t,z)$$
$$= \Big[A(t,z) - P(t,\hat{x})C^{\mathrm{T}}(t,\hat{x})W^{-1}C(t,z)\Big]Z(t,z)$$

and

$$\frac{d}{dt}\Big\{Z^{\mathrm{T}}(t,z)P^{-1}(t,\hat{x})Z(t,z)\Big\} = \big[\dot{Z}(t,z)\big]^{\mathrm{T}}P^{-1}(t,\hat{x})Z(t,z) + Z(t,z)\dot{P}^{-1}(t,\hat{x})Z(t,z) + Z(t,z)P^{-1}(t,\hat{x})\dot{Z}(t,z)$$

Therefore,

$$\frac{d}{dt}\Big\{Z^{\mathrm{T}}(t,z)P^{-1}(t,\hat{x})Z(t,z)\Big\} = Z^{\mathrm{T}}(t,z)\Pi Z(t,z),$$

where

$$\Pi = A^{\mathrm{T}}(t,z)P^{-1}(t,\hat{x}) + P^{-1}(t,\hat{x})A(t,z) + \dot{P}^{-1}(t,\hat{x}) - C(t,\hat{x})W^{-1}C(t,z) - C^{\mathrm{T}}(t,z)W^{-1}C(t,\hat{x}).$$

Finally,

$$\begin{aligned}\dot{P}^{-1}(t,\hat{x}) &= -P^{-1}(t,\hat{x})\dot{P}^{-1}(t,\hat{x})P^{-1}(t,\hat{x}) \\ &= -P^{-1}(t,\hat{x})A(t,\hat{x}) - A^{\mathrm{T}}(t,\hat{x})P^{-1}(t,\hat{x}) - V + C^{\mathrm{T}}(t,\hat{x})W^{-1}C(t,\hat{x}).\end{aligned}$$

That is

$$\begin{aligned}&C^{\mathrm{T}}(t,\hat{x})W^{-1}C(t,\hat{x}) - C^{\mathrm{T}}(t,\hat{x})W^{-1}C(t,z) - C^{\mathrm{T}}(t,z)W^{-1}C(t,\hat{x}) = \\ &-\mathcal{C}^{\mathrm{T}}W^{-1}\mathcal{C} + C^{\mathrm{T}}(t,z)W^{-1}C(t,z).\end{aligned}$$

□

We choose two symmetric matrices Y_1 and Y_2, then describe a partial order implying $Y_1 \leq Y_2$ whereas $Y_2 - Y_1$ is positive semidefinite. We need the following Lemma [50].

Lemma 4.3.2. *Suppose $0 \leq \gamma < \underline{v}/(2\overline{\alpha})$. For each $t \geq 0$ and $r(t) > 0$ such that all z satisfy $\|z - \hat{x}(t)\| \leq r(t)$, we have*

$$P(t,\hat{x})\mathcal{A}^{\mathrm{T}} + \mathcal{A}P(t,\hat{x}) + P^{-1}(t,\hat{x})\mathcal{C}^{\mathrm{T}}(t,\hat{x},z)W^{-1}\mathcal{C}(t,\hat{x},z)P^{-1}(t,\hat{x}) \leq V - 2\gamma P(t,\hat{x}) + P(t,\hat{x})C^{\mathrm{T}}(t,z)W^{-1}C(t,z)P(t,\hat{x}). \tag{4.23}$$

Proof. One may choose $z = \hat{x}$, in which case the right-hand side of (4.23) is considered a positive definite matrix, and the left-side of (4.23) can be canceled as well. □

Given any time t, the vectors z away from $\hat{x}(t)$ with the maximum distance $r(t)$ are in the region of contraction, and equality of these vectors in Lemma 4.3.1 can be written as

$$\frac{d}{dt}\Big\{Z^{\mathrm{T}}(t,z)P^{-1}(t,\hat{x})Z(t,z)\Big\} \leq -2\gamma\left(P^{-1}(t,\hat{x})Z(t,z)\right) \tag{4.24}$$

which means differential inequality. This yields that the metric in (4.20) between particular trajectories of the virtual system in this ball will tend to decay, with a rate of γ.

4.4 Contraction Region for a Classical Model of Power System

In this section, we aim to describe the contraction region for the multimachine power system. Full mathematical details and physical assumptions can be found in previous chapters. The power system dynamics of ith generator can be written as follows:

$$\begin{aligned}
\dot{\delta}_i &= \omega_i, \\
\dot{\omega}_i &= \frac{1}{M_i}\left(P_{mi} - E'_{qi}I_{qi} - D_i\omega_i\right), \\
\dot{E}'_{qi} &= \frac{1}{T'_{doi}}\Big[E_{fdi} - E'_{qi}(t) + (X_{di} - X'_{di})I_{di}\Big],
\end{aligned} \tag{4.25}$$

where

$$\begin{aligned}
I_{di} = &\sum_{j=1}^{n}\left[G_{ij}\cos(\delta_i - \delta_j) + B_{ij}\sin(\delta_i - \delta_j)\right]E'_{dj} \\
&+ \sum_{j=1}^{n}\left[B_{ij}\cos(\delta_i - \delta_j) - G_{ij}\sin(\delta_i - \delta_j)\right]E'_{qj}
\end{aligned} \tag{4.26}$$

and

$$\begin{aligned}
I_{qi} = &\sum_{j=1}^{n}\left[G_{ij}\cos(\delta_i - \delta_j) + B_{ij}\sin(\delta_i - \delta_j)\right]E'_{qj} \\
&- \sum_{j=1}^{n}\left[B_{ij}\cos(\delta_i - \delta_j) - G_{ij}\sin(\delta_i - \delta_j)\right]E'_{dj}.
\end{aligned} \tag{4.27}$$

We are interested in a two-machine system, since it is the simplest model to show the contraction region. Assuming $P_{ei} = E'_{qi}I_{qi}$, the electrical equations of the currents

can be expressed as:

$$I_{di} = \sum_{j=1}^{n} \left[B_{ij} \cos(\delta_i - \delta_j) - G_{ij} \sin(\delta_i - \delta_j) \right] E'_{qj}, \tag{4.28}$$

$$I_{qi} = \sum_{j=1}^{n} \left[G_{ij} \cos(\delta_i - \delta_j) + B_{ij} \sin(\delta_i - \delta_j) \right] E'_{qj}. \tag{4.29}$$

The above equations can be described for the two-machine system:

$$I_{d_1} = B_{11} E'_{q_1} + B_{12} E'_{q_2} \cos(\delta_1 - \delta_2) - G_{12} E'_{q_2} \sin(\delta_1 - \delta_2), \tag{4.30}$$

$$I_{d_2} = B_{22} E'_{q_2} + B_{21} E'_{q_1} \cos(\delta_2 - \delta_1) - G_{21} E'_{q_1} \sin(\delta_2 - \delta_1), \tag{4.31}$$

$$I_{q_1} = G_{11} E'_{q_1} + G_{12} E'_{q_2} \cos(\delta_1 - \delta_2) + B_{12} E'_{q_2} \sin(\delta_1 - \delta_2), \tag{4.32}$$

$$I_{q_2} = G_{22} E'_{q_2} + G_{21} E'_{q_1} \cos(\delta_2 - \delta_1) + B_{21} E'_{q_1} \sin(\delta_2 - \delta_1). \tag{4.33}$$

We write the equations for the model in the following state-space form:

$$\begin{aligned}
\dot{\delta}_1 &= \omega_1, \\
\dot{\omega}_1 &= \frac{1}{M_1} \Big[P_{m_1} - D_1 \omega_1 - G_{11} E'^2_{q_1} - G_{12} E'_{q_1} E'_{q_2} \cos(\delta_1 - \delta_2) - B_{12} E'_{q_1} E'_{q_2} \sin(\delta_1 - \delta_2) \Big], \\
\dot{E}'_{q_1} &= \frac{1}{T'_{do_1}} \Big[E_{fd_1} - E'_{q_1} + (X_{d_1} - X'_{d_1}) B_{11} E'_{q_1} + (X_{d_1} - X'_{d_1}) B_{12} E'_{q_2} \cos(\delta_1 - \delta_2) \\
&\quad - (X_{d_1} - X'_{d_1}) G_{12} E'_{q_2} \sin(\delta_1 - \delta_2) \Big], \\
\dot{\delta}_2 &= \omega_2, \\
\dot{\omega}_2 &= \frac{1}{M_2} \Big[P_{m_2} - D_2 \omega_2 - G_{22} E'^2_{q_2} - G_{21} E'_{q_1} E'_{q_2} \cos(\delta_1 - \delta_2) - B_{21} E'_{q_1} E'_{q_2} \sin(\delta_1 - \delta_2) \Big], \\
\dot{E}'_{q_2} &= \frac{1}{T'_{do_2}} \Big[E_{fd_2} - E'_{q_2} + (X_{d_2} - X'_{d_2}) B_{22} E'_{q_2} + (X_{d_2} - X'_{d_2}) B_{21} E'_{q_2} \cos(\delta_2 - \delta_1) \\
&\quad - (X_{d_2} - X'_{d_2}) G_{21} E'_{q_2} \sin(\delta_2 - \delta_1) \Big],
\end{aligned} \tag{4.34}$$

The two-machine system dynamics can be greatly simplified by using the new variables, resulting in

$$v_1 = \delta_1 - \delta_2 \,, \qquad v_2 = \omega_1 - \omega_2 \,, \qquad v_3 = E_1 \,, \qquad v_4 = E_2.$$

We next discuss our assumption.

Assumption 4.4.1. *To investigate whether the power system is contracting, we simply make use of the formulation* (2.47) *with using a well-known approximate equation*

$$P_i = \sum_{j=1}^{n} B_{ij}(\delta_i - \delta_j). \tag{4.35}$$

We make the following assumptions:

- *For most power networks,* $G \ll B$*, thus* $G = 0$*.*
- *For normal operating conditions,* $|\delta_i - \delta_j|$ *is less than* $10 - 15$ *degrees; therefore:*
  - $\sin(\delta_i - \delta_j) \approx \delta_i - \delta_j$
  - $\cos(\delta_i - \delta_j) \approx 1$
- *In per unit,* $|E_i|$ *and* $|E_j|$ *are close to 1, that is*
  - $|E_i||E_j| \approx 1$

These assumptions are used to prove contraction results. In our notation, we also get $D = D_1 = D_2$ and $M = M_1 = M_2$. Next, we write the power system dynamics:

$$\begin{aligned}
\dot{v}_1 &= v_2, \\
\dot{v}_2 &= \frac{1}{M}\Big[P_{m_1} - P_{m_2} - Dv_2 - G_{11}v_3^2 + G_{22}v_4^2 - G_{12}v_3v_4\cos(v_1) \\
&\quad + G_{21}v_3v_4\cos(-v_1) - B_{12}v_3v_4\sin(v_1) + B_{21}v_3v_4\sin(-v_1)\Big], \\
\dot{v}_3 &= \frac{1}{T'_{do_1}}\Big[E_{fd_1} - v_3 + (X_{d_1} - X'_{d_1})B_{11}v_3 + (X_{d_1} - X'_{d_1})B_{12}v_4\cos(v_1) \\
&\quad - (X_{d_1} - X'_{d_1})G_{12}v_4\sin(v_1)\Big], \\
\dot{v}_4 &= \frac{1}{T'_{do_2}}\Big[E_{fd_2} - v_4 + (X_{d_2} - X'_{d_2})B_{22}v_4 + (X_{d_2} - X'_{d_2})B_{21}v_3\cos(-v_1) \\
&\quad - (X_{d_2} - X'_{d_2})G_{21}v_3\sin(-v_1)\Big].
\end{aligned} \tag{4.36}$$

We now use the above assumptions with the neglecting conductances from the power

system dynamics. One can write

$$\begin{aligned}
\dot{v}_1 &= v_2, \\
\dot{v}_2 &= \frac{1}{M}\Big[P_{m_1} - P_{m_2} - Dv_2 - B_{12}v_3v_4\sin(v_1) + B_{21}v_3v_4\sin(-v_1)\Big], \\
\dot{v}_3 &= \frac{1}{T'_{do_1}}\Big[E_{fd_1} - v_3 + (X_{d_1} - X'_{d_1})B_{11}v_3 + (X_{d_1} - X'_{d_1})B_{12}v_4\cos(v_1)\Big], \\
\dot{v}_4 &= \frac{1}{T'_{do_2}}\Big[E_{fd_2} - v_4 + (X_{d_2} - X'_{d_2})B_{22}v_4 + (X_{d_2} - X'_{d_2})B_{21}v_2\cos(v_1)\Big].
\end{aligned} \tag{4.37}$$

We obtain the following results using the second and third assumptions under Assumption 4.4.1:

$$\begin{aligned}
0 &= v_2, \\
0 &= -Dv_2 - B_{12}v_1 - B_{21}v_1, \\
0 &= -v_3 + (X_{d_1} - X'_{d_1})B_{11}v_3 + (X_{d_1} - X'_{d_1})B_{12}v_4, \\
0 &= -v_4 + (X_{d_2} - X'_{d_2})B_{22}v_4 + (X_{d_2} - X'_{d_2})B_{21}v_3.
\end{aligned} \tag{4.38}$$

From this, we get $B = B_{12} = B_{21}$, $B_1 = B_{11}$, and $B_2 = B_{22}$. Then, we obtain the Jacobian matrix for the two-machine system:

$$\mathbf{J} = \begin{bmatrix} 0 & 1 & 0 & 0 \\ -2B & -D & 0 & 0 \\ 0 & 0 & -1 + B_1\Delta X_{d_1} & B\Delta X_{d_1} \\ 0 & 0 & B\Delta X_{d_2} & -1 + B_2\Delta X_{d_2} \end{bmatrix}, \tag{4.39}$$

where $\Delta X_{d_1} = X_{d_1} - X'_{d_1}$ and $\Delta X_{d_2} = X_{d_2} - X'_{d_2}$. The main result of this paper is the following proposition.

Proposition 4.4.1. *Under Assumption 4.4.1, we assume that the system has the form* (4.57) *with a two-machine system of the form* (4.59)*, and also consider the system of the form* (4.15) *to present the basic form of the observer design. If the system* $\mathbf{S}_i$ *is contracting, it naturally inherits a metric* $\mathbf{M}_i$ *with rate* β_i

$$\mathbf{M}_i = \mathbf{\Gamma}_i^{\mathrm{T}}\mathbf{\Gamma}_i. \tag{4.40}$$

Suppose also that the metric $\mathbf{M}_i$ *is compatible with a given system operating point in a feasible region. One can choose a diagonal positive definite metric* $\mathbf{M}_i$ *which is compatible for the given system. Associated with our system, a contraction system is induced by a constant diagonal metric which yields*

$$\mathbf{\Gamma}_i = \begin{bmatrix} 0 & 1 & 0 & 0 \\ 0 & 0 & 1 & 0 \\ 1 & 0 & 0 & 0 \\ 0 & 0 & 0 & 1 \end{bmatrix}. \tag{4.41}$$

Therefore, the system (4.58) *which is contracting in a constant metric* $\mathbf{M}_i$*, is said to be compatible with a convex feasible set.*

Proof. The generalized Jacobian is of the form

$$\mathbf{F} = (\dot{\mathbf{\Gamma}}_i + \mathbf{\Gamma}_i \mathbf{J})\mathbf{\Gamma}_i^{-1}, \tag{4.42}$$

where matrix $\mathbf{F}$ is defined by

$$\mathbf{F} = \begin{bmatrix} -D & 0 & -2B & 0 \\ 0 & -1 + B_1 \Delta X_{d_1} & 0 & B\Delta x_{d_1} \\ 1 & 0 & 0 & 0 \\ 0 & B\Delta X_{d_2} & 0 & -1 + B_2 \Delta x_{d_2} \end{bmatrix}. \tag{4.43}$$

The symmetric part of the generalized Jacobian is:

$$\mathbf{F}_s = \mathbf{F} + \mathbf{F}^{\mathrm{T}}. \tag{4.44}$$

Therefore, we can show the principal minors of the matrix $\mathbf{F}_s$

$$\begin{aligned} m_1 &= 2D, \\ m_2 &= -4D(-1 + B_1 \Delta X_{d_1}), \\ m_3 &= 2(2B-1)^2(-1 + B_1 \Delta X_{d_1}), \\ m_4 &= -(2B-1)(-2B^3 \Delta X_{d_1}^2 - 4B^3 \Delta X_{d_1} \Delta X_{d_2} - 2B^3 \Delta X_{d_2}^2 + B^2 \Delta X_{d_1}^2 \\ &\quad + 2B^2 \Delta X_{d_1} \Delta X_{d_2} + 8B_1 B_2 B \Delta X_{d_1} \Delta X_{d_2} - 8B_1 B \Delta X_{d_1} - 8B_2 B X_{d_1} \\ &\quad + 8B - 4B_1 B_2 \Delta X_{d_1} \Delta X_{d_2} + 4B_1 \Delta X_{d_1} + 4B_2 \Delta X_{d_2} - 4). \end{aligned} \tag{4.45}$$

As we know, the principal minors of the Jacobian matrix $\mathbf{F}_s$ are always positive. Hence, the principal minor m_1 is positive; m_2 and m_3 are negative. Here, m_2 must satisfy $B_1\Delta X_{d_1} < 1$ and m_3 must also satisfy $B_1\Delta X_{d_2} > 1$. In this case, it is not necessary to verify the last principle minor m_4. Thus, we cannot prove the contraction region of the uncontrolled case for model (4.25).

Let us write the Jacobian of the controlled system

$$\mathbf{J_c} = \begin{bmatrix} 0 & 1 & 0 & 0 \\ -2B & -D & 0 & 0 \\ k_1 & k_2 & -1 + B_1\Delta X_{d_1} & B\Delta X_{d_1} \\ 0 & 0 & B\Delta X_{d_1} & -1 + B_2\Delta X_{d_2} \end{bmatrix}. \tag{4.46}$$

$\mathbf{K}$ is the gain vector of the proposed controller. We have:

$$\mathbf{K} = \begin{bmatrix} k_1 & 0 & 0 & 0 \\ 0 & k_2 & 0 & 0 \end{bmatrix}. \tag{4.47}$$

The generalized Jacobian for the controlled case is:

$$\mathbf{F_c} = \begin{bmatrix} -D & 0 & -2B & 0 \\ k_2 & -1 + B_1\Delta X_{d_1} & k_1 & B\Delta x_{d_1} \\ 1 & 0 & 0 & 0 \\ 0 & B\Delta X_{d_2} & 0 & -1 + B_2\Delta x_{d_2} \end{bmatrix}. \tag{4.48}$$

The principal minors of the Jacobian of the controlled system are:

$$\begin{aligned} m_1 &= 2D, \\ m_2 &= -k_2^2 + 4D(1 - B_1\Delta X_{d_1}), \\ m_3 &= -Dk_1^2 + (2B-1)\left\{k_1k_2 - (2B-1)(1 - B_1X_{d_1})\right\}, \\ m_4 &= B^2(1 + 2X_{d_1}X_{d_2}(2B-1)^2 \\ &\quad + 4(1 - B_2X_{d_2})\Big[- Dk_1^2 + 2B - 1\left\{k_1k_2 - (2B-1)(1 - B_1X_{d_1})\right\}\Big]. \end{aligned} \tag{4.49}$$

Then, we can easily see that the conditions are:

$$\begin{aligned} 1 &> B_1 X_{d_1}, \\ B &> 0.5, \\ k_1 k_2 &> (2B-1)(1-B_1 X_{d_1}), \\ k_2^2 &> 4D(1-B_1 X_{d_1}), \\ D k_1^2 &> (2B-1)\left\{k_1 k_2 - (2B-1)(1-B_1 X_{d_1})\right\}. \end{aligned} \tag{4.50}$$

Finally, we conclude that all principal minors are positive, as desired. Therefore, the contraction region is obtained for the controlled case only. Here, we only give the proof for a two-machine system. Our detailed proof can be used for a three-machine system. The results of our simulations show that the contraction region exists. □

4.4.1 Computing of the Jacobian Matrix for Contraction Analysis: The Three-Machine System

In this subsection, we determine the Jacobian matrix of the three-machine system for contraction conditions. First, we write the system equations for the three-machine system:

$$\begin{aligned} \dot{\delta}_1 &= \omega_1, \\ \dot{\omega}_1 &= \frac{1}{M_1}\Big[P_{m_1} - D_1\omega_1 - G_{11}E_{q_1}'^2 - G_{12}E_{q_1}'E_{q_2}'\cos(\delta_1-\delta_2) \\ &\quad - G_{13}E_{q_1}'E_{q_3}'\cos(\delta_1-\delta_3) - B_{12}E_{q_1}'E_{q_2}'\sin(\delta_1-\delta_2) - B_{13}E_{q_1}'E_{q_3}'\sin(\delta_1-\delta_3)\Big], \\ \dot{E}_{q_1}' &= \frac{1}{T_{do_1}'}\Big[E_{fd_1} - E_{q_1}' - \Delta X_{d_1}G_{12}E_{q_2}'\sin(\delta_1-\delta_2) - \Delta X_{d_1}G_{13}E_{q_3}'\sin(\delta_1-\delta_3) \\ &\quad + \Delta X_{d_1}B_{11}E_{q_1}' + \Delta X_{d_1}B_{12}E_{q_2}'\cos(\delta_1-\delta_2) + \Delta X_{d_1}B_{13}E_{q_3}'\cos(\delta_1-\delta_3)\Big], \\ \dot{\delta}_2 &= \omega_2, \\ \dot{\omega}_2 &= \frac{1}{M_2}\Big[P_{m_2} - D_2\omega_2 - G_{21}E_{q_2}'^2 - G_{21}E_{q_2}'E_{q_1}'\cos(\delta_2-\delta_1) \\ &\quad - G_{23}E_{q_2}'E_{q_3}'\cos(\delta_2-\delta_3) - B_{21}E_{q_2}'E_{q_1}'\sin(\delta_2-\delta_1) - B_{23}E_{q_2}'E_{q_3}'\sin(\delta_2-\delta_3)\Big], \\ \dot{E}_{q_2}' &= \frac{1}{T_{do_2}'}\Big[E_{fd_2} - E_{q_2}' - \Delta X_{d_2}G_{21}E_{q_1}'\sin(\delta_2-\delta_1) - \Delta X_{d_2}G_{23}E_{q_3}'\sin(\delta_2-\delta_3) \\ &\quad + \Delta X_{d_2}B_{22}E_{q_2}' + \Delta X_{d_2}B_{21}E_{q_2}'\cos(\delta_2-\delta_1) + \Delta X_{d_2}B_{23}E_{q_3}'\cos(\delta_2-\delta_3)\Big], \end{aligned}$$

$$
\begin{aligned}
\dot{\delta}_3 &= \omega_3, \\
\dot{\omega}_3 &= \frac{1}{M_3}\Big[P_{m_3} - D_3\omega_3 - G_{33}E'^2_{q_3} - G_{31}E'_{q_3}E'_{q_1}\cos(\delta_3-\delta_1) \\
&\quad - G_{32}E'_{q_3}E'_{q_2}\cos(\delta_3-\delta_2) - B_{31}E'_{q_3}E'_{q_1}\sin(\delta_3-\delta_1) - B_{32}E'_{q_3}E'_{q_2}\sin(\delta_3-\delta_2)\Big], \\
\dot{E}'_{q_3} &= \frac{1}{T'_{do_3}}\Big[E_{fd_3} - E'_{q_3} - \Delta X_{d_3}G_{31}E'_{q_1}\sin(\delta_3-\delta_1) - \Delta X_{d_3}G_{32}E'_{q_2}\sin(\delta_3-\delta_2) \\
&\quad + \Delta X_{d_3}B_{33}E'_{q_3} + \Delta X_{d_3}B_{31}E'_{q_1}\cos(\delta_3-\delta_1) + \Delta X_{d_3}B_{32}E'_{q_2}\cos(\delta_3-\delta_2)\Big],
\end{aligned}
\tag{4.51}
$$

where $\Delta X_{d_3} = X_{d_3} - X'_{d_3}$. Next, we describe the new states:

$$
\begin{aligned}
v_1 &= \delta_1 - \delta_2\,, & v_4 &= \omega_1 - \omega_2\,, & v_7 &= E_1, \\
v_2 &= \delta_1 - \delta_3\,, & v_5 &= \omega_1 - \omega_3\,, & v_8 &= E_2, \\
v_3 &= \delta_2 - \delta_3\,, & v_6 &= \omega_2 - \omega_3\,, & v_9 &= E_3,
\end{aligned}
\tag{4.52}
$$

We assume that $v_3 = -v_1 + v_2$ and $v_6 = -v_4 + v_5$. Under Assumption 4.4.1, the model can be written:

$$
\begin{aligned}
\dot{v}_1 &= v_3, \\
\dot{v}_2 &= v_4, \\
\dot{v}_3 &= \frac{1}{M}\Big[P_{m_1} - P_{m_2} - Dv_3 - B_{12}v_5v_6\sin(v_1) - B_{13}v_5v_7\sin(v_2) + B_{21}v_5v_6\sin(-v_1) \\
&\quad + B_{23}v_5v_6\sin(-v_1+v_2)\Big], \\
\dot{v}_4 &= \frac{1}{M}\Big[P_{m_2} - P_{m_3} - Dv_4 - B_{12}v_5v_6\sin(v_1) - B_{13}v_5v_7\sin(v_2) + B_{31}v_5v_7\sin(-v_2) \\
&\quad + B_{32}v_6v_3\sin(v_1-v_2)\Big], \\
\dot{v}_5 &= \frac{1}{T'_{do_1}}\Big[E_{fd_1} - v_5 + \Delta X_{d_1}B_{11}v_5 + \Delta X_{d_1}B_{12}v_6\cos(v_1) + \Delta X_{d_1}B_{13}v_7\cos(v_2)\Big], \\
\dot{v}_6 &= \frac{1}{T'_{do_2}}\Big[E_{fd_2} - v_6 + \Delta X_{d_2}B_{22}v_6 + \Delta X_{d_2}B_{21}v_5\cos(-v_1) \\
&\quad + \Delta X_{d_2}B_{23}v_7\cos(-v_1+v_2)\Big], \\
\dot{v}_7 &= \frac{1}{T'_{do_3}}\Big[E_{fd_3} - v_7 + \Delta X_{d_3}B_{23}v_7 + \Delta X_{d_3}B_{31}v_5\cos(-v_1) \\
&\quad + \Delta X_{d_3}B_{32}v_6\cos(v_1-v_2)\Big].
\end{aligned}
\tag{4.53}
$$

Again, using Assumption 4.4.1, we obtain:

$$
\begin{aligned}
0 &= v_3, \\
0 &= v_4, \\
0 &= -Dv_3 - B_{12}v_1 - B_{13}v_2 - B_{31}v_1 - B_{23}v_1 + B_{23}v_2, \\
0 &= -Dv_4 - B_{12}v_1 - B_{13}v_2 - B_{31}v_2 - B_{32}v_2 + B_{32}v_1, \\
0 &= -v_5 + \Delta X_{d_1}B_{11}v_5 + \Delta X_{d_1}B_{12}v_6 + \Delta X_{d_1}B_{13}v_7, \\
0 &= -v_6 + \Delta X_{d_2}B_{22}v_6 + \Delta X_{d_1}B_{21}v_6 + \Delta X_{d_2}B_{23}v_7, \\
0 &= -v_7 + \Delta X_{d_3}B_{23}v_7 + \Delta X_{d_1}B_{31}v_5 + \Delta X_{d_3}B_{32}v_6.
\end{aligned}
\tag{4.54}
$$

We can write the above equations in a more compact form:

$$
\begin{aligned}
0 &= v_3, \\
0 &= v_4, \\
0 &= -Dv_3 - v_1(B_{12} + B_{31} + B_{23}) - v_2(B_{13} + B_{23}), \\
0 &= -Dv_4 - v_1(B_{12} + B_{32}) - v_2(B_{13} + B_{31} + B_{32}), \\
0 &= -v_5(1 - \Delta X_{d_1} B_{11}) + \Delta X_{d_1} B_{12} v_6 + \Delta X_{d_1} B_{13} v_7, \\
0 &= -v_6(1 - \Delta X_{d_2} B_{11}) + \Delta X_{d_1} B_{21} v_6 + \Delta X_{d_2} B_{13} v_7, \\
0 &= -v_7(1 - \Delta X_{d_3} B_{11}) + \Delta X_{d_1} B_{31} v_5 + \Delta X_{d_3} B_{32} v_6.
\end{aligned}
$$

We assume that $B = B_{12} = B_{21} = B_{31} = B_{23} = B_{13} = B_{23}$, $B_1 = B_{11}$, $B_2 = B_{22}$, and $B_3 = B_{33}$. Finally, we write:

$$
\begin{aligned}
0 &= v_3, \\
0 &= v_4, \\
0 &= -Dv_3 - 3Bv_1 - 2Bv_2, \\
0 &= -Dv_4 - 2Bv_1 - 3Bv_2, \\
0 &= -v_5(1 - X_{d_1} B_1) + X_{d_1} B v_6 + X_{d_1} B v_7, \\
0 &= -v_6(1 - X_{d_2} B_2) + X_{d_2} B v_5 + X_{d_2} B v_7, \\
0 &= -v_7(1 - X_{d_3} B_3) + X_{d_3} B v_5 + X_{d_3} B v_6.
\end{aligned}
\tag{4.55}
$$

Therefore, the Jacobian matrix of the three machine system is given:

$$
\mathbf{J} = \begin{bmatrix}
0 & 0 & 1 & 0 & 0 & 0 & 0 \\
0 & 0 & 0 & 1 & 0 & 0 & 0 \\
-3B & -2B & -D & 0 & 0 & 0 & 0 \\
-2B & -3B & 0 & -D & 0 & 0 & 0 \\
0 & 0 & 0 & 0 & -1 + B_1 \Delta X_{d_1} & B \Delta X_{d_1} & B \Delta X_{d_1} \\
0 & 0 & 0 & 0 & B \Delta X_{d_2} & -1 + B_2 \Delta X_{d_2} & B \Delta X_{d_2} \\
0 & 0 & 0 & 0 & B \Delta X_{d_3} & B \Delta X_{d_3} & -1 + B_3 \Delta X_{d_3}
\end{bmatrix}.
\tag{4.56}
$$

4.5 Decentralized Control Using Deterministic Kalman Observer

We start by discussing the role that observer-based control can play for the decentralized control of power systems. As a representative model of a power system application, we focus on model (2.60) related to power system dynamics. In this section, we discuss the three-machine system, because its dimension is higher than that of the two-machine system. The readers can follow the same procedure found in the previous section. Unlike the model of the two-machine bus system, this model has the relative angles $\delta_1 - \delta_3$ and $\delta_2 - \delta_3$, the angular velocities $\omega_1 - \omega_3$ and $\omega_2 - \omega_3$, and the quadrature axis internal voltage E_3. We also resort to numerical simulations to carry out this analysis for the two-machine system and three-machine system.

Let δ be the power angle, ω the relative speed, and the transient electric potential is E. The system equations to model SMIB are

$$\begin{aligned}
\dot{\delta}(t) &= \omega(t), \\
\dot{\omega}(t) &= -\lambda\omega(t) + P_m(t) - GE(t) - E(t)Y\sin(\delta - \theta), \\
\dot{E}(t) &= -aE(t) + bE(t)\cos(\delta + \theta) + E_f + u.
\end{aligned} \tag{4.57}$$

The definition of the Kalman estimation problem is formulated in the previous sections. We now provide a deterministic nonlinear observer for the design of decentralized control in power systems made of neighboring subsystems or machines, which have access to local measurements and the measurements from neighboring subsystems. Therefore, we first describe the idea of the observer design for a power network governed by the dynamics equations with the case of three subsystems. The corresponding observer design takes the form

$$(\Sigma)\begin{cases}
\dot{x}_1 = f_1(x_1, x_2, x_3, u), \\
\dot{x}_2 = f_2(x_2, x_1, x_3, u), \\
\dot{x}_3 = f_3(x_3, x_2, x_3, u), \\
y = (h_1(x_1), h_2(x_2), h_3(x_3)) = (y_1, y_2, y_3)^{\mathrm{T}}.
\end{cases} \tag{4.58}$$

With this respect, $x = [x_1, x_2, x_3]^{\mathrm{T}} = [\delta, \omega, E]^{\mathrm{T}}$ is the state vector.

Using the model (4.57), the model structure for the three machine system can be established:

$$
\begin{aligned}
\dot{\delta}_1 &= \omega_1, \\
\dot{\omega}_1 &= -D_1\omega_1 + P_1 - G_1E_1^2 - E_1E_2Y_{12}\sin(\delta_1 - \delta_2 + \alpha_{12}) - E_1E_3Y_{13}\sin(\delta_1 - \delta_3 + \alpha_{13}), \\
\dot{E}_1 &= -a_1E_1 + b_1E_2\cos(\delta_1 - \delta_2 + \alpha_{12}) + b_1E_3\cos(\delta_1 - \delta_3 + \alpha_{13}) + \frac{1}{\tau_1}(E_{f1} - V_1), \\
\dot{\delta}_2 &= \omega_2, \\
\omega_2 &= -D_2\omega_2 + P_2 - G_2E_2^2 - E_2E_1Y_{21}\sin(\delta_2 - \delta_1 + \alpha_{21}) - E_2E_3Y_{23}\sin(\delta_2 - \delta_3 + \alpha_{23}), \\
\dot{E}_2 &= -a_2E_2 + b_2E_1\cos(\delta_2 - \delta_1 + \alpha_{21}) + b_1E_3\cos(\delta_2 - \delta_3 + \alpha_{23}) + \frac{1}{\tau_2}(E_{f2} - V_2), \\
\dot{\delta}_3 &= \omega_3, \\
\dot{\omega}_3 &= -D_3\omega_3 + P_3 - G_3E_3^2 - E_3E_1Y_{31}\sin(\delta_3 - \delta_1 + \alpha_{31}) - E_3E_2Y_{32}\sin(\delta_3 - \delta_2 + \alpha_{32}), \\
\dot{E}_3 &= -a_3E_3 + b_3E_1\cos(\delta_3 - \delta_1 + \alpha_{31}) + b_3E_2\cos(\delta_3 - \delta_2 + \alpha_{32}) + \frac{1}{\tau_3}(E_{f3} - V_3).
\end{aligned}
\tag{4.59}
$$

The main motivation for using contraction theory is that contraction properties of the EKF are employed under the three-machine model of a power system. This case study illustrates how our numerical results can be used in order to preserve both contraction of the power system and diagonality of the metric.

4.6 Simulation Results

4.6.1 Simulation Methodology

In preparing a simulation for observer-based control using the EKF, we considered a power system represented by a multimachine power system. We are concerned with several different models of power systems [54]. Parameter values of the two-machine system are listed in Table 4.1.

Table 4.1: Parameter values of the two-machine bus system

Gen 1		Gen 2	
a_1	9.9854	a_2	11.0906
b_1	3.9168	b_2	4.6220
Y_{12}	16.3799	Y_{21}	24.9939
G_1	8.1542	G_2	7.1505
α	0.5432	α	0.5432
Ef_1	6.5	Ef_2	7.1
P_1	52.4412	P_1	48.8031
D_1	0.71	D_2	0.71
τ_1	1	τ_2	1

In addition, parameter values of the three-machine system are shown in Table 4.2.

Table 4.2: Parameter values of the three-machine bus system

Gen 1		Gen 2		Gen 3	
a_1	9.9854	a_2	11.0906	a_3	12.1234
b_1	3.9168	b_2	4.6220	b_3	4.4147
Y_{12}	16.3799	Y_{21}	24.9939	Y_{31}	17.6127
Y_{13}	21.1234	Y_{23}	19.1234	Y_{32}	23.2529
G_1	8.1542	G_2	7.1505	G_3	6.3936
α_{12}	0.51	α	0.5432	α_{31}	0.49
α_{13}	0.51	α_{23}	0.52	α_{32}	0.49
Ef_1	6.5	Ef_2	7.1	Ef_3	6.1
P_1	52.4452	P_1	48.8031	P_3	50.1234
D_1	0.71	D_1	0.71	D_3	0.71
τ_1	1	τ_2	1	τ_3	1

The performance of the simulation results confirm the stability of the multimachine system with nonlinear interconnections between different generators. Using the

decentralized observer-based design method, the observation errors of the states of the multimachine power system converge to zero. This implies the effectiveness of the proposed observer. For simulations of the proposed control scheme, MATLAB is used as a simulation tool.

In addition to the proposed control scheme based on a decentralized observer, the original system dynamics (4.57) can be written in the nine-order model for the three machine system. We begin by defining the new states $\{v_1 \dots v_9\}$ as

$$\begin{aligned} v_1 &= \delta_1 - \delta_2\,, & v_4 &= \omega_1 - \omega_2\,, & v_7 &= E_1, \\ v_2 &= \delta_1 - \delta_3\,, & v_5 &= \omega_1 - \omega_3\,, & v_8 &= E_2, \\ v_3 &= \delta_2 - \delta_3\,, & v_6 &= \omega_2 - \omega_3\,, & v_9 &= E_3, \end{aligned} \tag{4.60}$$

and the model can be rewritten in the form

$$\begin{aligned} \dot{v}_1 &= v_4, \\ \dot{v}_2 &= v_5, \\ \dot{v}_3 &= v_6, \\ \dot{v}_4 &= -Dv_4 + P_1 - P_2 - G_1 v_7^2 + G_2 v_8^2 - Y_{12} v_7 v_8 \sin(v_1 + \alpha) - Y_{21} v_7 v_8 \sin(v_1 - \alpha) \\ &\quad - Y_{13} v_7 v_9 \sin(v_2 + \alpha) - Y_{23} v_8 v_9 \sin(v_3 + \alpha), \\ \dot{v}_5 &= -Dv_5 + P_1 - P_3 - G_1 v_7^2 + G_3 v_9^2 - Y_{12} v_7 v_8 \sin(v_1 + \alpha) - Y_{32} v_8 v_9 \sin(v_3 - \alpha) \\ &\quad - Y_{13} v_7 v_9 \sin(v_2 + \alpha) - Y_{31} v_7 v_9 \sin(v_2 - \alpha), \\ \dot{v}_6 &= -Dv_6 + P_2 - P_3 - G_2 v_8^2 + G_3 v_9^2 - Y_{21} v_7 v_8 \sin(v_1 - \alpha) - Y_{23} v_8 v_9 \sin(v_3 + \alpha) \\ &\quad - Y_{31} v_7 v_9 \sin(v_2 - \alpha) - Y_{32} v_8 v_9 \sin(v_3 - \alpha), \\ \dot{v}_7 &= -a_1 v_7 + b_1 v_8 \cos(v_1 + \alpha) + b_1 v_9 \cos(v_2 - \alpha) + \frac{1}{\tau_1}(E_{f1} + V_1), \\ \dot{v}_8 &= -a_2 v_8 + b_2 v_7 \cos(-v_1 + \alpha) + b_2 v_9 \cos(v_3 + \alpha) + \frac{1}{\tau_2}(E_{f2} + V_2), \\ \dot{v}_9 &= -a_3 v_9 + b_3 v_7 \cos(-v_2 + \alpha) + b_3 v_8 \cos(-v_3 + \alpha) + \frac{1}{\tau_3}(E_{f3} + V_3). \end{aligned} \tag{4.61}$$

Finally, the model used for the implementation of the proposed control is obtained.

4.6.2 Case Study: Two-Machine System

The simulation results for the two-machine system are grouped into two cases. We simulate the behavior of the two-machine power system for both uncontrolled and controlled cases.

4.6.2.1 Case 1

The first case demonstrates the uncontrolled cases. We simulate the behavior of the states of the two-machine system.

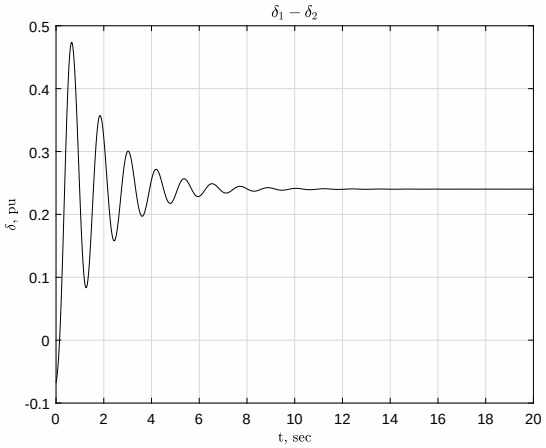

Figure 4.1: Rotor angle variations of the two-machine system

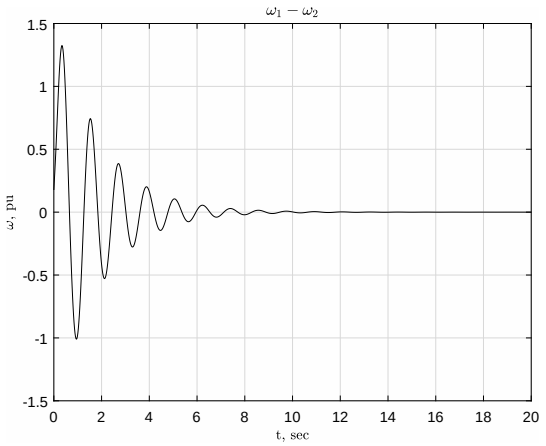

Figure 4.2: Relative speed variations of the two-machine system for the uncontrolled case

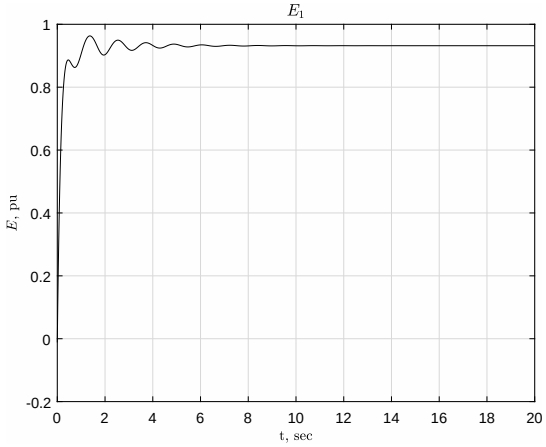

Figure 4.3: Internal voltage of the first generator for the uncontrolled case

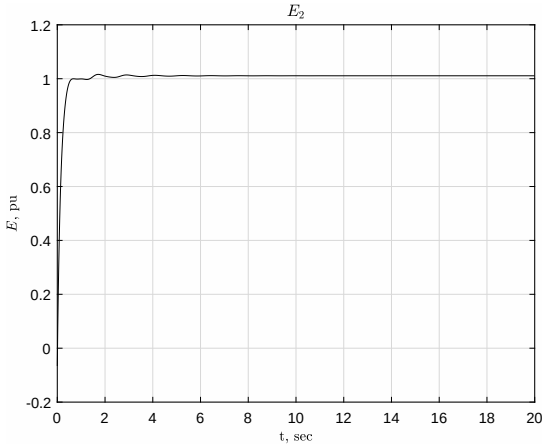

Figure 4.4: Internal voltage of the second generator for the uncontrolled case

Here, the states are the relative angle $\delta_1 - \delta_2$, the relative speed $\omega_1 - \omega_2$, and internal voltages E_1 and E_2. From these simulation results, we observe that the settling time is greater for the uncontrolled case than for the controlled case. In this case, the system is stable. In the theoretical direction, contraction theory for the two-machine system can be investigated analytically. The contraction region is fully analyzed in the model using some assumptions. Theoretical results for the model are thus verified by our simulation results. In a large power system, the contraction region may be unavailable to ensure stability over a wide range of operating conditions.

4.6.2.2 Case 2

The second case presents simulations for the controlled case. In this case, the observer errors of the states are also presented.

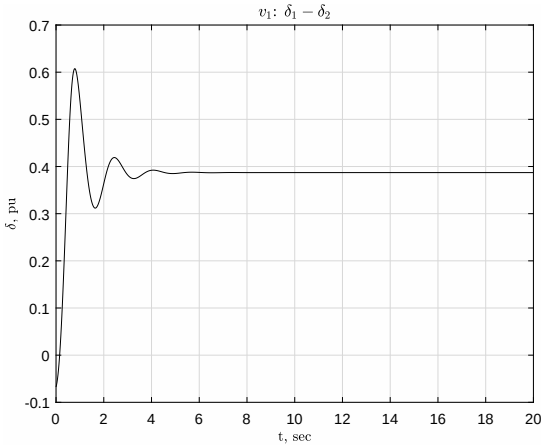

Figure 4.5: Rotor angle variations of the two-machine system for the controlled case

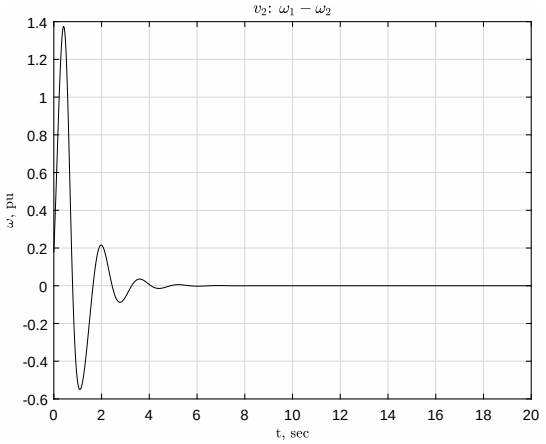

Figure 4.6: Relative speed variations of the two-machine system for the controlled case

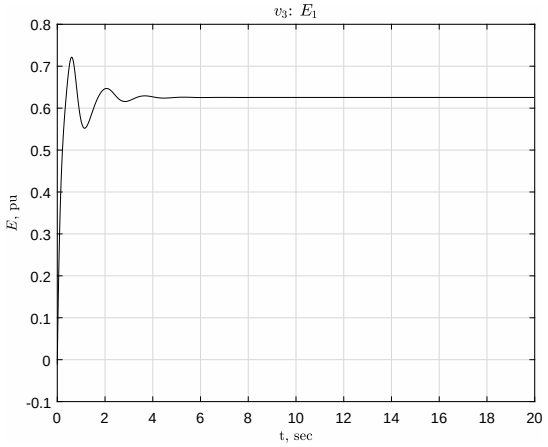

Figure 4.7: Internal voltage of the first generator for the controlled case

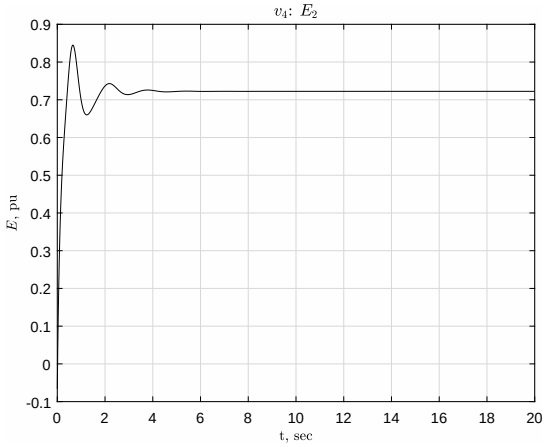

Figure 4.8: Internal voltage of the second generator for the controlled case

In Fig. 4.5–4.8, when the proposed control strategy is applied, it is clear that the settling time is less for the controlled case than for the uncontrolled case. Thus, in the controlled case, the system reaches equilibrium faster. The decentralized control scheme is sufficient to enhance the stability of the two-machine system.

Next, we demonstrate observer error dynamics. The dynamics of the state estimation error of rotor angles, relative speeds, and internal voltages are presented.

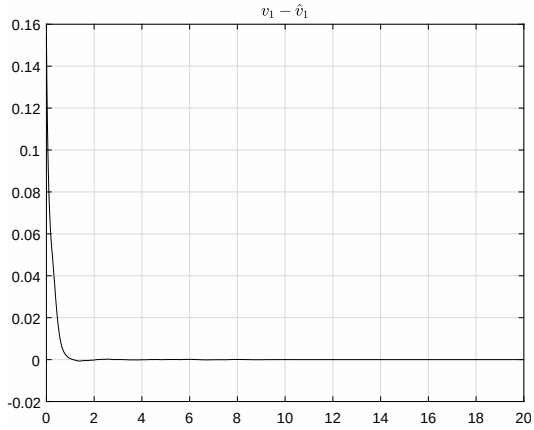

Figure 4.9: The estimation error of rotor angles for the two-machine system

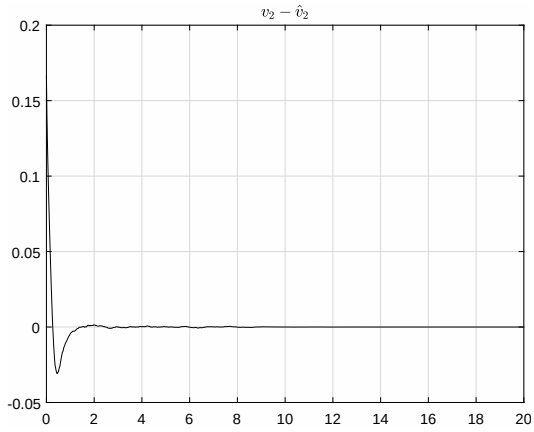

Figure 4.10: The estimation error of relative speeds for the two-machine system

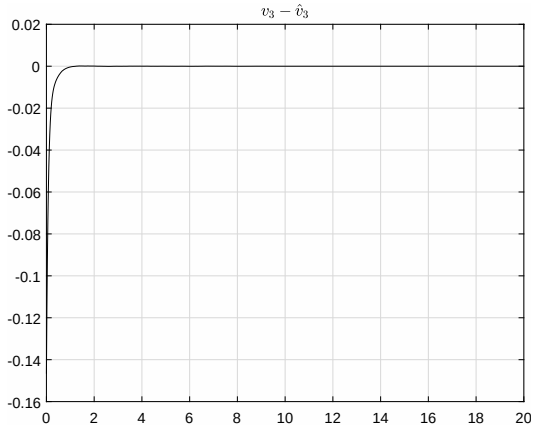

Figure 4.11: The estimation error of internal voltages for the first generator

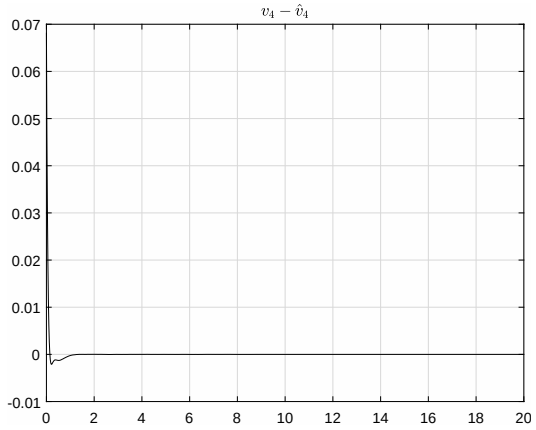

Figure 4.12: The estimation error of internal voltages for the second generator

In Fig. 4.9–4.12, the observation errors for the four states of the two-machine system converge rapidly to zero. The effectiveness of the design observer is thus illustrated.

4.6.3 Case Study: Three-Machine System

The simulation results for the three-machine system are demonstrated by the two cases presented. Again, we simulate the behavior of the three-machine power system for the same two cases discussed in the previous subsection.

4.6.3.1 Case 1

We start with the uncontrolled case. Similar to the two-machine system, we observe the states of relative angle $\delta_1 - \delta_3$ and $\delta_2 - \delta_3$, the relative speed $\omega_1 - \omega_3$ and $\omega_2 - \omega_3$, and internal voltage E_3.

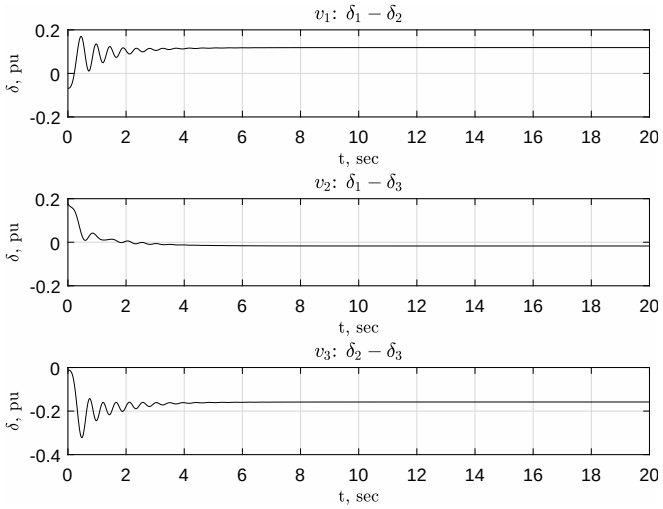

Figure 4.13: Rotor angle variations of the three-machine system

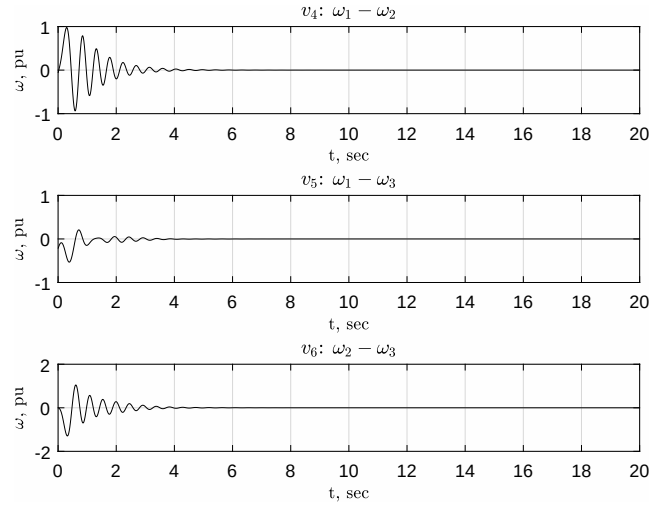

Figure 4.14: Relative speed variations of the three-machine system

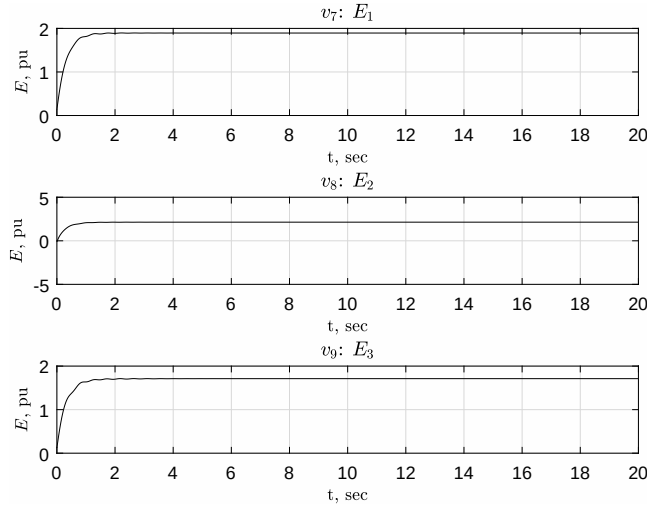

Figure 4.15: Internal voltages of the three-machine system

In Fig. 4.13–4.15, the system without control is stable, but it exhibits significant oscillations. In this case, the analytical investigation of a contraction region for the three-machine system is a diffucult task. Instead, it is more practical and realistic for our simulation results to present the contraction conditions.

4.6.3.2 Case 2

In this case, we present the simulations for the controlled case.

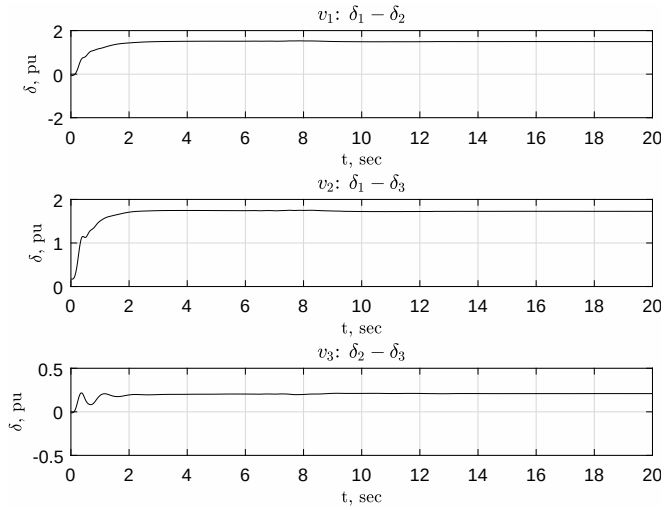

Figure 4.16: Rotor angle variations of the three-machine system for the controlled case

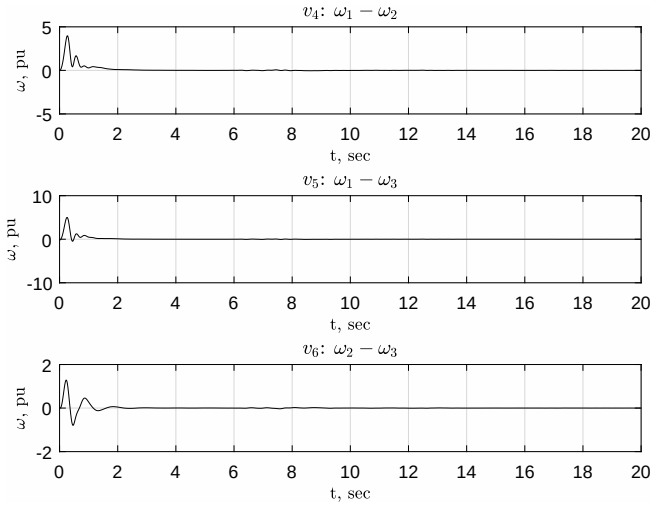

Figure 4.17: Relative speed variations of the three-machine system for the controlled case

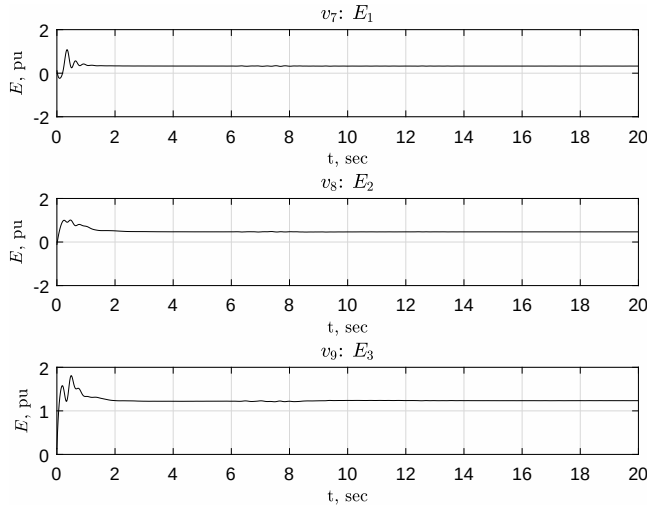

Figure 4.18: Internal voltage of the generators for the controlled case

From the simulation results in Fig. 4.16–4.18, it is clear that, despite the nonlinear interactions among different generators, the proposed control scheme is sufficient enough to enhance system stability and rapidly dampen the osculations for the three-machine system.

Finally, we present observer error dynamics for the three-machine system. The corresponding figures show the behaviors of different observation errors of the states of the system.

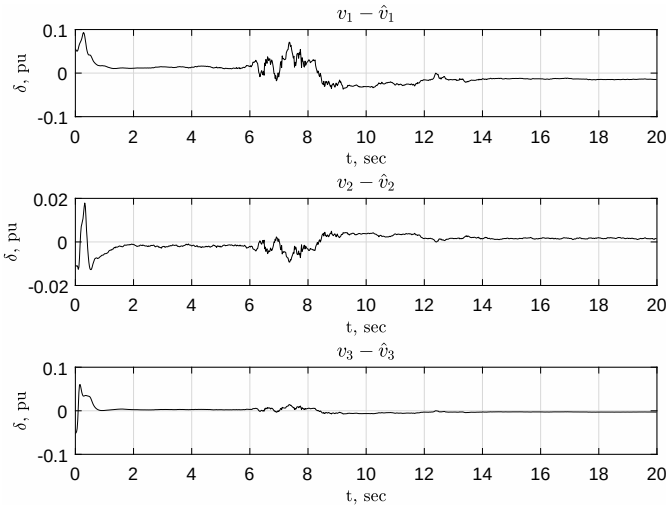

Figure 4.19: The estimation errors of rotor angles for the three-machine system

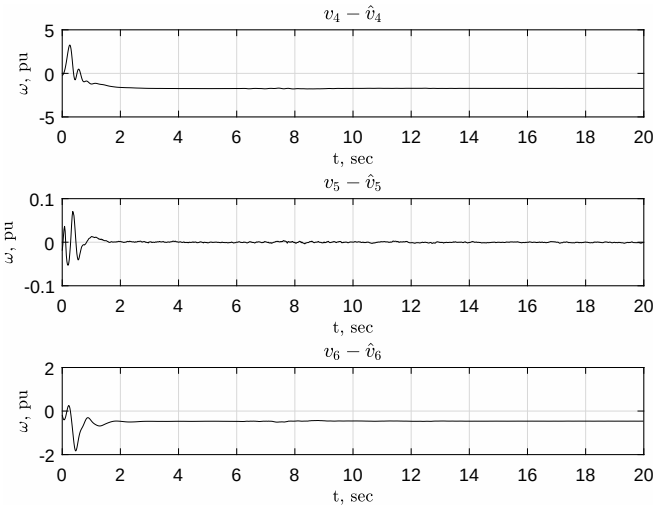

Figure 4.20: The estimation errors of relative speeds for the three-machine system

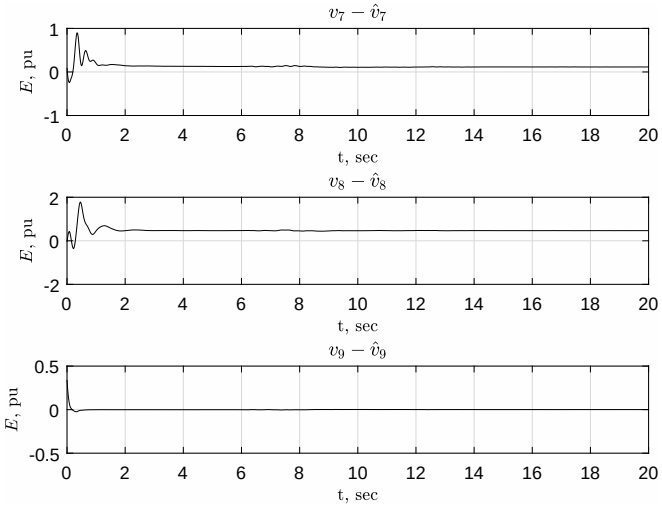

Figure 4.21: The estimation errors of internal voltages for the three-machine system

Finally, the observation errors of the three-machine system tend towards to zero with the desired convergence property. The estimation errors may lie outside in the origin but the EKF is consistent. Therefore, the effectiveness of the desired observer is established.

Chapter 5

The Integration of Renewables with Demand Participation

5.1 Introduction

Conic optimization is a powerful optimization technique that concerns the problem of minimizing a linear function over the intersection of an affine set and a closed convex cone, and is completely equivalent to convex optimization [298]. Many optimization problems such as linear programs, second-order cone programs, and semidefinite programs are convex optimization problems and can be recast in terms of conic optimization. Semidefinite optimization is an important class of conic optimization, which includes a special case where the cone is selected as both the semidefinite and the nonnegative matrices cone. Convex optimization problems are solved by primal-dual interior-point methods in practice. This chapter mainly presents fundamental results for solving the convex optimization problem that is applied to the optimal power flow problem.

The OPF problem aims to determine a steady-state (or optimal) operating point for an electric power system that minimizes an objective function which satisfies the system's different control schemes, operating constraints, and security requirements [299]. The variables of the OPF problem include both a set of dependent and control variables. The dependent variables include the complex voltages, as well as the reactive power, of generators performing voltage control at each bus. The control variables may include the apparent power output of the generator connected to each bus with a transformer and a phase shifter. The equality and inequality constraints of OPF are summarized as network equality constraints, and mainly include the power-flow equations that represent the relationship between bus voltages and power injections (i.e., the power balanced constraints); operating and physical limits such as inequality constraints on voltage magnitudes, active and reactive power generations, transmission line flows, and transformer taps; and operating capacity constraints on

shunt capacitors, reactors, etc. The sum of variable generation cost per unit time is usually selected as a desirable or appropriate cost function corresponding to an objective function. The objective function of an OPF problem can be seen in many different forms according to special-purpose applications. Despite the fact that the OPF problem is generally nonconvex, it is NP-hard in the worst case due to the nonlinearity of power-flow equations involving active power, reactive power, and voltage magnitude. To solve the OPF problem, numerous solution techniques and algorithms have been developed, including nonlinear programming (NLP), quadratic programming, Newton's methods, linear programming (LP) and mixed integer nonlinear programming, Lagrange relaxation, interior-point methods, decomposition methods, genetic algorithms, fuzzy logic, artificial intelligence, artificial neural networks, and particle swarm optimization [58], [59].

Semidefinite optimization is an important class of optimization problems and has been known as an efficient method in the theory and practice of approximation algorithms for over a decade. However, the nonconvex NLP formulation of the OPF problem, including certain constraints on power and voltage variables, entered the field of power systems considerably earlier, through a fundamental paper [299] which introduced a solution of nonconvexity of the OPF problem. The OPF problem is often reformulated as an NLP problem and is solved by NLP solvers. The SDP technique is used to reformulate the OPF problem into the SDP model to find a new solution for the OPF problem using interior-methods for SDP [46]. The main advantage of this techinique is to present an efficient approach to obtain Hessian and Jacobian-free solutions for the OPF problem. Thus, an OPF problem that is a highly nonconvex problem is accurately transformed into the SDP model, which is referred to as a convex optimization problem. To obtain an approximation of the global optimum solution, SDP relaxation in polynomial time is implemented for the OPF problem. The SDP has a zero duality gap and the SDP relaxation guarantees a zero duality gap or a strong duality; therefore, the SDP problem converges on the global optimum solution of the original OPF problem [68]. In practice, it is often difficult to obtain the global optimum solution for the OPF problem because the resulting SDP relaxation is too large to solve, and the solutions are not numerically (or physically) meaningful.

A few attempts demonstrate the failure of SDP relaxation in some of the test cases [63]. One of the main difficulties of the OPF is to transform and relax into SDP. The efficiency of solving the OPF problem by SDP mainly depends on two requirements. The first is the size of the square matrix variables (or the size of the LMI constraints), and the second is the number equalities (or the number of real variables). Here, the number of real variables of the problem is quadratic with the number of buses in the power system. To solve the larger square matrix variable for the SDP, more elapsed time and memory are required [300]. SDP relaxation with a large number of inequalities can be computationally intractable. From this perspective, the size of the SDP increases with the square of the number of buses in the system, which makes the solution of the OPF problem by the SDP computationally challenging for large power systems. Also, from a semidefinite programming perspective, a significant increase in the size of the SDP problem can be achieved by exploiting the sparsity of data matrices through matrix completion [301],[302]. In addition, most power system matrices are large and sparse. Power system matrices include large-scale semidefinite constraints which can also be decomposed into reduced-size constraints [303]. If their size is small, the SDP can be solved more efficiently. Moreover, if the reduced-size matrices obtained from these decompositions satisfies a rank condition, the large-scale semidefinite matrix also satisfies the rank condition. Then it is possible to find an optimal solution.

Throughout this chapter, in order to avoid some mathematical nuisances, we consider that all of the cones are closed convex cones and closed pointed convex cones with nonempty interiors. We then use standard notation: $\mathbb{S}$ is the set of real numbers, and $\mathbb{S}_+$ is the set of nonnegative integers. $\mathbb{S}^n$ denotes the real symmetric matrices of dimension $n \times n$. $\mathbb{S}^n_+$ is the cone of positive semidefinite matrices from $\mathbb{S}^n$. Notation $\preceq$ and $\succeq$ refer to matrix inequality signs in the positive semidefinite sense. We use $A \succeq 0$ to denote that $A \in \mathbb{S}^n$ (or $\mathbb{S}^n_+$) is a positive semidefinite matrix, and also use $A \succ 0$ to indicate that A is positive definite matrix. When we mention that a real matrix is positive semidefinite, we say that it is symmetric and has nonnegative eigenvalues. If a complex matrix is positive semidefinite, therefore it is Hermitian and has nonnegative eigenvalues. $\mathrm{Tr}(A)$ and A^{-1} trace and inverse a square matrix A, and A^{T} denotes a transpose of matrix A.

5.2 Semidefinite Program

Semidefinite programming (SDP) is a specific kind of convex optimization problem where a linear objective function of a symmetric matrix variable is optimized over the cone of a positive semidefinite and nonnegative matrix, and additional constraints are the positive semidefinite matrix [304]. All the matrices are restricted to be diagonal. However, SDP contains linear programming, convex quadratic programming, etc. In general, these problems cannot be formulated analytically. Rather, efficient methods such as primal-dual interior-point methods should be used to solve the convex optimization problem in practice. SDP can be solved with the worst-case complexity by using the primal-dual interior-point methods. In addition, we can easily solve problems including a large number of variables and constraints in a short computation time. The structured sparsity can be exploited, thus a large-scale problem with many thousands of variables and constraints can be solved using these methods. The major benefit of semidefinite programming is that optimization problems can be solvable in polynomial time. SDP problems can be handled reasonably and efficiently in practice using any installed solver package, or alternatively implemented by the user. Moreover, SDP can be used to obtain approximate solutions referred to as difficult problems, such as nonlinear or even nonconvex problems, for which one can not expect to obtain meaningful numerical results. In such cases, one has to rely on approximate solutions. SDP problems play a crucial role in a wide range of practical applications in research areas such as control theory, graph theory, circuit design, signal processing, and communication systems [305].

We can describe SDP relaxations using primal and dual methods referring to a primal-dual relationship. The SDP problem, which is considered to be a primal-dual pair of linear convex optimization problems, is formulated in matrix variables of the following form:

$$\begin{aligned} \text{minimize} \quad & \mathrm{Tr}(CX) \\ \text{subject to} \quad & \mathrm{Tr}(A_i X) = b_i \quad (i = 1, \ldots, m), \\ & X \in \mathcal{C}, \end{aligned} \tag{5.1}$$

where $\mathcal{C}$ is the cone of semidefinite and nonnegative matrices. That is, $\mathcal{C}$ represents

the matrices whose quadratic forms have nonnegative values on $\mathbb{S}_+^n$:

$$\mathcal{C} = \{A \in \mathbb{S}^n : x^{\mathrm{T}} A x \geq 0 \text{ for all } x \in \mathbb{S}_+^n\} \tag{5.2}$$

Here, the constraint x can be replaced by the matrix variable $X \in \mathbb{S}^n$ (unknown). Following this, the dual of (5.1)

$$\begin{aligned} &\text{maximize} && b^{\mathrm{T}} y \\ &\text{subject to} && \sum_{i=1}^{m} y_i A_i + S = C, \\ & && S \in \mathcal{C}^* \end{aligned} \tag{5.3}$$

where the matrix variable is $S \in \mathbb{S}^n$; the coefficient matrix A_p and the input data are a matrix C and may be considered to be symmetric without loss of generality; and $b \in \mathbb{R}^m$ and $y \in \mathbb{R}^m$ are two vector variables. Notice that the primal program (5.1) involves a corresponding dual program which is a maximization problem over the dual cone $\mathcal{C}^*$. To explain this concept in more detail, the triple $\{X, y, S\}$ is an optimal solution of SDP (5.1) and (5.3) if X is a minimum solution for a primal problem and $\{y, S\}$ is a maximum solution of dual problem. We conclude that X and $\{y, S\}$ are feasible solutions for primal and dual problems, respectively. X is the feasible solution for a primal problem and $\{y, S\}$ is a feasible solution for a dual problem that satisfies $X \succeq 0$ and $S \succeq 0$, respectively.

The equality standard form of SDP can equivalently be rewritten without using the dual variable S:

$$\begin{aligned} &\text{maximize} && b^{\mathrm{T}} y \\ &\text{subject to} && C - \sum_{i=1}^{m} y_i A_i \succeq 0 \end{aligned} \tag{5.4}$$

Therefore, the constraint (5.4) is a linear matrix inequality form of SDP. In contrast to primal problem (5.1), the dual problem (5.4) belongs to the cone $\mathcal{C}^*$ which is completely composed of positive matrices. In this case, both $\mathcal{C}$ and $\mathcal{C}^*$ are convex cones, thus (5.1) and (5.4) are called convex optimization problems.

For convex optimization problems, a nonzero duality gap can exist when either the primal or the dual problem is feasible. Duality in convex optimization problems can be stated with two fundamental definitions [304].

Definition 5.2.1 (**Weak Duality**). *Any primal-dual pair of convex (and even non-convex) programs can be expressed in the most common standard form* (5.1) *and* (5.3) *as* inf(P) *and* sup(D)*, respectively. The weak duality relation satisfies the inequality* $\inf(\mathrm{P}) \geq \sup(\mathrm{D})$.

For minimization and maximization, the notations inf and sup can be used, respectively. If $\tilde{X}$ is feasible for (P), and $\{\tilde{y}, \tilde{S}\}$ for (D), then the optimal objective values are denoted as $\mathrm{P}(\tilde{X})$ and $\mathrm{D}(\tilde{y}, \tilde{S})$. The above equation implies that the duality gap $\mathrm{P}(\tilde{X}) - \mathrm{D}(\tilde{y}, \tilde{S})$ is nonnegative for feasible solutions. The primal (resp. dual) is *unbounded* when $\mathrm{P}(\tilde{X}) = -\infty$ (resp. $\mathrm{D}(\tilde{y}, \tilde{S}) = +\infty$); it is *infeasible* when there is no feasible solution, which occurs when $\mathrm{P}(\tilde{X}) = +\infty$ (resp. $\mathrm{D}(\tilde{y}, \tilde{S}) = -\infty$). One problem can also be solved when its optimal value $\mathrm{P}(\tilde{X})$ (resp. $\mathrm{D}(\tilde{y}, \tilde{S})$) is obtained by at least one feasible primal (resp. dual) solution [306].

Definition 5.2.2 (**Strong Duality**). *The dual (resp. primal) problem guarantees a strictly feasible solution, i.e., equality of the optimal values ensures* $\mathrm{P}(\tilde{X}) = \mathrm{D}(\tilde{y}, \tilde{S})$ *and the dual (resp. primal) problem is either attained or infeasible.*

Following the LP case, if either the primal or the dual problem has a feasible solution, then both have feasible solutions, and there is no duality gap. In other words, the duality gap is zero, unless both problems are infesible. This implies strong duality for LP. On the other hand, this may be infeasible for SDP problems. In addition, even if the duality gap is zero, the optimal value cannot be attained for primal or dual problems. To overcome these difficulties, the form of SDP and its dual problem are satisfied by imposing a constraint qualification to get strong duality. The goal of constraint qualification is to ensure the existence of Lagrange multipliers at optimal conditions. The corresponding Lagrange multipliers are a feasible solution for the dual problem; indeed, the constraint qualification considers that both problems are feasible, and one of them is strictly feasible, and thus the constraint qualification guarantees that strong duality holds. In this way, it is possible to achieve primal and dual feasibility without admitting a zero duality gap. The most common constraint qualification is the Slater's constraint qualification which requires an interior point. If the primal problem has an interior point, then there is no gap between the primal-dual solution. Finally, it is easy to show that the Slater's constraint qualification

holds for an SDP problem, thus it attempts to generate a feasible matrix which is positive definite for the SDP problem of interest, see [298] for details.

5.2.1 Positive Semidefinite Matrices

A square matrix A is said to be positive semidefinite or nonnegative definite if $x^{\mathrm{T}}Ax \geq 0$. Similarly, the matrix A is said to be positive definite, which satisfies the condition for strict positivity for all $x \neq 0$. Obviously, the space of positive definite matrices is assumed from bounded sets $\mathbb{S}_{+}^{n}$ into bounded sets $\mathbb{S}^{n}$, and the set $\mathbb{S}_{+}^{n} \subset \mathbb{S}^{n}$ of positive semidefinite matrices is called a closed convex cone which is symbolized by $\mathcal{C}$.

Definition 5.2.3 (**Positive Semidefinite Matrix**). *Positive semidefinite matrices are the set of all positive semidefinite $n \times n$ matrices.*

However, a positive semidefinite matrix is a real matrix A that is symmetric (i.e., $A^{\mathrm{T}} = A$ has only principal minors and eigenvalues that are nonnegative. In other words, a symmetric matrix is positive semidefinite if, and only if, all its (real) eigenvalues are nonnegative. The trace and determinant of a positive semidefinite matrix are also non-negative. In addition, there exists matrix U such that $A = U^{\mathrm{T}}U$. Indeed, when A is an $n \times n$ Hermitian matrix, it means that $A > 0$ if and (only if) the determinant of every leading principal minor of A is positive, and $A \geq 0$ if (and only if) the determinant of every principal minor of A is nonnegative.

We can state one more important condition of positive semidefinite matrices.

Definition 5.2.4 (**Shur Complements**). *The matrix*

$$\begin{pmatrix} A & B \\ B^{\mathrm{T}} & C \end{pmatrix} \tag{5.5}$$

is positive semidefinite definite if, and only if, A is positive definite and $C - B^{\mathrm{T}}A^{-1}B$ is positive semidefinite definite.

The matrix $C - BA^{-1}B^{\mathrm{T}}$ is called the Shur Complement of A. We refer to [298],[304] for other definitions, theorems, and references therein.

5.3 Standard AC OPF Problem

We start with the definition of all buses along with the electric loads and generators connected to them. The system is represented by a power network formed of n-buses, with $\mathcal{N} = \{1, 2, \ldots, n\}$. Denote $\mathcal{G}$ and $\mathcal{N} - \mathcal{G}$ as the set of generator buses and non-generator buses (or load buses), respectively. $\mathcal{L}$ is all line flows, with the size of $\mathcal{N} \times \mathcal{N}$. P_{G_k} and Q_{G_k} are the active and reactive power of the generator at bus $k \in \mathcal{G}$. There is a known constant power load with the complex value $S_{D_k} = P_{D_k} + Q_{D_k}$, where P_{D_k} and Q_{D_k} are the active and reactive demands at bus $k \in \mathcal{N}$. $V_k = V_{d_k} + jV_{q_k}$ represents the voltage phasors in rectangular form at each bus $k \in \mathcal{N}$. S_{lm} is the apparent power on line $(l, m) \in \mathcal{L}$. $\mathbf{Y} \in \mathbb{C}^{n \times n}$ is the network admittance matrix, and is denoted as $\mathbf{Y} = \mathbf{G} + \mathbf{jB}$, where $\mathbf{G}$ and $\mathbf{B}$ are conductance and susceptance matrices, respectively. The standard formulation of a quadratic cost function can be written for each generator $k \in \mathcal{N}$,

$$C_k(P_{G_k}) = \sum_{k=1}^{n} \left(\alpha P_{G_k}^2 + \beta P_{G_k} + \gamma \right), \tag{5.6}$$

where α, β, and γ are system cost coefficient parameters. The objective function represents the cost minimization of active power generation to formulate the OPF problem. The standard OPF problem can be represented using either polar or rectangular forms. Here the vector of complex voltage is expressed by its real and imaginary parts in the rectangular form. Thus, the general formulation of the standard OPF problem in rectangular form is

$$\text{minimize} \quad \sum_{k\in\mathcal{G}} C_k(P_{G_k}) \tag{5.7a}$$

$$\text{subject to} \quad \underline{P}_{G_k} \le P_{G_k} \le \overline{P}_{G_k} \qquad \forall k \in \mathcal{G}, \tag{5.7b}$$

$$\underline{Q}_{G_k} \le Q_{G_k} \le \overline{Q}_{G_k} \qquad \forall k \in \mathcal{G}, \tag{5.7c}$$

$$\underline{V}_k \le |V_k| \le \overline{V}_k \qquad \forall k \in \mathcal{N}, \tag{5.7d}$$

$$|S_{lm}| \le \overline{S}_{lm} \qquad \forall (l,m) \in \mathcal{L}, \tag{5.7e}$$

$$P_k = V_{d_k} \sum_{i=1}^{n} (G_{ki}V_{di} - B_{ki}V_{qi}) + V_{q_k} \sum_{i=1}^{n} (B_{ki}V_{di} + G_{ki}V_{qi}) \qquad \forall k \in \mathcal{N}, \tag{5.7f}$$

$$Q_k = V_{d_k} \sum_{i=1}^{n} (-B_{ki}V_{di} - G_{ki}V_{qi}) + V_{q_k} \sum_{i=1}^{n} (G_{ki}V_{di} - B_{ki}V_{qi}) \qquad \forall k \in \mathcal{N}, \tag{5.7g}$$

where the net active and reactive power injection

$$P_k = P_{G_k} - P_{D_k} \quad \forall k \in \mathcal{G}\,, \qquad P_k = -P_{D_k} \quad \forall k \in \mathcal{N} - \mathcal{G}\,,$$
$$Q_k = Q_{G_k} - Q_{D_k} \quad \forall k \in \mathcal{G}\,, \qquad Q_k = -Q_{D_k} \quad \forall k \in \mathcal{N} - \mathcal{G}\,,$$

$\underline{P}_{G_k}$, $\overline{P}_{G_k}$, $\underline{Q}_{G_k}$, $\overline{Q}_{G_k}$, $\underline{V}_k$ and $\overline{V}_k$ are given lower/upper network constraints for active and reactive power limits and bus voltages, respectively. $\overline{S}_{lm}$ is the maximum limit of branch flow on line $(l-m)$. The power-flow equations P_k and Q_k-in other words, the nodal power balancing equations- are nonlinear equality constraints. However, the variable limits include inequality constraints on the upper and lower limits on all bus voltages, active and reactive sources, and branch flows. For the OPF problem (5.7), unknown parameters (or optimization variables) are the vectors of complex voltage V_k and the vectors of generator active and reactive power injections, P_{G_k} and Q_{G_k}. P_k and Q_k are also known as independent control variables; V_k (here the magnitude and phase angle of voltage at node k) is the dependent variable for the optimization problem. The main objective of the standard OPF is to minimize the objective function $C_k(P_{G_k})$ over the unknown parameters subject to power-flow

equations (5.7f) and (5.7g) for each bus by representing physical and operating constraints such as limits on branch flows or bus voltages. In the OPF problem (5.7), the cost function is convex; the constraints on the active and reactive power generations, the complex voltages, and line flows are also convex, but the equality constraints (5.7f), (5.7g) are nonconvex; thus, the OPF problem (5.7) is nonconvex [222].

Alternatively, the nodal real and reactive power balancing equations are represented in the polar form. The variables are the voltage magnitude and phase angle at each bus and the real and reactive power flows in polar form. Thus, we have

$$P_k = V_k \sum_{i=1}^{n} V_i \left(G_{ki} \cos(\delta_k - \delta_i) + B_{ki} \sin(\delta_k - \delta_l) \right), \tag{5.8}$$

$$Q_k = V_k \sum_{i=1}^{n} V_i \left(G_{ki} \sin(\delta_k - \delta_i) - B_{ki} \cos(\delta_k - \delta_i) \right). \tag{5.9}$$

The voltage magnitudes must be nonnegative to maintain feasibility of the OPF problem. The relationship between the OPF problem and the power-flow problem is that solutions of the power-flow problem satisfy all transmission line limits and include the bounds on voltages and active and reactive powers; thus, the solutions specify a feasible solution for the OPF problem.

The power-flow problem is a nonlinear problem, which requires the solution of a large set of nonlinear equations for bus voltages and bus phase angles [275]. Nonlinear problems are usually numerically solved through a process of linearization and iterative methods [246]. In solving a power-flow problem, the buses in the power system can be classified into three types: load, generator, and slack buses. Firstly, at load buses, which are also called PQ buses, P and Q are specified as known quantities, and the equations (5.8), (5.9) are enforced at bus k; thus, the complex voltage (V, θ) at bus k is to be determined. Secondly, for the generator buses, which are also called PV buses, P and V are specified as known quantities, and enforces the active power equation (5.8); thus, Q and θ at bus k are to be determined.

In addition, the generator buses may have some controllable reactive power sources, and evaluating the reactive power is required at a bus to maintain voltage magnitude at that bus. Power flows in the generator buses are also solved to obtain the change in reactive power resulting from the change in voltage magnitude. As we have previously stated, as part of the linearization methods, the power-flow problem constructs the

Jacobian matrix, which results from linearization of nonlinear power-flow equations. The Jacobian matrix gives the linearized relationship between small changes in voltage angle and voltage magnitude and the small changes in real and reactive power. After finding a power-flow solution, power flows check whether a specified tolerance is acceptable given the calculating power mismatches. In the case that the tolerance is acceptable, then the calculated reactive power of each generator is checked to determine whether it is within upper limits, and the columns and rows of the Jacobian matrix that correspond to this generator bus are deleted because the voltage magnitude of the generator bus is known. Otherwise, if the generator reactive limit is reached, the generator bus will be changed into a load bus, keeping the columns and rows of the Jacobian matrix that are corresponding to this generator bus. Similarly, if generator bus violate their reactive power limits, they are considered to be load buses.

Thirdly, in power systems, only one arbitrary bus is chosen as a slack bus. The slack bus is an accepted fictitious idea. All loads are constant and all generator outputs are fixed expect one bus that is slack. It is characterized a fixed voltage magnitude and phase angle; thus, we do not know its active power injection. V and θ are known quantities for a slack bus. P and Q need to be solved, and also can vary. The generator bus is selected as slack supplies to the power network. The system losses are not known until the final solution is calculated. The solution having the least slack bus active power generation results in the solution with the lowest losses [223].

5.4 RESs Injection to the OPF Problem

Throughout this work, intermittent RESs are mainly considered as wind turbines and PV generators. We neglect uncertainties due to intermittency in generation. RESs are integrated to the power system using the power-flow equations of the standard OPF problem in (5.7). The semidefinite relaxation of the OPF problem is enhanced through demand-side participation for RESs which permits the reformulation of additional variables, costs and/or constraints. In this regard, the power-flow equations including conventional generators and RESs, may be written in rectangular form the OPF problem.

The electrical network can be modeled by power-flow equations with the rectangular formulation as complex voltages $V_{d_k} + V_{q_k}$ and the sum of the complex admittance $G_{ki} + jB_{ki}$. It is assumed that the bus power injections can be supplied by both conventional generation and renewable generation. The power-flow equations at bus $k \in \mathcal{N}$ are given by

$$\begin{aligned} P_{G_k} + P^r_{k,\text{inj}} - P_{D_k} = V_{d_k} \sum_{i=1}^{n} (G_{ik} V_{d_i} - B_{ik} V_{q_i}) \\ + V_{q_k} \sum_{i=1}^{n} (B_{ik} V_{d_i} + G_{ik} V_{q_i}), \end{aligned} \tag{5.10}$$

$$\begin{aligned} Q_{G_k} + Q^r_{k,\text{inj}} - Q_{D_k} = V_{d_k} \sum_{i=1}^{n} (-B_{ik} V_{d_i} - G_{ik} V_{q_i}) \\ + V_{q_k} \sum_{i=1}^{n} (G_{ik} V_{d_i} - B_{ik} V_{q_i}), \end{aligned} \tag{5.11}$$

where $P^r_{k,\text{inj}}$ and $Q^r_{k,\text{inj}}$ denote active and reactive renewable power injections for some $k \in \mathcal{N}$. The voltage magnitude equation is

$$|V_k|^2 = V_{d_k}^2 + V_{q_k}^2 \qquad \forall k \in \mathcal{N}, \tag{5.12}$$

and must be satisfied at all buses, and only two nonlinear equations (5.7f) and (5.7g) are directly enforced for some bus k when solving the power-flow problem. For conventional resources, the active powers are measured at all buses. The reactive powers are measured at $(\mathcal{N} - \mathcal{G})$ buses, and voltage magnitudes are measured at all buses. On the other hand, for unconventional resources, the $\mathcal{G}$ buses and/or $(\mathcal{N} - \mathcal{G})$ buses may contain RESs. Then the active power generation $P^r_{G_k}$ and the reactive power generation $Q^r_{G_k}$ are injected to the corresponding buses. The network constraints, including both conventional and unconventional energy generation, are described by the following equation

$$\begin{aligned} \{P_{G_k}\}_{k\in\mathcal{G}} + \left\{P^r_{k,\text{inj}}\right\}_{k\in\mathcal{N}} + \left\{Q^r_{k,\text{inj}}\right\}_{k\in\mathcal{N}-\mathcal{G}} = \left\{|V_k|^2\right\}_{k\in\mathcal{N}} \\ + \{P_{D_k}\}_{k\in\mathcal{G}} + \{S_{D_k}\}_{k\in\mathcal{N}-\mathcal{G}} \end{aligned} \tag{5.13}$$

where P_{G_k} is the active power generation in $\mathcal{G}$ buses produced from conventional sources, $P^r_{k,\text{inj}}$ is the active renewable power generation for all $\mathcal{N}$ buses, $Q^r_{k,\text{inj}}$ is the

reactive renewable power generation for $(\mathcal{N}-\mathcal{G})$ buses, P_{D_k} is the active load demand in $\mathcal{G}$ buses, and S_{D_k} is the active and reactive load demand for all non-slack buses.

From now on, we will restrict our attention to renewable resource outputs for only the active power generation. Therefore, we assume that the reactive power generation $Q^r_{G_k}$ is zero unless otherwise specified. The active renewable power is a positive (random) value. The renewable power generation in each period T, and the renewable generation estimations in a $(T-1)$ period, are assumed to be known. Thus,

$$\hat{P}^r_{G_k}(T-1) > 0 \qquad \forall k \in \mathcal{N}, \tag{5.14}$$

$$\hat{Q}^r_{G_k}(T-1) > 0 \qquad \forall k \in \mathcal{N}-\mathcal{G}, \tag{5.15}$$

and its cost $C_r(P^r_{G_k}(T))$ for some $k \in \mathcal{G}$. Moreover, we assume real-time measurements of the active renewable generation, where

$$P^r_{G_k}(T) := g\left(\hat{P}^r_{G_k}(T-1)\right), \tag{5.16}$$

$$\hat{Q}^r_k(T) := g\left(\hat{Q}^r_k(T-1)\right), \tag{5.17}$$

and where $g(\cdot)$ is a piecewise-defined function which bears all information on the nonlinearity of RESs dynamics. Next, the active and reactive renewable power generation must lie between lower and upper bounds

$$\underline{P}^r_{G_k} \le P^r_{G_k}(T) \le \overline{P}^r_{G_k} \qquad \forall k \in \mathcal{N}, \tag{5.18}$$

$$\underline{Q}^r_{G_k} \le Q^r_{G_k}(T) \le \overline{Q}^r_{G_k} \qquad \forall k \in \mathcal{N}-\mathcal{G}. \tag{5.19}$$

The variable $P^r_{G_k}(T)$ is denoted as the renewable generation and allows electric loads to be satisfied, which is represented as a *negative demand* in practice [37],[208]. Indeed, the $P^r_{G_k}(T)$ is assumed to be nondispatchable renewable generation for some $k \in \mathcal{N}-\mathcal{G}$. Again,

$$0 \le P^r_{G_k}(T) \le \overline{P}^r_{G_k} \qquad \forall k \in \mathcal{N}. \tag{5.20}$$

Similarly, the load-demand estimation is also assumed to be known as

$$P_{D_k}(T) = h\big(P_{D_k}(T-1)\big) \qquad \forall k \in \mathcal{N}-\mathcal{G}, \tag{5.21}$$

where $h(\cdot)$ is the load estimation function, which can be obtained from the load estimation techniques in relevant literature, see [307],[308],[309]. P_{D_k} is the actual loads for each $k \in \mathcal{N} - \mathcal{G}$. From this,

$$\Delta P_{D_k}(T) = P_{D_k}(T) - P^r_{G_k}(T) \qquad \forall k \in \mathcal{N} - \mathcal{G}, \tag{5.22}$$

where $\Delta P_{D_k}(T)$ is the excess load demand (supply) and $P^r_{G_k}(T)$ appears on negative loads. Then, $\sum_{k\in\mathcal{G}} P_{G_k} = \Delta P_{D_k}(T)$ unless $\Delta P_{D_k}(T) < 0$ for every $k \in \mathcal{N} - \mathcal{G}$. Note that, $\sum_{k\in\mathcal{G}} P_{G_k}$ represents dispatchable (conventional) generation units. To this end, the active load demand constrains are

$$\underline{P}_{D_k} \leq P_{D_k}(T) \leq \overline{P}_{D_k}, \tag{5.23}$$

$$\overline{P}_{D_k} \leq \sum_k P_{D_k}(T) \qquad \forall k \in \mathcal{N} - \mathcal{G}. \tag{5.24}$$

Finally, the balancing active power including RESs is

$$P_{b_k}(T) = \sum_{k\in\mathcal{G}} P_{G_k} - \Delta P_{D_k}(T) \qquad \forall k \in \mathcal{N}. \tag{5.25}$$

In view of the above expressions, results following the OPF problem, including demand-side participation for RESs, can be written as follows:

$$\begin{aligned} \text{minimize} \quad & \sum_{k\in\mathcal{G}} C_k(P_{G_k}) \\ \text{subject to} \quad & \underline{P}_{G_k} \leq P_{G_k} \leq \overline{P}_{G_k} \qquad \forall k \in \mathcal{G}, \\ & (5.14),\ (5.16),\ (5.20),\ (5.21),\ (5.22),\ (5.23),\ (5.24), \\ & \sum_{k\in\mathcal{G}} P_{G_k} = \sum_k \Delta P_{D_k}(T) \qquad \forall k \in \mathcal{N} - \mathcal{G}. \end{aligned} \tag{5.26}$$

5.5 SDP Reformulation

In this section, the standard OPF problem in (5.7) and the optimization problem in (5.26) are transformed into the SDP problem [68],[62]. In order to describe our results, one needs to represent the matrices used in the semidefinite programming relaxation of the OPF problem. To do this, the following matrices are formulated for

the active and reactive power injections, and the square of the voltage magnitude at bus k, respectively. We obtain,

$$\mathbf{Y}_k = 0.5 \begin{bmatrix} \mathrm{Re}(Y_k + Y_k^{\mathrm{T}}) & \mathrm{Im}(Y_k^{\mathrm{T}} - Y_k) \\ \mathrm{Im}(Y_k - Y_k^{\mathrm{T}}) & \mathrm{Re}(Y_k + Y_k^{\mathrm{T}}) \end{bmatrix}, \tag{5.27}$$

$$\hat{\mathbf{Y}}_k = -0.5 \begin{bmatrix} \mathrm{Im}(Y_k + Y_k^{\mathrm{T}}) & \mathrm{Re}(Y_k^{\mathrm{T}} - Y_k) \\ \mathrm{Re}(Y_k - Y_k^{\mathrm{T}}) & \mathrm{Im}(Y_k + Y_k^{\mathrm{T}}) \end{bmatrix}, \tag{5.28}$$

$$\mathbf{M}_k = \begin{bmatrix} e_k e_k^{\mathrm{T}} & \mathbf{0} \\ \mathbf{0} & e_k e_k^{\mathrm{T}} \end{bmatrix}, \tag{5.29}$$

where the matrix $\mathbf{Y}_k = e_k e_k^{\mathrm{T}} \mathbf{Y}$ and $e_k \in \mathbb{R}^n$ has its kth entry equal to 1, and the other entries have zeros. Therefore,

$$e_1 = [1, 0, \ldots, 0]\,,\ e_2 = [0, 1, \ldots, 0]\,, \ldots,\ e_n = [0, 0, \ldots, n]\,. \tag{5.30}$$

The set $\{e_1, \ldots, e_n\}$ is also known as the unit vector in the appropriate dimension. Then we define the SDP variable matrix $\mathbf{X} \in \mathbb{R}^{2n}$ involving the vector of the real and imaginary parts of bus voltages

$$\mathbf{X} = \begin{bmatrix} \mathrm{Re}\{\mathbf{V}\}^{\mathrm{T}} & \mathrm{Im}\{\mathbf{V}\}^{\mathrm{T}} \end{bmatrix}^{\mathrm{T}}. \tag{5.31}$$

Based on these definitions, the formulations of the OPF problem can be rewritten in terms of the SDP variable matrix $\mathbf{X}$, and it can be factorized as $\mathbf{X}\mathbf{X}^T$. In this case, by defining the variable (or loading vector), matrix $\mathbf{X}$ is lifted into a symmetric, positive semidefinite, and rank-one matrix $\mathbf{W} \in \mathbb{R}^{2n \times 2n}$-that is, $\mathbf{W} = \mathbf{X}\mathbf{X}^{\mathrm{T}}$. $\mathrm{Tr}\{\mathbf{Y}_k \mathbf{W}\}$, $\mathrm{Tr}\{\hat{\mathbf{Y}}_k \mathbf{W}\}$, and $\mathrm{Tr}\{\mathbf{M}_k \mathbf{W}\}$ represent the active and reactive power injections, and the square of the voltage magnitude at the bus k, respectively.

Using the matrices (5.27),(5.29), the net active power injection with each bus k can be written in the following form:

$$P_{G_k} - P_{D_k} = \sum_{i=1}^{n} \mathrm{Re}\{Y_{ki}\}\,(V_{d_k} V_{d_i} + V_{q_k} V_{q_i}) - \mathrm{Im}\{Y_{ki}\}\,(V_{d_k} V_{q_i} - V_{q_k} V_{d_i})\,. \tag{5.32}$$

We can verify that $P_{G_k} - P_{D_k} = \mathrm{Tr}\{\mathbf{Y}_k \mathbf{W}\}$. Hence, we give a proof.

Proof.

$$
\begin{aligned}
P_k &= \mathrm{Re}\left\{V_k I_k^*\right\} \\
&= \underbrace{\mathrm{Re}\left\{ \begin{bmatrix} V_1 \\ \vdots \\ V_n \end{bmatrix}^* \begin{bmatrix} e_1 \\ \vdots \\ e_n \end{bmatrix} \begin{bmatrix} e_1 \\ \vdots \\ e_n \end{bmatrix}^{\mathrm{T}} \begin{bmatrix} Y_{11} & \cdots & Y_{1n} \\ \vdots & \ddots & \vdots \\ Y_{n1} & \cdots & Y_{nn} \end{bmatrix} \begin{bmatrix} V_1 \\ \vdots \\ V_n \end{bmatrix} \right\}}_{\mathrm{Re}\left\{\mathbf{V}^* e_k e_k^* \mathbf{I}\right\}}. \\
&= \underbrace{\mathrm{Re}\left\{ \begin{bmatrix} V_1 \\ \vdots \\ V_n \end{bmatrix}^* \begin{bmatrix} Y_{11} & \cdots & Y_{1n} \\ \vdots & \ddots & \vdots \\ Y_{n1} & \cdots & Y_{nn} \end{bmatrix} \begin{bmatrix} V_1 \\ \vdots \\ V_n \end{bmatrix} \right\}}_{\mathrm{Re}\{\mathbf{V}^* Y_k \mathbf{V}\} \text{ where } Y_k = e_k e_k^{\mathrm{T}} Y.} \\
&= \mathrm{Re}\left\{ \begin{bmatrix} V_{d_1} + jV_{q_1} \\ \vdots \\ V_{d_n} + jV_{q_n} \end{bmatrix}^* \begin{bmatrix} Y_{11} & \cdots & Y_{1n} \\ \vdots & \ddots & \vdots \\ Y_{n1} & \cdots & Y_{nn} \end{bmatrix} \begin{bmatrix} V_{d_1} + jV_{q_1} \\ \vdots \\ V_{d_n} + jV_{q_n} \end{bmatrix} \right\} \\
&= \begin{bmatrix} V_{d_1} & \cdots & V_{d_n} \end{bmatrix} \mathrm{Re}\left\{Y_n\right\} \begin{bmatrix} V_{d_1} \\ \vdots \\ V_{d_n} \end{bmatrix} + \begin{bmatrix} V_{q_1} & \cdots & V_{q_n} \end{bmatrix} \mathrm{Re}\left\{Y_n\right\} \begin{bmatrix} V_{q_1} \\ \vdots \\ V_{q_n} \end{bmatrix} \\
&- \begin{bmatrix} V_{d_1} & \cdots & V_{d_n} \end{bmatrix} \mathrm{Im}\left\{Y_n\right\} \begin{bmatrix} V_{q_1} \\ \vdots \\ V_{q_n} \end{bmatrix} + \begin{bmatrix} V_{q_1} & \cdots & V_{q_n} \end{bmatrix} \mathrm{Im}\left\{Y_n\right\} \begin{bmatrix} V_{d_1} \\ \vdots \\ V_{d_n} \end{bmatrix}.
\end{aligned}
\tag{5.33}
$$

The SDP variable matrix $\mathbf{X}$ can be written into a 2×2 block structure including the real and imaginary parts of the bus voltages:

$$
\mathbf{X} = \begin{bmatrix} V_{d_k}^2 & V_{d_k} V_{q_k} & V_{d_k} V_{d_i} & V_{d_k} V_{q_i} \\ V_{q_k} V_{d_k} & V_{q_k}^2 & V_{q_k} V_{d_i} & V_{q_k} V_{q_i} \\ V_{d_i} V_{d_k} & V_{d_i} V_{q_k} & V_{d_i}^2 & V_{d_i} V_{q_i} \\ V_{q_i} V_{d_k} & V_{q_i} V_{q_k} & V_{q_i} V_{d_i} & V_{q_i}^2 \end{bmatrix}. \tag{5.34}
$$

Thus, the active power injected at bus k is obtained as

$$
\mathbf{X}^{\mathrm{T}} \begin{bmatrix} \mathrm{Re}\left\{Y_k\right\} & -\mathrm{Im}\left\{Y_k\right\} \\ \mathrm{Im}\left\{Y_k\right\} & \mathrm{Re}\left\{Y_k\right\} \end{bmatrix} \mathbf{X}. \tag{5.35}
$$

However, consider Eq. (5.35), and its symmetric $P_k + P_k^{\mathrm{T}}$. Following this, a sum of the symmetric matrix $P_k = 1/2(P_k + P_k^{\mathrm{T}})$, since

$$\begin{aligned} &= \frac{1}{2}\mathbf{X}^{\mathrm{T}} \begin{bmatrix} \mathrm{Re}(Y_k + Y_k^{\mathrm{T}}) & \mathrm{Im}(Y_k^{\mathrm{T}} - Y_k) \\ \mathrm{Im}(Y_k - Y_k^{\mathrm{T}}) & \mathrm{Re}(Y_k + Y_k^{\mathrm{T}}) \end{bmatrix} \mathbf{X} \\ &= \mathbf{X}^{\mathrm{T}}\mathbf{Y}_k\mathbf{X} \end{aligned} \tag{5.36}$$

where

$$\mathbf{Y}_k = \frac{1}{2} \begin{bmatrix} \mathrm{Re}(Y_k + Y_k^{\mathrm{T}}) & \mathrm{Im}(Y_k^{\mathrm{T}} - Y_k) \\ \mathrm{Im}(Y_k - Y_k^{\mathrm{T}}) & \mathrm{Re}(Y_k + Y_k^{\mathrm{T}}) \end{bmatrix}.$$

Moreover, taking $\mathbf{W} = \mathbf{X}\mathbf{X}^{\mathrm{T}}$ and using the properties of the trace operator, we derive the net active power injection

$$P_k = \mathrm{Tr}\{\mathbf{Y}_k\mathbf{W}\}. \tag{5.37}$$

□

In a similar way, the net reactive power injection can be rewritten as

$$Q_{G_k} - P_{D_k} = -\sum_{i=1}^{n} \mathrm{Re}\left\{Y_{ki}\right\}\left(V_{d_k}V_{q_i} - V_{q_k}V_{d_i}\right) + \mathrm{Im}\left\{Y_{ki}\right\}\left(V_{q_k}V_{q_i} + V_{d_k}V_{d_i}\right), \tag{5.38}$$

and $\mathrm{Tr}\{\hat{\mathbf{Y}}_k\mathbf{W}\}$ and $\mathrm{Tr}\{\mathbf{M}_k\mathbf{W}\}$ can be proved in the same way. Based on these analyses, the corresponding results are given in the following equations:

$$Q_k = \mathrm{Tr}\{\hat{\mathbf{Y}}_k\mathbf{W}\} \qquad \forall k \in \mathcal{N}, \tag{5.39}$$

$$|V_k|^2 = \mathrm{Tr}\{\mathbf{M}_k\mathbf{W}\} \qquad \forall k \in \mathcal{N}. \tag{5.40}$$

In conclusion, the power balance equation can be rewritten in terms of SDP reformulation:

$$P_k + jQ_k = V_k I_k^{\star} = (e_k^* V)(e_k I_k^*) = \mathrm{Tr}\{VV^*Y^*e_k e_k^*\} \qquad \forall k \in \mathcal{N}. \tag{5.41}$$

Now, both problems (5.7) and (5.26) are rewritten in terms of the matrix variable

$\mathbf{W}$ as follows,

$$\text{minimize} \quad \sum_{1}^{T}\left(\sum_{k\in\mathcal{G}} s_k\right) \tag{5.42a}$$

$$\text{subject to} \quad \underline{P}_{G_k} \le P_{G_k} \le \overline{P}_{G_k} \qquad \forall k \in \mathcal{G}, \tag{5.42b}$$

$$P_{b_k}(T) = \text{Tr}\{\mathbf{Y}_k\mathbf{W}\} \qquad \forall k \in \mathcal{N}, \tag{5.42c}$$

$$\underline{Q}_{b_k} \le \text{Tr}\{\hat{\mathbf{Y}}_k\mathbf{W}\} \le \overline{Q}_{b_k} \qquad \forall k \in \mathcal{N}, \tag{5.42d}$$

$$(\underline{V}_k)^2 \le \text{Tr}\{\mathbf{M}_k\mathbf{W}\} \le (\overline{V}_k)^2 \qquad \forall k \in \mathcal{N}, \tag{5.42e}$$

$$\begin{bmatrix} a_{k1} & a_{k2} \\ a_{k2} & -1 \end{bmatrix} \preceq 0 \qquad \forall k \in \mathcal{G}, \tag{5.42f}$$

$$\mathbf{W} \succeq 0, \tag{5.42g}$$

$$\text{rank}(\mathbf{W}) = 1, \tag{5.42h}$$

where

$$a_{k1} = \beta\left[\text{Tr}\{\mathbf{Y}_k\mathbf{W}\} + P_{D_k}\right] - s_k, \tag{5.43a}$$

$$a_{k2} = \sqrt{\gamma}\left[\text{Tr}\{\mathbf{Y}_k\mathbf{W}\} + P_{D_k}\right] \tag{5.43b}$$

for every $k \in \mathcal{G}$, and

$$\underline{Q}_{b_k} = \sum_{k\in\mathcal{G}} \underline{Q}_{G_k} - Q_{D_k} \qquad \text{for all } k \in \mathcal{N}, \tag{5.44}$$

$$\overline{Q}_{b_k} = \sum_{k\in\mathcal{G}} \overline{Q}_{G_k} - Q_{D_k} \qquad \text{for all } k \in \mathcal{N}. \tag{5.45}$$

Here, if $\mathbf{W}$ is an optimal solution to the above problem, then $\mathbf{W} \succeq 0$ and $\mathbf{rank}(\mathbf{W}) = 1$ mean that we have $\mathbf{W} = \mathbf{X}\mathbf{X}^{\text{T}}$ a with unit trace. In other words, the SDP variable matrix X appears solely through $\mathbf{W} = \mathbf{X}\mathbf{X}^{\text{T}}$. We thus reformulate the OPF problem in terms of $\mathbf{X}$ only, and $\mathbf{X}\mathbf{X}^{\text{T}}$ is equivalent to $\text{Tr}(\mathbf{X}) = 1$, $\mathbf{W} \succeq 0$ and $\text{rank}(\mathbf{W}) = 1$. In addition, s_k is a scalar; using the the equivalence (5.42f), $\left(\alpha P_{G_k}^2 + \beta P_{G_k} + \gamma\right) \preceq s_k$ can be seen using Schur's complement formula [310],[66].

Remark 7. *$P_{G_k}^r$ is considered as negative load for every $k \in \mathcal{N} - \mathcal{G}$ buses. It means that*

$$\begin{cases} P_{G_k}^r, \ \textit{nondispatchable} & \textit{if } k \in \mathcal{N} - \mathcal{G}; \\ \quad \textit{dispatchable} & \textit{otherwise.} \end{cases}$$

Also, $P_{D_k} = 0$ *and* $Q_{D_k} = 0$ *for* $k \in \mathcal{G}$ *buses. In addition* $P_{G_k} = 0$ *and* $Q_{G_k} = 0$ *for every* $k \in \mathcal{N} - \mathcal{G}$ *buses.*

Remark 8. *The renewable generation outputs* $P^r_{G_k}$ *for every* $k \in \mathcal{G}$ *in optimization problem* (5.42) *are not considered to be decision variables. The problem* (5.42) *without renewable generation includes* P_{G_k}, $k \in \mathcal{G}$ *and the number of generators corresponding to the decisions being made. The solution of* (5.42) *specifies the optimal decisions* P_{G_k}, Q_{G_k} *and* V_k *to satisfy the excess demand* ΔP_{D_k}.

The problem (5.42) has a linear cost function and convex constraints. As expected, the constraint (5.42h) is nonconvex, hence we cannot expect to obtain a global solution. To remove the rank constraint, we formulate the optimization problem (5.42) using SDP in the dual formulation. Then we make use of the fact that the auxiliary variables, called Lagrange multipliers, are introduced. These multipliers provide an optimal solution for the dual problem. Here, the triple Lagrange multipliers $\{\lambda_k, \gamma_k, \mu_k\}_{k\in\mathcal{N}}$ are given by

$$\Lambda_k = \begin{cases} \overline{\lambda}_k - \underline{\lambda}_k + a_{k1} + 2\sqrt{a_{k2}}\ \mathbf{r}_k & \text{if } k \in \mathcal{G}\,, \\ \overline{\lambda}_k - \underline{\lambda}_k & \text{otherwise}\,. \end{cases} \tag{5.46}$$

$$\Gamma_k = \overline{\gamma}_k - \underline{\gamma}_k \qquad \text{for all } k \in \mathcal{N}, \tag{5.47}$$

$$\Psi_k = \overline{\psi}_k - \underline{\psi}_k \qquad \text{for all } k \in \mathcal{N}. \tag{5.48}$$

With these definitions, the cost function is

$$\begin{aligned} h = &- \sum_{1}^{T} \sum_{i\in\mathcal{G}} r_{2i} - \sum_{i\in\mathcal{G}_r} \rho_i \\ &+ \sum_{1}^{T} \sum_{k\in\mathcal{N}} \Big\{ \Lambda_k \Delta P_{D_k} + \Gamma_k Q_{D_k} + \underline{\lambda}_k \underline{P}_{G_k} - \overline{\lambda}_k \overline{P}_{G_k} \\ &+ \underline{\gamma}_k \underline{Q}_{G_k} - \overline{\gamma}_k \overline{Q}_{G_k} + \underline{\psi}_k (\underline{V}_k)^2 - \overline{\psi}_k (\overline{V}_k)^2 + \underline{\xi}_k \underline{P}^r_{G_k} \\ &- \overline{\xi}_k \overline{P}^r_{G_k} \Big\}, \end{aligned} \tag{5.49}$$

where $\mathcal{G}_r$ is the number of renewable resources in the power grid.

Remark 9. *We assume that the marginal cost of renewable power* $C_r(P^r_{G_k}(T)) \equiv 0$ *for every* $k \in \mathcal{G}_r$. *We also assume that, for each period* T, $P_{b_k}(T)$ *is the balancing*

power and $C_b(P_{b_k}(T))$ *is its cost for every* $k \in \mathcal{N}$. $\mathcal{C}_b(\cdot, T)$ *is convex and continuously differentiable with* $C_b(0,T) = 0$. *The total cost consists of the cost* C_b *of the balancing power from the conventional resources in the power grid.*

Next, the nonconvex rank constraint (5.42h) is removed and we introduce the dual formulation of the SDP relaxation for the OPF problem (5.42), which is defined as follows:

$$\begin{aligned}
&\text{maximize} && h && (5.50a)\\
&\text{subject to} && \sum_{k\in\mathcal{N}} \left\{\Lambda_k \mathbf{Y}_k + \Gamma_k \hat{\mathbf{Y}}_k + \Psi_k \mathbf{M}_k\right\} \succeq 0, && (5.50b)\\
& && \begin{bmatrix} 1 & r_{1k} \\ r_{1k} & r_{2k} \end{bmatrix} \succeq 0 \qquad \forall k \in \mathcal{G}, && (5.50c)
\end{aligned}$$

where $\mathbf{r}_k$ is the symmetric matrix, and r_{1k} and r_{2k} are the optimization variables. The dual OPF problem (5.50) also satisfies

$$\underline{\lambda}_k, \overline{\lambda}_k \geq 0 \quad \text{for (5.42c)}, \tag{5.51}$$

$$\underline{\gamma}_k, \overline{\gamma}_k \geq 0 \quad \text{for (5.42d)}, \tag{5.52}$$

$$\underline{\psi}_k, \overline{\psi}_k \geq 0 \quad \text{for (5.42e)}. \tag{5.53}$$

If a zero duality gap exists, it obviously yields a feasible (and physically meaningful) solution of the SDP relaxation. Since if, and only if, the nullspace of the constraint (5.50b) has a dimension less than two– that is, the rank-one condition –it always admits a zero duality gap. In addition, the matrix $\mathbf{W}$ corresponding to the generalized Lagrange multiplier of the constraint (5.50b) is expected to have a rank-one solution with a zero duality gap for obtaining the global optimal solution. However, a duality gap of zero means that the OPF (5.42) problem and its dual form (5.50b) have the same optimal values. This is also called strong duality. In contrast, when the duality gap is nonzero, the dual OPF problem is not solvable [258],[46].

Remark 10. *The optimization problem* (5.42) *corresponds to a Lagrangian dual problem of* (5.50) *which guarantees strong duality but it does not have the rank constraint* (5.42h).

Remark 11. *Adding additional constraints such as power flow and thermal line limits to semidefinite relaxation of the OPF problem will not affect the modeling structure or problem solving strategy. For the sake of simplicity, we neglect power flow and thermal line limits in this chapter. The additional constraints to be added to the formulation of OPF problem with SDP can be seen in [68],[62].*

We conclude that the renewable power injection to the OPF problem does not change the dual variables and dual formulation of the problem. Our results are identical to the results in [68].

5.6 Methodology for Demand-Side Participation

The main contribution of this section is a program to solve OPF with renewable generation. In this section, a practical algorithm is adopted to the OPF problem, which is reformulated as SDP. In this way, random renewable generation is realized. According to this algorithm, we choose the candidate non-generator buses. Random renewable power is injected, and then maximized using the selected buses. To do this, we give a random value, such as real power generation. In fact, real power generation is treated as renewable power generation to the load buses. We first take an initial renewable power value which corresponds to zero; this means that the initial value equals the amount of the injected renewable power into the grid, which holds the current value. The current value of penetrated renewable power is added to the non-generator bus as a negative load. Problem (5.50) is solved for this case. If a feasible solution is obtained, the penetration of renewable generation is increased gradually. These penetrations, or non-negative random values, continue to add the non-generator buses in each case. The process of increasing renewable generation for the given buses has continued until the OPF problem with SDP no longer converges on the global solution of the test system. At the end of this process, the maximum value of the renewable power generation for the test system is obtained. It is clear that there is no feasible solution for higher penetration of renewable generation. Thus, after obtaining OPF solutions with SDP for the base case, we run the program for scenarios in order to solve the OPF problem under various amounts of renewable generation. The highest penetration rate for the test system is determined. Finally,

the proposed program is summarized in Algorithm 1.

Algorithm 1 Algorithm for Demand Participation

1: Initially choose ΔP_G^r
2: Select the candidate $\mathcal{N} - \mathcal{G}$ buses
3: Initialize $P_G^r = 0$ and converge flag = 1
4: $P_G^r = P_G^r + \Delta P_G^r$ **then** $P_D = P_D + P_G^r$
5: Add the initial value of P_G^r to $\mathcal{N} - \mathcal{G}$ buses
6: Solve the SDP relaxation for an optimal solution.
7: **if** converge flag=0 **then**
8: $P_D = P_D - \Delta P_G^r$
9: $P_G^r = P_G^r + \Delta P_G^r$
10: **else**
11: Increment $P_G^r = P_G^r + \Delta P_G^r$
12: **end if**
13: Set converge flag=1
14: **if** converge flag=0 **then**
15: **return** step 4.
16: **else**
17: the total amount of renewable penetration, $P_D = P_D - \Delta P_G^r$
18: **end if**

5.7 Numerical Results

In this section, we investigated the effects of renewable generation of the OPF problem by means of a semidefinite programming (SDP) relaxation. In order to carry out these investigations, the penetrations of RESs are demonstrated as negative load to provide the demand-side participation. Then we develop a program to inject renewable power gradually. The resulting optimization problem is solved using the SDP. We find the global optimum solution for each incremental change of renewable generation. Numerical results confirm that the SDP fails to provide a physically meaningful solution for the higher penetrations. Throughout this section, we have reported our results regarding a base-case SDP solution of the OPF problem and the SDP solution for the penetration of the RESs. The proposed methodology is demonstrated on the IEEE 9-bus and IEEE 39-bus systems. All data can be found in [293]. To solve the OPF problem we partially use MATPOWER [293] with the SDP solver [62]. The numerical results are performed by YALMIP [294] and Sedumi [53].

5.7.1 Case Study: 9–Bus System

We first present the behavior of the IEEE 9-bus system. The single-line diagram of the 9-bus test system is shown in Fig. 5.1.

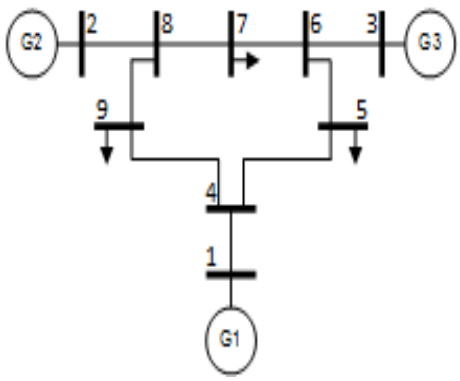

Figure 5.1: 9-bus system

In addition, the active power generated by generators and active power consumed by loads of the test system can be seen in Table 5.1.

Table 5.1: Generation and demand data for the 9-bus system

Bus	P_G (MW)	Bus	P_D (MW)
1	0	5	90
2	163	7	100
3	85	9	125
Total	248	Total	315

The base-case SDP solutions are given in Table 5.2. The base-case solution indicates the actual operating point. Under this condition, it satisfies necessary requirements for the power transaction at each bus. The base case means that there is no current flow from the power system. As a matter of fact, the base-case solution gives information about the system's operating condition. We start with solving the base case so that we obtain an operating point before the random renewable energy is penetrated. In this way, we calculate power-flow quantities such as power flows from the transmission lines, line flows, bus voltage information and other power flow in network components. Here the base-case solution treats the case where there is no renewable energy supply, that is $P_G^r \equiv 0$. To get the base-case solution, the OPF problem starts iterations with an initial guess; that is, all bus voltage angles are set to zero degrees, magnitudes of load-bus voltages are set to 1.0 per unit, and magnitudes of generator-bus voltages are kept at the given values. The voltage limits are selected between 0.95 and 1.05, then, the global solution is shown in Table 5.2.

Table 5.2: Base-case SDP solution of the modified 9-bus system

Bus	V(p.u)	δ(deg)	P_G(MW)	Q_G(MVAr)
1	1.050	0.00	90.21	18.00
2	1.050	5.32	134.28	6.52
3	1.040	3.50	94.20	−18.29
4	1.041	−2.72		
5	1.030	−4.40		
6	1.050	0.61		
7	1.038	−1.36		
8	1.049	0.95		
9	1.016	−5.11		

The optimal objective value for the SDP solution is $5306.38 per hour.

Next, we consider that the penetration of the RESs are located at the non-generator buses 5, 7, 9, which can be seen in Fig. 5.2.

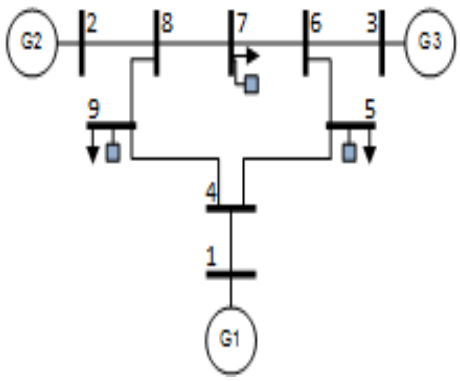

Figure 5.2: 9-bus system with renewable penetration

The procedure described above is followed to achieve the optimization problem in (5.42). The random renewable power is injected to related load buses 5, 7, 9 as negative load. An initial value has been set to 1 MW for this test system. This value can be chosen by the user. Here, the amount of renewable generation for demand participation can be considered to be 1 MW. This means that for any 1 MW injected at buses 5, 7, and 9, the optimization problem is resolved for this incremental value and also meets a convergent solution. Due to changing demand for the increasing renewable generation, the resulting power flow is not feasible. Thus, the maximum value of renewable capacity using the demand-side participation has been obtained as 280 MW. The global solution of the of the system can be seen in Table 5.3.

Table 5.3: Global solution of the modified 9-bus system with renewable penetration

Bus	V(p.u)	δ (deg)	P_G(MW)	Q_G(MVAr)
1	1.050	0.00	10.00	0.99
2	1.043	0.48	14.35	−9.19
3	1.037	0.58	10.77	−23.57
4	1.049	−0.30		
5	1.049	−0.10		
6	1.050	0.24		
7	1.042	−0.07		
8	1.048	0.00		
9	1.034	−0.83		

Here, the lowest voltage value is increased to 1.034. The optimal objective value for this solution is \$1205.72 per hour. However, there are constraints on the voltage magnitude, active and reactive power at every bus, and also the apparent power at every line. We deal with the voltage constraints, active and reactive power constraints. Firstly, the voltage bounds at load and generator buses and the active and reactive power limits are given by

$$\underline{V}_k = \overline{V}_k = 1 \qquad \forall k \in \mathcal{N} - \mathcal{G}, \tag{5.54}$$

$$\underline{V}_k = 0.95 \quad \text{and} \quad \overline{V}_k = 1.05 \qquad \forall k \in \mathcal{G}, \tag{5.55}$$

$$\underline{P}_k = \underline{Q}_k = -\infty \qquad \forall k \in \mathcal{G}, \tag{5.56}$$

$$\overline{P}_k = \overline{Q}_k = +\infty \qquad \forall k \in \mathcal{G}. \tag{5.57}$$

In this case, we first seek the possible solution by modifying the constraints. The SDP solution of the OPF problem fails to give physically meaningful results. On the other hand, using MATLAB Interior Point Solver (MIPS), convergence is reached. Here the lowest voltage is 0.962 p.u. As another scenario, we attempt to constrain the voltage magnitudes at load buses below the base case results. Thus, the voltage bounds at load buses are chosen between 0 and 0.95; $\overline{P}_k$ is set as the base case condition and $\underline{P}_k$ is set to zero, then the SDP solution of the OPF problem converges. In addition, the upper limit of the voltage magnitude is set to 1 and the lower limit of the voltage magnitude is set to zero. The SDP finds multiple solutions for both scenarios, which are summarized in Table 5.4.

Table 5.4: The two solutions of the modified 9-bus system

Bus	V(p.u)	δ (deg)	P_G(MW)	V(p.u)	δ(deg)	P_G(MW)
1	0.985	0.00	90.89	1.000	0.00	90.53
2	0.966	6.46	134.30	1.000	5.87	134.34
3	0.961	4.27	94.26	0.995	3.80	94.27
4	0.965	−3.16		0.998	−3.02	
5	0.947	−5.07		0.975	−4.87	
6	0.967	0.86		1.000	0.62	
7	0.950	−1.45		0.984	−1.54	
8	0.963	1.30		0.996	1.03	
9	0.931	−5.94		0.960	−5.69	

We now attempt to solve the SDP problem with acceptable voltage profiles for higher demands. To do this, all real loads are multiplied by a factor of 2.3 [311] while other parameters are the same as the base case condition. If loads are increased even further in the 9-bus system, the problem fails. The solution is shown in Table 5.5.

Table 5.5: Global solution of the modified 9-bus system with scaled demands

Bus	V(p.u)	δ (deg)	P_G(MW)	Q_G(MVAr)
1	1.050	0.00	232.60	91.63
2	1.050	6.34	242.43	61.06
3	1.050	10.00	269.68	−50.16
4	1.008	−7.27		
5	0.975	−11.26		
6	1.033	1.62		
7	1.004	−5.67		
8	1.024	−1.76		
9	0.956	−14.76		

5.7.2 Case Study: 39–Bus System

We use the IEEE 39-bus test system with 10 generators to illustrate the effects of RESs using the solution procedure discussed in previous sections. The single-line diagram of the 39-bus test system is shown in Fig. 5.3.

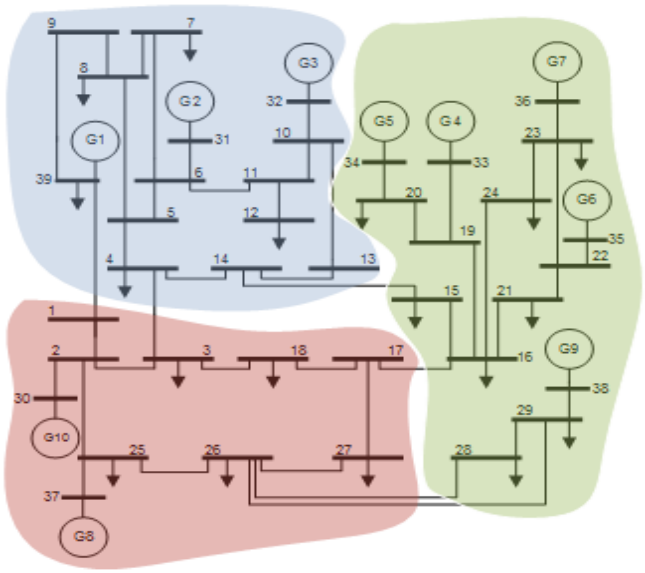

Figure 5.3: 39-bus system with three regions

The following Table 5.6 shows the generation and demand capacity of the system for each region.

Table 5.6: Generation and demand capacity of regions

Region	P_G (MW)	P_D (MW)
Region 1	2327	2384
Region 2	790	1221
Region 3	3180	2648
Total	6297	6253

Now, we investigate the base-case solution for the 39-bus system [293], [62]. Again, the voltage bounds are chosen between 0.95 and 1.05. The base-case solution is for the 39-bus system is given in Table 5.7. Then, the optimal objective value is obtained is \$41901.14 per hour. In this case, if the load voltage limits at load buses are chosen between 0 and 0.95, the solution is not feasible.

Table 5.7: Base-case SDP solution of the modified 39-bus system

Bus	V(p.u)	δ (deg)	Bus	V(p.u)	δ (deg)	P_G(MW)	Q_G(MVAr)
1	1.034	−13.60	21	1.033	−4.80		
2	1.044	−5.52	22	1.049	−0.21		
3	1.035	−9.13	23	1.041	−0.37		
4	1.024	−10.58	24	1.040	−7.17		
5	1.033	−9.87	25	1.050	−4.61		
6	1.037	−9.16	26	1.050	−7.69		
7	1.025	−11.63	27	1.038	−9.20		
8	1.023	−12.32	28	1.047	−6.30		
9	1.049	−15.34	29	1.045	−4.20		
10	1.049	−6.68	30	1.037	1.08	671.88	140.00
11	1.044	−7.52	31	1.029	0.00	646.00	300.00
12	1.031	−7.47	32	1.030	0.94	671.23	300.00
13	1.043	−7.30	33	0.999	2.86	652.00	119.46
14	1.034	−8.76	34	1.050	1.34	508.00	142.37
15	1.025	−8.86	35	1.050	4.83	661.44	222.80
16	1.035	−7.34	36	1.050	7.91	580.00	64.99
17	1.037	−8.47	37	1.022	2.56	564.00	10.79
18	1.035	−9.15	38	1.016	1.47	654.78	-24.16
19	1.050	−2.51	39	1.033	−17.22	691.16	100.50
20	0.988	−3.91					

Next, we assume that the test system includes three regions and is penetrated by renewables. Suppose further that renewable generation units are placed at non-generator buses 4, 7, 8, 18, 20, 24, 25, 26, 27, 28, and 29 to achieve demand-side participation. Simulations are performed to determine the global solution of the test system for the penetration of RESs. The SDP solution returns a feasible solution only if the generation capacity is adequate to satisfy and balance supply and demand in response to temporal deviations in RESs and loads with the given security constraint limits. The optimization values in this case are $\mathbf{V}$, $\mathbf{P}_G$, and $\mathbf{Q}_G$.

We start by investigating the feasible solution for the 39-Bus system. A diagram of the buses with the penetration of renewable generation is shown in Fig. 5.4.

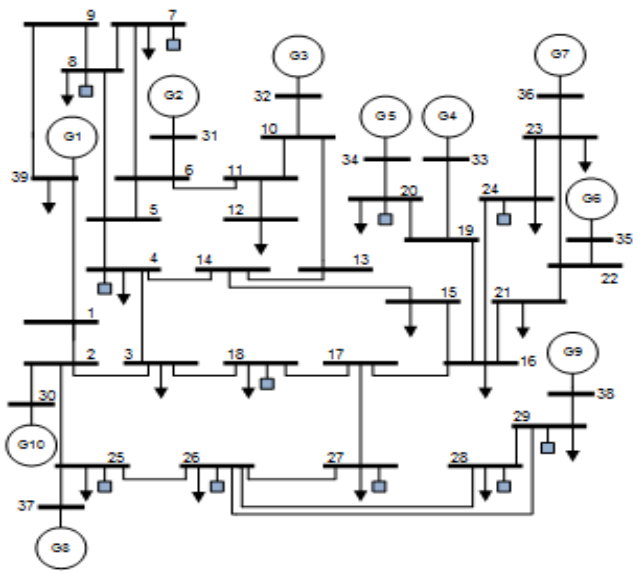

Figure 5.4: 39-bus system with demand participation

Then, we adopt the following procedure to solve the optimization problem: the random renewable power is injected to related load buses as mentioned before, and an initial value has been set to 10 MW or any reasonable value. As a part of our algorithm, the related load buses have been equally increased by 10 MW. The SDP is run under the conditions of this change and provided with a convergent solution. The process of increasing renewable generation to load buses has continued until the solution no longer converges and the problem is not feasible due to line limits. At the end of this process, the maximum value of renewable capacity using the demand-side participation has been calculated as 720 MW, which is equal to slightly more than 10% of the total generation capacity. In this case, the reactive power limits are kept at the given values. Again, this occurs when the voltage limits on load buses are chosen between 0 and 0.95. The optimal objective value is found to be \$31.020 per hour. Finally, the global solution of the test system is given in Table 5.8.

Table 5.8: Global solution of the modified 39-bus system with renewable penetration

Bus	V(p.u)	δ (deg)	Bus	V(p.u)	δ (deg)	P_G(MW)	Q_G(MVAr)
1	1.022	−13.38	21	1.032	−3.61		
2	1.038	−3.90	22	1.049	0.30		
3	1.031	−7.16	23	1.042	0.28		
4	1.023	−8.83	24	1.038	−3.28		
5	1.032	−8.46	25	1.050	−2.34		
6	1.036	−7.86	26	1.046	−4.00		
7	1.024	−10.00	27	1.035	−5.76		
8	1.021	−10.72	28	1.046	1.36		
9	1.040	−15.05	29	1.050	2.34		
10	1.046	−5.73	30	1.033	1.60	553.10	140.00
11	1.041	−6.45	31	1.031	0.00	556.98	300.00
12	1.028	−6.40	32	1.017	0.65	553.32	282.00
13	1.041	−6.22	33	0.998	3.44	538.22	110.66
14	1.033	−7.35	34	1.007	3.49	508.00	145.83
15	1.016	−7.05	35	1.050	4.42	542.36	211.12
16	1.032	−5.48	36	1.050	7.98	540.04	58.02
17	1.034	−6.04	37	1.020	4.41	529.54	0.00
18	1.032	−6.68	38	1.027	6.81	526.01	12.86
19	1.050	−6.99	39	1.021	−17.84	571.31	109.04
20	0.989	−1.75					

It is worth noting that all load buses are increased by the same amount of active power injection. However, some load buses can be enforced under various amounts of renewable generation. It is possible to find a global optimal solution which does not have a duality gap between the original problem and the dual SDP problem. We conclude that if the OPF problem is solved with the given voltage limits, then the solutions can be infeasible. We show the solutions that lie within acceptable voltage limits and converge to the global solutions.

5.7.3 Contingency Scenarios

In this subsection, we provide the contingency scenarios on the modified 39-bus system. The contingency effect in each case is tested by the SDP relaxation of the test system. We assume that the test system is operated under normal operating conditions. The renewable energy injections at the load buses of interest are ignored. These results can be found in our previous work [73]. The event of contingency is

performed with various generation and transmission outages on the test system. For all contingency scenarios in this section, voltage constraints remain within a range of 90 to 105% of nominal voltage on the test system. The transmission lines between these regions are given in Table 5.9.

Table 5.9: Connection lines between the regions of the 39-bus system

Regions	Line number
$1-2$	$4-3$
	$39-1$
$1-3$	$14-15$
$2-3$	$17-16$
	$26-29$
	$26-28$

5.7.3.1 Double Contingency Scenarios of Transmission or Generation and Transmission Outages–Scheduled Cases

Line outages: In this scenario, we only consider the test system under transmission line failures. With each transmission line loss, its outage increases the load on the rest of the transmission lines, power flows are redispatched to another transmission lines, and voltages on the remaining system are degraded. According to this scenario, double transmission outages occur at transmission lines 14-15 and 26-28, then the SDP is run on the system with the remaining transmission and generation facilities. The unavailability of these transmission lines does not cause an unstable operating condition; thus, a feasible solution is obtained. In addition, the transmission line 14-15 is the central transmission line between the regional systems 1 and 3. After the important line outages occur between the regional systems 1 and 3, these regional systems can be operated safely. When an unplanned line outage occurs at line 39-1, the test system is not able to safely withstand another contingency; this may lead to a cascading outage so the power-flow model fails to solve. The loss of any triple combination of transmission lines between the regions $1-2$, $1-3$, and $2-3$ does not jeopardize the remaining facilities in this system. The corrective active power generation when two contingencies occur is given in Table 5.10. The last row of the

table shows another double contingency combination of transmission outages at the lines 14-15 and 26-29.

Table 5.10: The rescheduled active power generations for the line outages

Bus	Region code	P_G(MW)		
		Before cont.	First cont.	Second cont.
30	2	671.88	672.46	673.22
31	1	646.00	646.00	646.00
32	1	671.23	672.56	673.33
33	3	652.00	652.00	652.00
34	3	508.00	508.00	508.00
35	3	661.44	661.78	662.59
36	3	580.00	580.00	580.00
37	2	564.00	564.00	564.00
38	3	654.78	651.95	649.55
39	1	691.16	692.02	692.80

Following the corrective active power generation for each generator in case of contingency, we observe that the rescheduled generation of the generation unit located at bus 38 decreases by 3 MW. When the line 26-28 is tripped, the power flows through to line 26-29. Similarly, the cause of transmission line contingency slightly decreases the generation unit's active power output at bus 38. On the other hand, the rescheduled generation of the generating units, such as at bus 33, 34, and 36, remain the same since these three generation units are independent from the rest of the system. However, the power generation in the remaining system is satisfied to its point of demand within acceptable voltage limits. We also observe that the generating units at bus 30 and 39 increase from 671.88 MW to 672.46 MW and 691.16 MW to 692.02 MW, respectively.

Line and generator outages: According to this scenario, the event of planned contingency occurs at both transmission line and a generation unit in the system. The possible events in this scenario are the loss of the single line 14-15 and a power generation unit at bus 30. Thus, the lost generation is 250 MW in the system. If only one generation unit is lost, the remaining generation units are able to meet the demand of the system. The feasible solution is obtained.

When line $26-29$ is lost as a second contingency, the system still remains feasible.

Table 5.11: The rescheduled active power generations for the line and generator outages

Bus	Region code	P_G(MW) planned cont.
31	1	646.00
32	1	725.00
33	3	652.00
34	3	508.00
35	3	687.00
36	3	580.00
37	2	564.00
38	3	865.00
39	1	1076.61

The value of the active power generation at bus 39 increases to 1081.00 MW. Even though line 3-4 or line 39-1 is lost, the SDP solution can be obtained. Finally, the results of double contingency scenarios of transmission or generation and transmission outages are summarized in Table 5.12.

Table 5.12: The results of the double contingency scenarios

First Cont.	Second Cont.	Solvability	Third Cont.	Solvability
Line 14-15	Line 26–28	feasible	Line 39–1	infeasible
Line 14-15	line 26–29	feasible		
Gen 30	Line 14–15	feasible		
Gen 30	Line 26–29	feasible	Line 39–1	feasible
Gen 30	Line 26–29	feasible	Line 3–4	feasible

Finally, the contingencies of the transmission and generation facilities are shown in Fig. 5.5

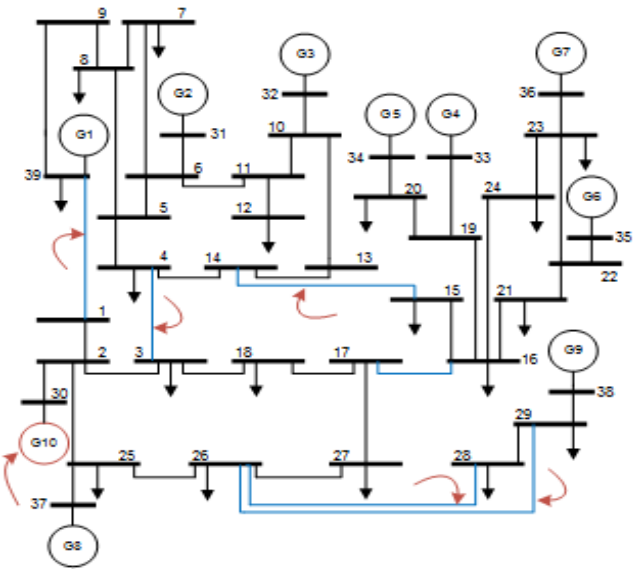

Figure 5.5: 39-bus system with line and generator contingencies

5.7.3.2 The Worst Case Contingencies–Unscheduled Cases

In this subsection, we provide results for the worst-case contingency situations, assuming the unanticipated outages of generation units only, transmissions lines only and generation-transmission combinations.

Line and generator outages: In this scenario, generation outage occurs at bus 30, transmission line outage occurs line 26-29, and the system loses 250 MW. Here, power generation is shifted to other lines, and the SDP method for OPF returns a feasible solution. Thus, the system is operated securely before the second contingency. With a third outage, the result of the outage of transmission line 10-13, the actual power flows are infeasible. Note that transmission line 10-13 is not particularly important for our scenario. Remaining generation capacity, transmission capacity, and fixed loads and generator and line constraints in the system cause load/generation mismatch. Finally, the SDP results become infeasible. To return the system to a secure operating condition, the load-shedding scheme is designed to restore system voltage and frequency to account for abnormal condition. In fact, the load shedding is to address voltage decays and frequency declines, as well as stabilize frequency and voltage. In this way, load-shedding is intended to the load and generation balance in the system. According to our load-shedding analysis, or in general, the loads are shed at

the closest location of the generators and transmission lines that tripped. In this case, the SDP returns a feasible solution, shedding 170 MW of load at bus 4 and 70 MW at bus 26. Moreover, we observe that the loss of the generator at bus 30 and the loss of the most important transmission facilities 26-29, 39-1, and 14-15 do not affect the remaining facilities in the system. Therefore, the test system is still feasible.

Lines outages: This type of contingency involves a cascading lines failure in the power network. In this case, the line contingencies occur at lines 14-15, 26-28. The system still remains operational and safe. The new worst contingency occurs at line 39-1. These transmission lines are critical for their control area. The tripping of the generation unit at bus 30 or bus 37 is an alternative solution before the load-shedding scheme. If load-shedding of 322 MW occurs at bus 30, the system can be failed.

Generator outages: We consider that several generation units shut down for our scenario. Generation outage occurs at bus 30 and 34. These generators are the smallest units in the test system, and the loss of generation supply in the system is approximately 758 MW in total. To maintain generation-demand balance, a total of 485 MW has to be shed from bus 20. Finally, power transactions and the redispatch of generation beyond the system are evaluated after load shedding has occurred.

Table 5.13: The results of the worst-case contingency scenarios

Case	First Cont.	Second Cont.	Third Cont.	Load Shed (MW)
1	Gen 30	Line 26–29	Line 10-13	240
2	Line 14-15	Line 26–28	Line 39-1	322
3	Gen 30	Gen 34		485

5.8 Conclusion

In this chapter, we aim to solve the OPF problem for integrating RESs with demand participation in electric grids. The injections of renewable generation for the OPF problem are performed by means of a SDP relaxation. Here, the penetrations of RESs are demonstrated as negative load to provide the demand-side participation. In other words, the demand participation is provided by demand-side resources to reduce the

actual or aggregate load, which means that the penetration of renewable generation is increased. To do this, the electric generation from renewables as a supplier is randomly realized using an algorithm. The first contribution in this chapter is that we have developed a practical algorithm to inject renewable power gradually. This program is integrated to the SDP solver. The classical OPF problem is reformulated for the penetrating RESs with demand-side participation in the power network. The resulting optimization problem, accommodating the renewable generation, is solved by using the SDP method. Additionally, the formulations of the SDP method are explained clearly. Next, we find the global optimum solution for each incremental change of renewable generation. We observe that the SDP fails to provide a physically meaningful solution for the higher penetrations.

The second contribution of this chapter is our test of the SDP method for contingency scenarios. Here, we use the 39-bus system as the test case to run an SDP approach, and to find the amount of load to be shed. Our scenarios are performed to better understand the impact of the contingency conditions on the grid. These contingencies involve primary tasks such as shedding load, dropping or tripping generation, or tripping transmission lines to maintain a reliable grid. All tasks intend to achieve feasible power transactions, which are adjusted continuously to control frequency, voltage, and line loadings. We introduce contingency scenarios in this chapter, including generation unit failures or transmission lines outages (either individually or in combination with one another). The effect of contingency in each case is measured in terms of load shedding. This is necessary for the SDP approach to return a feasible solution. After single and multiple contingency events, the SDP method for the OPF problem returns a feasible solution only if the supply and demand match with the existing transmission constraints. We conclude that the SDP method is fairly robust and is capable of withstanding single or multiple contingency events.

Chapter 6

Conclusions

6.1 Contributions

The theoretical contributions of this dissertation are summarized under some titles.

6.1.1 Decentralized Voltage Control

This work enhances both our understanding and the crucial role of decentralized control in power systems. We implement decentralized control action in uncertain model cases, and in this respect, seek to control both the terminal voltage and frequency of generators. We suggest a methodology that provides successful analysis of power systems under various uncertainties in the model.

6.1.1.1 Modelling

Power system models are represented as a set of parameter-dependent nonlinear differential equations with parameter variation. We identify these time-varying parameters as an explanation for the nonlinear dynamical behaviors observed in power systems. Then, power system states are defined by the generator rotor angles, generator velocity deviations (speeds), mechanical powers, field voltages, or electrical output power of generators. Power plant dynamics are represented as a lower-dimensional model and, as a consequence, the terminal voltage of synchronous generators is described as a system state. In this case, the electrical output power acts as a control input. The terminal voltage of the generator depends only on the parameters being varied, which are referred to as uncertain parameters. The terminal voltage state is not only affected by uncertain parameters, but is also a highly nonlinear function of the rotor angle and the power output of the generator. These uncertain (or unknown) deterministic parameters capture the dynamic nature of synchronous generators. More precisely, any change in the operating conditions of the power system will cause parameter changes,

and thus the voltage will vary. In the present work, reasonable operating limits are set for the power system models. These limits are used in defining uncertain parameters and determining their allowable uncertainty ranges. The resulting decentralized voltage control action allows us to ensure that these parameters shift in the interval of interest within the operating range of the power system. Additionally, power system dynamics are represented using a higher-order model which is used a power system stabilizer. The extended dynamic model involves uncertain design parameters which belong to the power system stabilizer. These design parameters are computed-in fact, optimized-when the terminal voltage dynamics containing uncertain parameters are changed.

6.1.1.2 Solving

In Chapter 3, we present state feedback control and output feedback control design approaches. We first formulate the state feedback control problem, and discuss some necessary mathematical concepts related to the linear feedback design for non-linear systems subject to uncertain time-varying parameters. We show a technique to compute the upper and lower bounds of these uncertain parameters. Subsequently, a numerical algorithm including linear inequalities is presented; thus, the solution of the decentralized voltage control problem is obtained using the known ranges of uncertain parameters. We indicate that the structure of the controller design may vary in time. We also confirm that the system is stable for certain ranges of uncertain parameters. The solution method is guaranteed to converge quadratically. In addition, we present a novel approach for designing an output feedback controller. This approach is illustrated by a much more complex model than the previous approach, effectively enhancing the solution procedure of power system dynamics. We then implement a bisection algorithm for solving the output feedback problem, since the model contains some additional uncertainties or design parameters. Our goal is to find the maximum values of design parameters when a feasible solution of the output feedback problem is obtained. In this contribution, the design parameters are restated for unknown variation of uncertain parameters which possibly depend on time and are bounded as reliable and secure operation intervals of the power system. In both state and

output feedback cases, we verify that the solution procedures allow us to take over all existing parametric uncertainties while also determining the design parameters of the power system stabilizer. Applying our procedure, the gain matrices for both cases are finally obtained. We also present the numerical calculation for computing the worst-case norm using time-varying parameter uncertainties in the model.

6.1.2 Observer Design for Power Systems

We have designed an observer-based control methodology for power systems. The observer-based control enhances stability with a contraction theory-based analysis. We then present a contraction theory to analyse the contraction alongside the convergence properties of the Kalman filter when it is used as an observer for power systems.

6.1.2.1 State Observer

We extend a decentralized control scheme using observer-based control for the multimachine power system with respect to the nonlinear interconnections between generators. The decentralized control of the multimachine power system is made by a deterministic observer. Thus, we have solved the state estimation and/or state observation problem. State estimates are obtained through the use of the extended Kalman filter. The proposed observer characterizes the stability properties of the deterministic EKF based on contraction theory. Contraction analysis is constructed for the classical model of power systems, then it is applied to the problem of state observation.

6.1.2.2 A Contraction Theory-Based Analysis of the Stability

We demonstrate the necessary conditions for the existence of contraction for EKF underlying the proposed power system model. The state estimates are generated by the proposed observer. A virtual and true system framework with contraction theory is used. We explain the contraction properties of the virtual system, which is relevant to a particular solution of the EKF and to the solution of the true system. The estimation error (or trajectory) of the EKF exponentially converges to the true system's

state or the true trajectory of the system. Our simulation results, indeed, agree with these convergence results. The contraction metric is defined for the classical model of the power system. We seek the necessary conditions under which the multimachine power system model is contracting in a diagonal metric with standard assumptions. The Jacobian matrix corresponds to the model as a generalized Jacobian matrix; we first show the principal minors of the generalized Jacobian matrix. For the uncontrolled case, these principal minors are unstable, since we observe that some principal minors of the Jacobian matrix are not negative. We demonstrate that this case is very similar to those used in our simulations; however, when we apply this method to the controlled case, the region of contraction is obtained. In this case, we observe that the principal minors are stable. To this end, we confirm that a contraction interval is found for the classical model of power systems. The contraction theory is thus proved.

6.1.2.3 Simulation Results for EKF

We design simulation results for EKF using a two-machine power system and a three-machine power system model. We develop the programs to be used for simulation results. These programs simulate the behavior of multimachine power system cases. For the analytical investigation of obsever-based control for the models, analytical results are obtained for power system models through the use of contraction theory. Theoretically, the contraction theory is only described in detail for a two-machine power system. Our research results confirm that necessary conditions for a Kalman observer are provided, and that the state stability of nonlinear power system model is guaranteed.

6.1.3 Integrating Renewables in Power Grids

We primarily solve the OPF problem for achieving renewable energy integration in power grids. Demand-side participation is used to facilitate the integration of renewable generation resources. According to our scenario, we supply renewable production or penetration as negative load from the demand sides; in other words, the demand adapts to the variable generation. Renewable production units are enabled

for the demand-side participation. Using the concept of demand participation, we raise the demand participation for reducing and/or shifting usage peak load periods and adapting elastic demand to fluctuating generations in electricity grids. In achieving our scenarios, we develop an algorithm to provide demand participation. This algorithm is integrated into the SDP program. The integration of renewable generation is gradually increased using this algorithm , which enables a higher integration of renewable energy. We assume that renewable power is a random variable. Each penetration level is tested by the OPF problem, and is performed by means of an SDP relaxation. We observe the feasibility of the solutions. If-and when-this penetration reaches significant levels, the highest level of renewable energy generation is obtained for our scenarios.

6.1.3.1 Semidefinite Optimization

We present the interior-point based semidefinite programming solutions for the optimal power flow problem when integrating renewables into power grids. The SDP based OPF problem is redesigned for demand participation. The formulations of a converted semidefinite program for OPF are investigated. The solutions of the SDP-based OPF problem are obtained for each incremental change of renewable generation. We guarantee the global optimal solution of the SDP-based OPF problem. However, the semidefinite relaxation fails for higher penetrations. The results are tested for both a 9-bus system and a 39-bus system.

6.1.3.2 Contingency Cases

We present the SDP solutions for contingency analyses. Contingency scenarios are performed for the 39-bus system with three regions. According to our scenarios, contingency analyses are performed by generation and line losses. Contingency scenarios are considered to be possible events. These events may be single contingencies, such as a generation unit failures or transmission line failures, or they may be double contingencies. Transmission line contingencies occur with the loss of critical lines of the transmission grid on the system. After single or multiple contingencies occur, it is required to shed some load, drop or trip the generation, or trip transmission lines for

maintaining secure grid operations. In our contingency scenarios, we basically determine the appropriate amount of load to be shed. In this case, the SDP based OPF problem is tested for feasible transactions and generation dispatches in the system. if such action is feasible, the global optimal solution of the SDP-based OPF problem is guaranteed. In addition, the impact of worst-case contingency is examined for our test system. The amount of load shedding required is thus obtained.

6.2 Further Study

6.2.1 Efficient Solution Ways to Solve Parameter Uncertainties

The uncertainty of the power system translates to uncertain parameters in the model. The upper and lower bounds of these parameters are known and are varied within an allowable bound. By specifying a range for the uncertain parameters, we notice that the controller is based on assumptions of the operating range of the power system. To find the largest intervals for uncertain parameters without using these operating ranges is a central issue for decentralized control. The solution strategies can be improved with nonconvex optimization methods. The model for synchronous machine can also be expanded with wind turbine and photovoltaic system. In addition to parameter uncertainties, the model can involve state dependent parameters. The deriving the model including both parameter uncertainty and state dependent parameters should be a future direction. The Sum of Square (SOS) and polynomial optimization methods can be used to solve multiple parameter uncertainties.

6.2.2 Power Network Synchronization

Contraction analysis has two fundamental approaches: nonlinear observer design and synchronization. In this work, we choose the Extended Kalman Filter for nonlinear observer design. This observer design is restricted to well-known structure and/or reliable knowledge of power systems. Instead of Kalman-like observer, the advanced observer design can be used for nonlinear power systems, which do not a *priori* satisfy the structure of power system. The observer design can be extended to interconnection-based and transformation-based designs. Due to modelling errors in the different forms of structured and unstructured uncertainties, the observer may not be already

available. To do this, interconnected observers have ability to interconnected between subsystems or hierarchical layers each of which would admit an observer if the states of the other subsystems were known. Then a candidate observer for the interaction with these subsystems has capability that interconnect available sub-observers. The candidate observer running in nonlinear power system may be adequately incorporate into the model, and thus estimate the physical state of the system. On the other hand, the transformation-based approach can be turned into one of these forms by an appropriate transformation as well as changing of state coordinates. From this perspective, if the relation between decentralized agents or plants and the structure of their interactions are not available or clear for an observer design, but are equivalent to a system(s) which does have some appropriate structure, then the physical state of the current system can be obtained using the original system. In the cyber-physical systems such as smart grids, the power plant has not only physical states, but also cyber states. The continuous physical state and the discrete cyber state of the system can be integrated into the observer design. In addition, the synchronization is the most efficient approach of Contraction theory. This approach aims to design robust and resilient control for the physical power systems. The physical state of the system such as frequency and terminal voltage is subject to a disturbance and can be a control input. The cyber state is controlled by the attack/defense mechanism used by the network administrator. Here, the physical state(s) is assumed a synchronous state(s) for the model. The cyber state(s) can be defined non-synchronous state(s) for all system. Here, we need synchrony or perfect correlation for both physical and cyber states when disturbances and attacks occur. In other words, the physical states must synchronize with cyber states. This indicates that they synchronize all in the system. This approach can be use for real-time phase measurement unit (PMU) based tools. The main target is a better control design for contributing to stable (synchronized) grid, electromechanical response, and good frequency and voltage regulation.

6.2.3 Virtual Power Plants

Today's distribution system tends to accommodate a large number of distributed generations, storage systems, and inelastic loads. These highly distributed units participating with the transmission grid use modern information and communication technologies, and have a high cost. Instead, decentralized control architectures with increased penetration of DERs can reduce the high computational complexity of system operation. To do this, the concept of Virtual Power Plant is introduced. A VPP is called Virtual Utility, acting as a cluster of dispersed generating units, inelastic loads, and storage units that are combined in order to operate as a single facility or entity. The centralized and decentralized generating units in the VPP can fueled from both fossil fuel (coal, gas), large hydro, nuclear fuel, and RESs such as photovoltaic, wind, small hydro, fuel cells, biomass fired generators and other RESs. Here, VPP optimizes the energy production and consumption and maximizes the benefit of consumers, and at the same time the provider's benefit. Thus, it can be used to maximize the performance of the power grid. In addition to optimal and robust control, stochastic programming techniques for optimal decision making under uncertainty can be used for the basic different components of a VPP.

Bibliography

[1] K. Bhattacharya, M. Bollen, and J. E. Daalder. *Operation of Restructured Power Systems*. Springer, 2001.

[2] M. Ilic, F. Galiana, and L. Fink. *Power Systems Restructuring*. Springer, 1998.

[3] F. I. Denny and D. E. Dismukes. *Power System Operations and Electricity Markets*. CRC Press, 2013.

[4] H.-P. Chao, S. Oren, and R. Wilson. Reevaluation of vertical integration and unbundling in restructured electricity markets. In Fereidoon Sioshansi, editor, *Competitive Electricity Markets*, chapter 1, pages 27–64. Elsevier Science, 2008.

[5] M. E. El-Hawary. The smart grid-state-of-the-art and future trends. *Electric Power Components and Systems*, 42(3–4):239–250, Feb 2014.

[6] H.-D. Chiang. Application of bifurcation analysis to power systems. In Guanrong Chen, David J. Hill, and Xinghuo Yu, editors, *Bifurcation Control*, chapter 1, pages 1–23. Springer, 2003.

[7] M. D. Ilic and J. Zaborszky. *Dynamics and Control of Large Electric Power Systems*. Wiley Interscience, 2000.

[8] R. Sioshansi, S. Oren, and R. O'neill. The cost of anarchy in self-commitment-based electricity markets. In Fereidoon Sioshansi, editor, *Competitive Electricity Markets*, chapter 6, pages 245–266. Elsevier Science, 2008.

[9] J. H. Chow, P. V. Kokotovic, and R. J. Thomas, editors. *Systems and Control Theory for Power Systems*. Springer, 1995.

[10] C. L. DeMarco, C. A. Baone, Y. Han, B. C. Lesieutre, A. Bose, P. Kansal, M. Kezunovic, and B. Matic-Cuka. Control and protection paradigms of the future. PSERC Publication 12-10, May 2012.

[11] G. T. Heydt, J. D. McCalley, and M. Venkatsubramanian. Electric energy challenges of the future. PSERC Publication 12-11, May 2012.

[12] J. M. Morales, A. J. Conejo, H. Madsen, P. Pinson, and M. Zugno. *Integrating Renewables in Electricity Markets*. Springer, 2014.

[13] P. Adib, E. Schubert, and S. Oren. Resource adequacy. In Fereidoon Sioshansi, editor, *Competitive Electricity Markets*, chapter 9, pages 327–362. Elsevier Science, 2008.

[14] B. M. Buchholz and Z. Styczynski. *Smart Grids-Fundamentals and Technologies in Electricity Networks*. Springer, 2014.

[15] N. Hadijsaid and J.-C. Sabonnadiere. Smartgrids: Motivation, stakes and perspectives. In Nouredine Hadjsaid and Jean-Claude Sabonnadiere, editors, *SmartGrids*, chapter 1, pages 1–31. Viley, 2012.

[16] M. D. Ilic and Q. Liu. Toward sensing, communications and control architectures for frequency regulation in systems with highly variable resources. In Aranya Chakrabortty and Marija D. Ilic, editors, *Control and Optimization Methods for Electric Smart Grids*, chapter 1, pages 1–33. Springer, 2012.

[17] M. D. Ilic and S. Liu. *Hierarchical Power Systems Control*. Springer, 1996.

[18] M. D. Ilic. From hierarchical to open access electric power systems. *Proceedings of the IEEE*, 95(5):1060–1084, May 2007.

[19] T. V. Cutsem and C. Vournas. *Voltage Stability of Electric Power Systems*. Springer, 2008.

[20] P. Kundur. *Power System Stability and Control*. McGraw-Hill, 1994.

[21] M. D. Ilic. Automating operation of large electric power systems over broad ranges of supply/demand and equipment status. In Joe. H. Chow, Felix. F. Wu, and James. J. Mamoh, editors, *Applied Mathematics for Restructured Electric Power Systems*, chapter 6, pages 105–137. Springer, 2005.

[22] J. Momoh. *Smart Grid Architectural Designs*, pages 1–15. Wiley-IEEE Press, 2012.

[23] K. Tomsovic, D. E. Bakken, V. Venkatasubramanian, and A. Bose. Designing the next generation of real-time control, communication, and computations for large power systems. *Proceedings of the IEEE*, 93(5):965–979, May 2005.

[24] Q. Zhu, C. Rieger, and T. Basar. A hierarchical security architecture for cyber-physical systems. In *2011 4th International Symposium on Resilient Control Systems*, pages 15–20, Aug 2011.

[25] A. A. Sallam and Om P. Malik. *Scada Systems and Smart Grid Vision*, pages 469–493. Wiley-IEEE Press, 2011.

[26] F. F. Wu, K. Moslehi, and A. Bose. Power system control centers: Past, present, and future. *Proceedings of the IEEE*, 93(11):1890–1908, Nov 2005.

[27] S. M. Amin and B. F. Wollenberg. Toward a smart grid: power delivery for the 21st century. *IEEE Power and Energy Magazine*, 3(5):34–41, Sep 2005.

[28] K. Moslehi and R. Kumar. Smart grid-a reliability perspective. In *2010 Innovative Smart Grid Technologies (ISGT)*, pages 1–8, Jan 2010.

[29] P. McDaniel and S. McLaughlin. Security and privacy challenges in the smart grid. *IEEE Security Privacy*, 7(3):75–77, May 2009.

[30] J. Zarnikau. Demand participation in restructured markets. In Fereidoon Sioshansi, editor, *Competitive Electricity Markets*, chapter 8, pages 297–324. Elsevier Science, 2008.

[31] A. F. Correlje and L. J. De Vries. Hybrid electricity markets: The problem of explaining different patterns of restructuring. In Fereidoon Sioshansi, editor, *Competitive Electricity Markets*, chapter 2, pages 65–93. Elsevier Science, 2008.

[32] A. J. Conejo, M .Carrin, and J. M. Morales. *Decision Making Under Uncertainty in Electricity Markets*. Springer, 2010.

[33] D. Bauknecht and G. Brunekreet. Distributed generation and the regulation of electricity networks. In Fereidoon Sioshansi, editor, *Competitive Electricity Markets*, chapter 13, pages 469–497. Elsevier Science, 2008.

[34] C. L. DeMarco, C. A. Baone, Y. Han, and B. Lesieutre. Primary and secondary control for high penetration renewables. PSERC Publication 12-06, May 2012.

[35] A. Mullane and M. O'Malley. The inertial response of induction-machine-based wind turbines. *IEEE Transactions on Power Systems*, 20(3):1496–1503, Aug 2005.

[36] J. Hossain and H. R. Pota. *Robust Control for Grid Voltage Stability: High Penetration of Renewable Energy*. Springer, 2014.

[37] L. Chen, Na Li, L. Jiang, and S. H. Low. Optimal demand response: Problem formulation and deterministic case. In Aranya Chakrabortty and Marija D. Ilic, editors, *Control and Optimization Methods for Electric Smart Grids*, chapter 1, pages 63–86. Springer, 2012.

[38] C. W. Gellings and J. H. Chamberlin. *Demand-Side Management: Concepts and Methods*. PennWell Books, 1993.

[39] H. Bervani. *Robust Power System Frequency Control*. Springer, 2009.

[40] Ibraheem, P. Kumar, and D. P. Kothari. Recent philosophies of automatic generation control strategies in power systems. *IEEE Transactions on Power Systems*, 20(1):346–357, Feb 2005.

[41] B. H. Chowdhury and H. T. Ma. Frequency regulation with wind power plants. In *2008 IEEE Power and Energy Society General Meeting-Conversion and Delivery of Electrical Energy in the 21st Century*, pages 1–5, Jul 2008.

[42] J. Duval and B. Meyer. Frequency behavior of grid with high penetration rate of wind generation. In *2009 IEEE Bucharest PowerTech*, pages 1–6, Jun 2009.

[43] S. Gill, I. Kockar, and G. W. Ault. Dynamic optimal power flow for active distribution networks. *IEEE Transactions on Power Systems*, 29(1):121–131, Jan 2014.

[44] P. W. Sauer. Reactive power and voltage conrol issues in electic power systems. In Joe H. Chow, Felix F. Wu, and James A. Momoh, editors, *Applied Mathematics for Restructured Electric Power Systems*, chapter 2, pages 11–24. Springer, 2005.

[45] T. Niknam, M. Zare, and J. Aghaei. Scenario-based multiobjective volt/var control in distribution networks including renewable energy sources. *IEEE Transactions on Power Delivery*, 27(4):2004–2019, Oct 2012.

[46] X. Bai, H. Wei, K. Fujisawa, and Y. Wang. Semidefinite programming for optimal power flow problems. *International Journal of Electrical Power amd Energy Systems*, 30(67):383–392, Jun 2008.

[47] D. J. Hill, Y. Guo, M. Larsson, and Y. Wang. Global control of complex power systems. In Guanrong Chen, David J. Hill, and Xinghuo Yu, editors, *Bifurcation Control*, chapter 1, pages 155–187. Springer, 2003.

[48] W. Lohmiller and J. J. E. Slotine. On contraction analysis for nonlinear systems. *Automatica*, 34(6):683–696, Jun 1998.

[49] G. Besancon. Observer design for nonlinear systems. In Antonio Loria and Francoise Lamnabhi-Lagarrigue, editors, *Advanced Topics in Control Systems Theory*, chapter 2, pages 61–89. Springer, 2005.

[50] S. Bonnabel and J. J. E. Slotine. A contraction theory-based analysis of the stability of the deterministic extended kalman filter. *IEEE Transactions on Automatic Control*, 60(2):565–569, Feb 2015.

[51] C. Zhu, R. Zhou, and Y. Wang. A new nonlinear voltage controller for power systems. *Internatinal Journal of Electrical Power Energy System*, 19(1):19–27, Jan 1997.

[52] F. Amato. *Robust Control of Linear Systems Subject to Uncertain Time-Varying Parameters*. Springer, 2006.

[53] J. F. Sturm. Using sedumi 1.02, a matlab toolbox for optimization over symmetric cones. *Optimization Methods and Software*, 11(1-4):625–653, 1999.

[54] C. Zhu, R. Zhou, and Y. Wang. An obsrver-based scheme for decentralized stabilization of large-scale systems with application to power systems. *Asian Journal of Control*, 17(1):124–132, Jan 2015.

[55] R. Kalman and R. Bucy. New results in linear filtering and prediction theory. *Journal of Basic Engineering*, 83(3):95–108, Mar 1961.

[56] J. Jouffroy and J. J. E. Slotine. Methodological remarks on contraction theory. In *2004 43rd IEEE Conference on Decision and Control (CDC)*, volume 3, pages 2537–2543, Dec 2004.

[57] K. Reif, F. Sonnemann, and R. Unbehaunen. An ekf-based nonlinear observer with a prescribed degree of stability. *Automatica*, 34(9):1119–1123, Sep 1998.

[58] J. A. Momoh, R. Adapa, and M. E. El-Hawary. A review of selected optimal power flow literature to 1993. i. nonlinear and quadratic programming approaches. *IEEE Transactions on Power Systems*, 14(1):96–104, Feb 1999.

[59] J. A. Momoh, M. E. El-Hawary, and R. Adapa. A review of selected optimal power flow literature to 1993. ii. newton, linear programming and interior point methods. *IEEE Transactions on Power Systems*, 14(1):105–111, Feb 1999.

[60] D. K. Molzahn, B. C. Lesieutre, and C. L. DeMarco. A sufficient condition for power flow insolvability with applications to voltage stability margins. *IEEE Transactions on Power Systems*, 28(3):2592–2601, Aug 2013.

[61] X. Bai and H. Wei. Semi-definite programming-based method for security-constrained unit commitment with operational and optimal power flow constraints. *IET Generation, Transmission Distribution*, 3(2):182–197, Feb 2009.

[62] D. K. Molzahn, J. T. Holzer, B. C. Lesieutre, and C. L. DeMarco. Implementation of a large-scale optimal power flow solver based on semidefinite programming. *IEEE Transactions on Power Systems*, 28(4):3987–3998, Nov 2013.

[63] B. C. Lesieutre, D. K. Molzahn, A. R. Borden, and C. L. DeMarco. Examining the limits of the application of semidefinite programming to power flow problems. In *2011 49th Annual Allerton Conference on Communication, Control, and Computing (Allerton)*, pages 1492–1499, Sep 2011.

[64] S. Sojoudi and J. Lavaei. Convexification of optimal power flow problem by means of phase shifters. In *2013 IEEE International Conference on Smart Grid Communications (SmartGridComm)*, pages 756–761, Oct 2013.

[65] R. Madani, S. Sojoudi, and J. Lavaei. Convex relaxation for optimal power flow problem: Mesh networks. In *2013 Asilomar Conference on Signals, Systems and Computers*, pages 1375–1382, Nov 2013.

[66] D. Gayme and U. Topcu. Optimal power flow with large-scale storage integration. *IEEE Transactions on Power Systems*, 28(2):709–717, May 2013.

[67] L. Gan, N. Li, U. Topcu, and S. H. Low. Exact convex relaxation of optimal power flow in radial networks. *IEEE Transactions on Automatic Control*, 60(1):72–87, Jan 2015.

[68] J. Lavaei and S. H. Low. Zero duality gap in optimal power flow problem. *IEEE Transactions on Power Systems*, 27(1):92–107, Feb 2012.

[69] V. Blondel and J. N. Tsitsiklis. Np-hardness of some linear control design problems. *SIAM Journal on Control and Optimization*, 35(6):2118–2127, Jul 1997.

[70] L. Xie, S. Puller, M. Ilic, and S. Oren. Quantifying benefits of demand response and look-ahead dispatch in systems with variable resources. PSERC Publication 13-41, Sep 2013.

[71] M. D. Ilic, L. Xie, and J. Y. Joo. Efficient coordination of wind power and price-responsive demand;part i: Theoretical foundations. *IEEE Transactions on Power Systems*, 26(4):1875–1884, Nov 2011.

[72] M. D. Ilic, L. Xie, and J. Y. Joo. Efficient coordination of wind power and price-responsive demand;part ii: Case studies. *IEEE Transactions on Power Systems*, 26(4):1885–1893, Nov 2011.

[73] M. Yilmaz and M. E. El-Hawary. Optimal power flow with demand participation of ress. In *2016 IEEE Electrical Power and Energy Conference (EPEC)*, pages 1–8, Oct 2016.

[74] P. W. Sauer and M. A. Pai. *Power System Dynamics and Stability*. Englewood Cliffs: Prentice Hall, 1998.

[75] P. M. Anderson and A. A. Fouad. *Power System Control and Stability*. IEEE Press, 2003.

[76] M. E. Sezer and D. D. Siljak. On decentralized stabilization and structure of linear large scale systems. *Automatica*, 17(4):641–644, Jul 1981.

[77] S. S. Stankovic, D. M. Stipanovic, and D. D. Siljak. Decentralized dynamic output feedback for robust stabilization of a class of nonlinear interconnected systems. *Automatica*, 43(5):861–867, May 2007.

[78] A. Zecevic and D. D. Siljak. *Control of Complex Systems*. Springer, 2010.

[79] Lubomir Bakule. Decentralized control: An overview. *Annual Reviews in Control*, 32:87–98, May 2008.

[80] Z. Qu, J. F. Dorsey, J. Bond, and J. D. McCalley. Application of robust control to sustained oscillations in power systems. *IEEE Transactions on Circuits and Systems I: Fundamental Theory and Applications*, 39(6):470–476, Jun 1992.

[81] S. Jain and F. Khorrami. Robust decentralized control of power systems utilizing only swing angle measurements. *International Journal of Control*, 66(4):581–602, Nov 1997.

[82] H. Jiang, H. Cai, J. F. Dorsey, and Z. Qu. Toward a globally robust decentralized control for large-scale power systems. *IEEE Transactions on Control Systems Technology*, 5(3):309–319, May 1997.

[83] Y. Wang, D. J. Hill, and G. Guo. Robust decentralized control for multimachine power systems. *IEEE Transactions on Circuits and Systems I: Fundamental Theory and Applications*, 45(3):271–279, Mar 1998.

[84] P. Varaiya, F. F. Wu, and Rong-Liang Chen. Direct methods for transient stability analysis of power systems: Recent results. *Proceedings of the IEEE*, 73(12):1703–1715, Dec 1985.

[85] J. W. Chapman, M. D. Ilic, C. A. King, L. Eng, and H. Kaufman. Stabilizing a multimachine power system via decentralized feedback linearizing excitation control. *IEEE Transactions on Power Systems*, 8(3):830–839, Aug 1993.

[86] C. A. King, J. W. Chapman, and M. D. Ilic. Feedback linearizing excitation control on a full-scale power system model. *IEEE Transactions on Power Systems*, 9(2):1102–1109, May 1994.

[87] G. Guo, Y. Wang, and D. J. Hill. Nonlinear output stabilization control for multimachine power systems. *IEEE Transactions on Circuits and Systems I: Fundamental Theory and Applications*, 47(1):46–53, Jan 2000.

[88] A. I. Zecevic, G. Neskovic, and D. D. Siljak. Robust decentralized exciter control with linear feedback. *IEEE Transactions on Power Systems*, 19(2):1096–1103, May 2004.

[89] D. D. Siljak, D. M. Stipanovic, and A. I. Zecevic. Robust decentralized turbine/governor control using linear matrix inequalities. *IEEE Transactions on Power Systems*, 17(3):715–722, Aug 2002.

[90] C. Concordia and L. K. Kirchmayer. Tie-line power and frequency control of electric power systems. *Transactions of the American Institute of Electrical Engineers. Part III: Power Apparatus and Systems*, 72(2), Jan 1953.

[91] N. Cohn. Considerations in the regulation of interconnected areas. *IEEE Transactions on Power Apparatus and Systems*, PAS-86(12):1527–1538, Dec 1967.

[92] M. Ilic, P. Skantze, C. N. Yu, L. Fink, and J. Cardell. Power exchange for frequency control (pxfc). In *IEEE Power Engineering Society. 1999 Winter Meeting*, volume 2, pages 809–819, Jan 1999.

[93] D. P. Kothari and I. J. Nagrath. *Modern Power System Analysis*. McGraw-Hill, 3rd edition, 2003.

[94] D. Apostolopoulou, P. W. Sauer, and A. D. Domnguez-Garca. Balancing authority area model and its application to the design of adaptive agc systems. *IEEE Transactions on Power Systems*, 31(5):3756–3764, Sep 2016.

[95] M. Andreasson, D. V. Dimarogonas, H. Sandberg, and K. H. Johansson. Distributed control of networked dynamical systems: static feedback, integral action and consensus. *IEEE Transactions on Automatic Control*, 59(7):1750–1764, Jul 2014.

[96] M. Andreasson, H. Sandberg, D. V. Dimarogonas, and K. H. Johansson. Distributed integral action: stability analysis and frequency control of power systems. In *2012 IEEE 51st IEEE Conference on Decision and Control (CDC)*, pages 2077–2083, Dec 2012.

[97] N. Jaleeli, L. S. VanSlyck, D. N. Ewart, L. H. Fink, and A. G. Hoffmann. Understanding automatic generation control. *IEEE Transactions on Power Systems*, 7(3):1106–1122, Aug 1992.

[98] Y. G. Rebours, D. S. Kirschen, M. Trotignon, and S. Rossignol. A survey of frequency and voltage control ancillary services;part i: Technical features. *IEEE Transactions on Power Systems*, 22(1):350–357, Feb 2007.

[99] Y. G. Rebours, D. S. Kirschen, M. Trotignon, and S. Rossignol. A survey of frequency and voltage control ancillary services;part ii: Economic features. *IEEE Transactions on Power Systems*, 22(1):358–366, Feb 2007.

[100] J. W. Ingleson and E. Allen. Tracking the eastern interconnection frequency governing characteristic. In *IEEE PES General Meeting*, pages 1–6, Jul 2010.

[101] A. J. Wood and B. F. Wollenberg. *Power Generation, Operation and Control*. Wiley, 1996.

[102] Ibraheem, P. Kumar, and D. P. Kothari. Recent philosophies of automatic generation control strategies in power systems. *IEEE Transactions on Power Systems*, 20(1):346–357, Feb 2005.

[103] C. E. Fosha and O. I. Elgerd. The megawatt-frequency control problem: A new approach via optimal control theory. *IEEE Transactions on Power Apparatus and Systems*, PAS-89(4):563–577, Apr 1970.

[104] E. C. Tacker, C. C. Lee, T. W. Reddoch, T. O. Tan, and P. M. Julich. Optimal control of interconnected electric energy systems: A new formulation. *Proceedings of the IEEE*, 60(10):1239–1241, Oct 1972.

[105] E. V. Bohn and S. M. Miniesy. Optimum load-frequency sampled-data control with randomly varying system disturbances. *IEEE Transactions on Power Apparatus and Systems*, PAS-91(5):1916–1923, Sep 1972.

[106] P. Kambale, H. Mukai, J. Spare, and J. Zaborszky. A reevaluation of the normal operating state control (agc) of the power system using computer control and system theory part iii. tracking the dispatch targets with unit control. *IEEE Transactions on Power Apparatus and Systems*, PAS-102(6):1903–1912, Jun 1983.

[107] C. Zhao, U. Topcu, and S. Low. Swing dynamics as primal-dual algorithm for optimal load control. In *2012 IEEE Third International Conference on Smart Grid Communications (SmartGridComm)*, pages 570–575, Nov 2012.

[108] D. Apostolopoulou, P. W. Sauer, and A. D. Dominguez-Garcia. Automatic generation control and its implementation in real time. In *2014 47th Hawaii International Conference on System Sciences*, pages 2444–2452, Jan 2014.

[109] G. Sharma, I. Nasiruddin, K.R. Niazi, and R.C. Bansal. Optimal agc of a multi-area power system with parallel ac/dc tie lines using output vector feedback control strategy. *International Journal of Electrical Power and Energy Systems*, 81:22–31, Oct 2016.

[110] H. Bervani. *Robust Power System Frequency Control*. Springer, 2009.

[111] Y. Wang, R. Zhou, and C. Wen. Robust load-frequency controller design for power systems. *IEE Proceedings C-Generation, Transmission and Distribution*, 140(1):11–16, Jan 1993.

[112] K. Y. Lim, Y. Wang, and R. Zhou. Robust decentralised load-frequency control of multi-area power systems. *IEE Proceedings-Generation, Transmission and Distribution*, 143(5):377–386, Sep 1996.

[113] M. T. Alrifai, M. F. Hassan, and M. Zribi. Decentralized load frequency controller for a multi-area interconnected power system. *International Journal of Electrical Power and Energy Systems*, 33(2):198–209, Feb 2011.

[114] D. Rerkpreedapong, A. Hasanovic, and A. Feliachi. Robust load frequency control using genetic algorithms and linear matrix inequalities. *IEEE Transactions on Power Systems*, 18(2):855–861, May 2003.

[115] W. Tan and H. Zhou. Robust analysis of decentralized load frequency control for multi-area power systems. *International Journal of Electrical Power and Energy Systems*, 43(1):996–1005, Dec 2012.

[116] Y. Wang, D. J. Hill, R. H. Middleton, and L. Gao. Transient stability enhancement and voltage regulation of power systems. *IEEE Transactions on Power Systems*, 8(2):620–627, May 1993.

[117] M. Gordon and D. J. Hill. Global transient stability and voltage regulation for multimachine power systems. In *2008 IEEE Power and Energy Society General Meeting-Conversion and Delivery of Electrical Energy in the 21st Century*, pages 1–8, Jul 2008.

[118] L. Gao, L. Chen, Y. Fan, and H. Ma. A nonlinear control design for power systems. *Automatica*, 28(5):975–979, Sep 1992.

[119] C. Zhu, R. Zhou, and Y. Wang. A new decentralized nonlinear voltage controller for multimachine power systems. In *2003 4th International Conference on Control and Automation Proceedings*, pages 525–530, Jun 2003.

[120] K. T. Law, D. J. Hill, and N. R. Godfrey. Robust controller structure for coordinated power system voltage regulator and stabilizer design. *IEEE Transactions on Control Systems Technology*, 2(3):220–232, Sep 1994.

[121] A. Heniche, H. Bourles, and M. P. Houry. A desensitized controller for voltage regulation of power systems. *IEEE Transactions on Power Systems*, 10(3):1461–1466, Aug 1995.

[122] O. Akhrif, F. A. Okou, L. A. Dessaint, and R. Champagne. Application of a multivariable feedback linearization scheme for rotor angle stability and voltage regulation of power systems. *IEEE Transactions on Power Systems*, 14(2):620–628, May 1999.

[123] D. J. Hill, I. A. Hiskens, and D. H. Popovic. Stability analysis of power system loads with recovery dynamics. *International Journal of Electrical Power and Energy Systems*, 16(4):277–286, Aug 1994.

[124] D. S. Popovic. Impact of secondary voltage control on voltage stability. *Electric Power Systems Research*, 40(1):51–62, Jan 1997.

[125] D. S. Popovic, V. A. Levi, and Z. A. Gorecan. Coordination of emergency secondary-voltage control and load shedding to prevent voltage instability. *IEE Proceedings-Generation, Transmission and Distribution*, 144(3):293–300, May 1997.

[126] D. H. Popovic, D. J. Hill, and Q. Wu. Optimal voltage security control of power systems. *International Journal of Electrical Power and Energy Systems*, 24(4):305–320, May 2002.

[127] H. Liu, Z. Hu, and Y. Song. Lyapunov based decentralized excitation control for global asymptotic stability and voltage regulation of multi-machine power systems. *IEEE Transactions on Power Systems*, 27(4):2262–2270, Nov 2012.

[128] F. Schweppe. *Uncertain Dynamic Systems*. Prentice Hall, 1973.

[129] K. Zhou, J. Doyle, and K. Glover. *Robust and Optimal Control*. Prentice Hall, 1996.

[130] S. Sastry. *Nonlinear Systems*. Springer, 1999.

[131] A. N. Michel, L. Hou, and D. Liu. *Stability of Dynamical Systems*. Birkhauser, 2015.

[132] K. Zhou and J. Doyle. *Essentials of Robust Control*. Prentice Hall, 1998.

[133] G. Dullerud and F. Paganini. *A Course in Robust Control Theory-A Convex Approach*. Springer, 2002.

[134] I. R. Petersen and R. Tempo. Robust control of uncertain systems: Classical results and recent developments. *Automatica*, 50(5):1315–1335, May 2014.

[135] A. Isadori. *Nonlinear Control Systems II*. Springer, 1999.

[136] G. Zames. On the input-output stability of time-varying nonlinear feedback systems part one: Conditions derived using concepts of loop gain and conicity and positivity. *IEEE Transactions on Automatic Control*, 11(2):228–238, Apr 1966.

[137] G. Zames. On the input-output stability of time-varying nonlinear feedback systems–part ii: Conditions involving circles in the frequency plane and sector nonlinearities. *IEEE Transactions on Automatic Control*, 11(3):465–476, Jul 1966.

[138] J. Doyle. Analysis of feedback systems with structured uncertainties. *IEE Proceedings D-Control Theory and Applications*, 129(6):242–250, Nov 1982.

[139] J. Cruz, J. Freudenberg, and D. Looze. A relationship between sensitivity and stability of multivariable feedback systems. *IEEE Transactions on Automatic Control*, 26(1):66–74, Feb 1981.

[140] B. Francis, J. Helton, and G. Zames. h_∞ optimal feedback controllers for linear multivariable systems. *IEEE Transactions on Automatic Control*, 29(10):888–900, Oct 1984.

[141] B. Francis and G. Zames. On h_∞ optimal sensitivity theory for siso feedback systems. *IEEE Transactions on Automatic Control*, 29(1):9–16, Jan 1984.

[142] J. Doyle, B. Francis, and A. Tannenbaum. *Feedback Control Theory*. Macmillan Publishing Company, 1992.

[143] P. Doroto. *Robust Control*. IEEE Press, 1987.

[144] P. Doroto and R. K. Yedavalli. *Recent Advances in Robust Control*. IEEE Press, 1990.

[145] J. M. Maciejowski. *Multivariable Feedback Design*. Addison-Wesley, 1989.

[146] P. Gahinet and P. Apkarian. Decentralized and fixed-structure h_∞ control in matlab. In *2011 50th IEEE Conference on Decision and Control and European Control Conference*, pages 8205–8210, Dec 2011.

[147] S. Xu and J. Lam. *Robust Control and Filtering of Singular Systems*. Springer, 2006.

[148] J. Doyle and G. Stein. Multivariable feedback design: Concepts for a classical/modern synthesis. *IEEE Transactions on Automatic Control*, 26(1):4–16, Feb 1981.

[149] K. Zhou and P. P. Khargonekar. Robust stabilization of linear systems with norm-bounded time-varying uncertainty. *Systems and Control Letters*, 10(1):17–20, Jan 1988.

[150] D. Peaucelle and D. Arzelier. Robust performance analysis with lmi-based methods for real parametric uncertainty via parameter-dependent lyapunov functions. *IEEE Transactions on Automatic Control*, 46(4):624–630, Apr 2001.

[151] T. Mori and H. Kokame. A parameter-dependent lyapunov function for a polytope of matrices. *IEEE Transactions on Automatic Control*, 45(8):1516–1519, Aug 2000.

[152] J. Ackermann. *Robust Control*. Springer, 1993.

[153] Y. Ohta and D.D. Siljak. Parametric quadratic stabilizability of uncertain nonlinear systems. *Systems and Control Letters*, 22(6):437–444, Jun 1994.

[154] P. P. Khargonekar, I. R. Petersen, and K. Zhou. Robust stabilization of uncertain linear systems: quadratic stabilizability and h_∞ control theory. *IEEE Transactions on Automatic Control*, 35(3):356–361, Mar 1990.

[155] F. Amato and A. Pironti. Quadratic stabilization with an h_∞ performance bound of uncertain linear time-varying systems. *Systems and Control Letters*, 28(2):103–114, Jun 1996.

[156] S. Xu, J. Lam, and C. Yang. Quadratic stability and stabilization of uncertain linear discrete-time systems with state delay. *Systems and Control Letters*, 43(2):77–84, Jun 2001.

[157] I. R. Petersen. Quadratic stabilizability of uncertain linear systems containing both constant and time-varying uncertain parameters. *Journal of Optimization Theory and Applications*, 57(3):439–461, Jun 1988.

[158] E. Feron, P. Apkarian, and P. Gahinet. Analysis and synthesis of robust control systems via parameter-dependent lyapunov functions. *IEEE Transactions on Automatic Control*, 41(7):1041–1046, Jul 1996.

[159] P. Apkarian and P. Gahinet. A convex characterization of gain-scheduled h_∞ controllers. *IEEE Transactions on Automatic Control*, 40(5):853–864, May 1995.

[160] P. Gahinet, P. Apkarian, and M. Chilali. Affine parameter-dependent lyapunov functions and real parametric uncertainty. *IEEE Transactions on Automatic Control*, 41(3):436–442, Mar 1996.

[161] S. Boyd, L. Ghaoui, E. Feron, and V. Balakrishnan. *Linear Matrix Inequalities in System and Control Theory*. SIAM, 1994.

[162] C. Scherer and S. Weiland. *Course on Linear Matrix Inequalities in Control. Lecture Notes DISC*. Springer, 2000.

[163] L. Ghaoui and S. Niculescu. *Advances in Linear Matrix Inequalities in Control*. SIAM, 2000.

[164] F. Amato, R. Ambrosino, M. Ariola, C. Cosentino, and A. Merola. State feedback control of nonlinear quadratic systems. In *46th IEEE Conference on Decision and Control*, pages 1699–1703, Dec 2007.

[165] D. Yue, Q.-L. Han, and C. Peng. State feedback controller design of networked control systems. *IEEE Transactions on Circuits and Systems II: Express Briefs*, 51(11):640–644, Nov 2004.

[166] S. S. Stankovic, D. M. Stipanovic, and D. D. Siljak. Decentralized dynamic output feedback for robust stabilization of a class of nonlinear interconnected systems. *Automatica*, 43(5):861–867, May 2007.

[167] S. Kanev, C. Scherer, M. Verhaegen, and B. De Schutter. Robust output-feedback controller design via local bmi optimization. *Automatica*, 40(7):1115–1127, Jul 2004.

[168] X.-H. Chang. *Robust Output Feedback H-infinity Control and Filtering for Uncertain Linear Systems*. Springer, 2014.

[169] A. I. Zecevic and D. D. Siljak. Design of robust static output feedback for large-scale systems. *IEEE Transactions on Automatic Control*, 49(11):2040–2044, Nov 2004.

[170] D. Henrion, J. Lofberg, M. Kocvara, and M. Stingl. Solving polynomial static output feedback problems with penbmi. In *Proceedings of the 44th IEEE Conference on Decision and Control*, pages 7581–7586, Dec 2005.

[171] D. Henrion and J. B. Lasserre. Convergent relaxations of polynomial matrix inequalities and static output feedback. *IEEE Transactions on Automatic Control*, 51(2):192–202, Feb 2006.

[172] M. Alamir. Optimization-based nonlinear observers revisited. *International Journal of Control*, 72(13):1204–1217, Nov 1999.

[173] M. Arcak and P. Kokotovic. Observer-based control of systems with slope-restricted nonlinearities. *IEEE Transactions on Automatic Control*, 46(7):1146–1150, Jul 2001.

[174] J. Tsinias. Observer design for nonlinear systems. *Systems and Control Letters*, 13(2):135–142, Aug 1989.

[175] A. J. Krener and A. Isidori. Linearization by output injection and nonlinear observers. *Systems and Control Letters*, 3(1):47–52, Jun 1983.

[176] C.-H. Lien. Robust observer-based control of systems with state perturbations via lmi approach. *IEEE Transactions on Automatic Control*, 49(8):1365–1370, Aug 2004.

[177] W.-H. Chen. Disturbance observer based control for nonlinear systems. *IEEE/ASME Transactions on Mechatronics*, 9(4):706–710, Dec 2004.

[178] D. Luenberger. Observers for multivariable systems. *IEEE Transactions on Automatic Control*, 11(2):190–197, Apr 1966.

[179] D. Luenberger. An introduction to observers. *IEEE Transactions on Automatic Control*, 16(6):596–602, Dec 1971.

[180] M. Zeitz. The extended luenberger observer for nonlinear systems. *Systems and Control Letters*, 9(2):149–156, Aug 1987.

[181] A. Gelb. *Applied Optimal Estimation*. MIT Press, 1992.

[182] M. Boutayeb, H. Rafaralahy, and M. Darouach. Convergence analysis of the extended kalman filter used as an observer for nonlinear deterministic discrete-time systems. *IEEE Transactions on Automatic Control*, 42(4):581–586, Apr 1997.

[183] J. Jouffroy. Some ancestors of contraction analysis. In *Proceedings of the 44th IEEE Conference on Decision and Control*, pages 5450–5455, Dec 2005.

[184] J. Jouffroy. A simple extension of contraction theory to study incremental stability properties. In *2003 European Control Conference (ECC)*, pages 1315–1321, Sep 2003.

[185] Q. C. Pham, N. Tabareau, and J. J. Slotine. A contraction theory approach to stochastic incremental stability. *IEEE Transactions on Automatic Control*, 54(4):816–820, Apr 2009.

[186] A. P. Dani, S. J. Chung, and S. Hutchinson. Observer design for stochastic nonlinear systems via contraction-based incremental stability. *IEEE Transactions on Automatic Control*, 60(3):700–714, Mar 2015.

[187] M. Alamir. Contraction-based nonlinear model predictive control formulation without stability-related terminal constraints. *Automatica*, 75:288–292, Jan 2017.

[188] H. M. T. Menegaz, J. Y. Ishihara, G. A. Borges, and A. N. Vargas. A systematization of the unscented kalman filter theory. *IEEE Transactions on Automatic Control*, 60(10):2583–2598, Oct 2015.

[189] J. P. Maree, L. Imsland, and J. Jouffroy. A convergence result for the unscented kalman-bucy filter using contraction theory. In *2013 European Control Conference (ECC)*, pages 2134–2139, Jul 2013.

[190] M. A. Belabbas and J. J. E. Slotine. Factorizations and partial contraction of nonlinear systems. In *Proceedings of the 2010 American Control Conference*, pages 3440–3445, June 2010.

[191] G. Russo and M. di Bernardo. Contraction theory and master stability function: Linking two approaches to study synchronization of complex networks. *IEEE Transactions on Circuits and Systems II: Express Briefs*, 56(2):177–181, Feb 2009.

[192] Q.-C. Pham and J. J. E. Slotine. Stable concurrent synchronization in dynamic system networks. *Neural Networks*, 20(1):62–77, Jan 2007.

[193] E. M. Aylward, P. A. Parrilo, and J. J. E. Slotine. Stability and robustness analysis of nonlinear systems via contraction metrics and sos programming. *Automatica*, 44(8):2163–2170, Aug 2008.

[194] I. R. Manchester and J. J. E. Slotine. Output-feedback control of nonlinear systems using control contraction metrics and convex optimization. In *2014 4th Australian Control Conference (AUCC)*, pages 215–220, Nov 2014.

[195] W. Lohmiller and J. J. E. Slotine. Nonlinear process control using contraction theory. *AICHE Journal*, 46(3):588–596, Mar 2000.

[196] B. B. Sharma and I. N. Kar. Contraction theory based adaptive synchronization of chaotic systems. *Chaos, Solitons and Fractals*, 41(5):2437–2447, Sep 2009.

[197] A. G. Richardson, M. C. Tresch, E. Bizzi, and J. J. E. Slotine. Stability analysis of nonlinear muscle dynamics using contraction theory. In *2005 IEEE Engineering in Medicine and Biology 27th Annual Conference*, pages 4986–4989, Jan 2005.

[198] C. Juarez and A. M. Stankovic. Contraction analysis of power system dynamics using time-varying omib equivalents. In *39th North American Power Symposium*, pages 385–391, Sep 2007.

[199] F. K. Bayat, M. Yilmaz, and M. E. El-Hawary. Observer-based synchronization of networked hindmarsh-rose neurons. In *IEEE 28th Canadian Conference on Electrical and Computer Engineering (CCECE)*, pages 1605–1611, May 2015.

[200] R. Weron. *Modeling and Forecasting Electricity Loads and Prices: A Statistical Approach*. Hugo Steinhaus Center, Wroclaw University of Technology, Jul 2006.

[201] A. P. S. Meliopoulos. Distributed energy sources: needs for analysis and design tools. In *2001 Power Engineering Society Summer Meeting Conference Proceedings*, volume 1, pages 548–550, Jul 2001.

[202] A. Papavasiliou and S. S. Oren. Large-scale integration of deferrable demand and renewable energy sources. *IEEE Transactions on Power Systems*, 29(1):489–499, Jan 2014.

[203] A. Subramanian, M. J. Garcia, D. S. Callaway, K. Poolla, and P. Varaiya. Real-time scheduling of distributed resources. *IEEE Transactions on Smart Grid*, 4(4):2122–2130, Dec 2013.

[204] E. A. DeMeo, W. Grant, M. R. Milligan, and M. J. Schuerger. Wind plant integration (wind power plants). *IEEE Power and Energy Magazine*, 3(6):38–46, Nov 2005.

[205] E. A. DeMeo, G. A. Jordan, C. Kalich, J. King, M. R. Milligan, C. Murley, B. Oakleaf, and M. J. Schuerger. Accommodating wind's natural behavior. *IEEE Power and Energy Magazine*, 5(6):59–67, Nov 2007.

[206] T. Ackermann, J. R. Abbad, I. M. Dudurych, I. Erlich, H. Holttinen, J. R. Kristoffersen, and P. E. Sorensen. European balancing act. *IEEE Power and Energy Magazine*, 5(6):90–103, Nov 2007.

[207] A. Papavasiliou and S. S. Oren. A stochastic unit commitment model for integrating renewable supply and demand response. In *2012 IEEE Power and Energy Society General Meeting*, pages 1–6, Jul 2012.

[208] N. Li, L. Chen, and S. H. Low. Optimal demand response based on utility maximization in power networks. In *2011 IEEE Power and Energy Society General Meeting*, pages 1–8, July 2011.

[209] D. S. Kirschen. Demand-side view of electricity markets. *IEEE Transactions on Power Systems*, 18(2):520–527, May 2003.

[210] A. I. Cohen and C. C. Wang. An optimization method for load management scheduling. *IEEE Transactions on Power Systems*, 3(2):612–618, May 1988.

[211] A. H. Mohsenian-Rad and A. Leon-Garcia. Optimal residential load control with price prediction in real-time electricity pricing environments. *IEEE Transactions on Smart Grid*, 1(2):120–133, Sep 2010.

[212] Y.-Y. Hsu and C.-C. Su. Dispatch of direct load control using dynamic programming. *IEEE Transactions on Power Systems*, 6(3):1056–1061, Aug 1991.

[213] D.-C. Wei and N. Chen. Air conditioner direct load control by multi-pass dynamic programming. *IEEE Transactions on Power Systems*, 10(1):307–313, Feb 1995.

[214] K. H. Ng and G. B. Sheble. Direct load control-a profit-based load management using linear programming. *IEEE Transactions on Power Systems*, 13(2):688–694, May 1998.

[215] J. Chen, F. N. Lee, A. M. Breipohl, and R. Adapa. Scheduling direct load control to minimize system operation cost. *IEEE Transactions on Power Systems*, 10(4):1994–2001, Nov 1995.

[216] Y. V. Makarov, C. Loutan, J. Ma, and P. de Mello. Operational impacts of wind generation on california power systems. *IEEE Transactions on Power Systems*, 24(2):1039–1050, May 2009.

[217] H. Holttinen. Optimal electricity market for wind power. *Energy Policy*, 33(16):2052–2063, May 2005.

[218] N. Ruiz, I. Cobelo, and J. Oyarzabal. A direct load control model for virtual power plant management. *IEEE Transactions on Power Systems*, 24(2):959–966, May 2009.

[219] H. Pandzic, I. Kuzle, and T. Capuder. Virtual power plant mid-term dispatch optimization. *Applied Energy*, 101:134–141, Jan 2013.

[220] H. Pandzic, J. M. Morales, A. J. Conejo, and I. Kuzle. Offering model for a virtual power plant based on stochastic programming. *Applied Energy*, 105:282–292, May 2013.

[221] F. Milano. *Optimal Power Flow Analysis*, pages 131–153. Springer, 2010.

[222] G. S. Christensen, M. E. El-Hawary, and S. A. Soliman. *Dynamic Optimal Load Flow*, pages 21–53. Springer, 1987.

[223] X.-F. Wang, Y. Song, and M. Irving. *Modern Power Systems Analysis*. Springer, 2008.

[224] M. Huneault and F. D. Galiana. A survey of the optimal power flow literature. *IEEE Transactions on Power Systems*, 6(2):762–770, May 1991.

[225] E. Dall'Anese, H. Zhu, and G. B. Giannakis. Distributed optimal power flow for smart microgrids. *IEEE Transactions on Smart Grid*, 4(3):1464–1475, Sep 2013.

[226] R. S. Ferreira, C. L. T. Borges, and M. V. F. Pereira. A flexible mixed-integer linear programming approach to the ac optimal power flow in distribution systems. *IEEE Transactions on Power Systems*, 29(5):2447–2459, Sep 2014.

[227] T. Erseghe. Distributed optimal power flow using admm. *IEEE Transactions on Power Systems*, 29(5):2370–2380, Sep 2014.

[228] M. J. Dolan, E. M. Davidson, I. Kockar, G. W. Ault, and S. D. J. McArthur. Distribution power flow management utilizing an online optimal power flow technique. *IEEE Transactions on Power Systems*, 27(2):790–799, May 2012.

[229] G. Hug-Glanzmann and G. Andersson. Decentralized optimal power flow control for overlapping areas in power systems. *IEEE Transactions on Power Systems*, 24(1):327–336, Feb 2009.

[230] M. E. El-Hawary and G. A. N. Mbamalu. A comparison of probabilistic perturbation and deterministic based optimal power flow solutions. *IEEE Transactions on Power Systems*, 6(3):1099–1105, Aug 1991.

[231] X. Li, Y. Li, and S. Zhang. Analysis of probabilistic optimal power flow taking account of the variation of load power. *IEEE Transactions on Power Systems*, 23(3):992–999, Aug 2008.

[232] H. Zhang and P. Li. Probabilistic analysis for optimal power flow under uncertainty. *IET Generation, Transmission Distribution*, 4(5):553–561, May 2010.

[233] A. G. Bakirtzis, P. N. Biskas, C. E. Zoumas, and V. Petridis. Optimal power flow by enhanced genetic algorithm. *IEEE Transactions on Power Systems*, 17(2):229–236, May 2002.

[234] M. Noroozian, L. Angquist, M. Ghandhari, and G. Andersson. Use of upfc for optimal power flow control. *IEEE Transactions on Power Delivery*, 12(4):1629–1634, Oct 1997.

[235] J. Yuryevich and Kit Po Wong. Evolutionary programming based optimal power flow algorithm. *IEEE Transactions on Power Systems*, 14(4):1245–1250, Nov 1999.

[236] V. Miranda and J. P. Saraiva. Fuzzy modelling of power system optimal load flow. *IEEE Transactions on Power Systems*, 7(2):843–849, May 1992.

[237] L. Shi, C. Wang, L. Yao, Y. Ni, and M. Bazargan. Optimal power flow solution incorporating wind power. *IEEE Systems Journal*, 6(2):233–241, Jun 2012.

[238] J. Liang, G. K. Venayagamoorthy, and R. G. Harley. Wide-area measurement based dynamic stochastic optimal power flow control for smart grids with high variability and uncertainty. *IEEE Transactions on Smart Grid*, 3(1):59–69, Mar 2012.

[239] H. Yu and W. D. Rosehart. An optimal power flow algorithm to achieve robust operation considering load and renewable generation uncertainties. *IEEE Transactions on Power Systems*, 27(4):1808–1817, Nov 2012.

[240] R. A. Jabr, S. Karaki, and J. A. Korbane. Robust multi-period opf with storage and renewables. *IEEE Transactions on Power Systems*, 30(5):2790–2799, Sep 2015.

[241] Y. Levron, J. M. Guerrero, and Y. Beck. Optimal power flow in microgrids with energy storage. *IEEE Transactions on Power Systems*, 28(3):3226–3234, Aug 2013.

[242] A. Gabash and P. Li. Active-reactive optimal power flow in distribution networks with embedded generation and battery storage. *IEEE Transactions on Power Systems*, 27(4):2026–2035, Nov 2012.

[243] B. Hayes, I. Hernando-Gil, A. Collin, G. Harrison, and S. Djokic. Optimal power flow for maximizing network benefits from demand-side management. *IEEE Transactions on Power Systems*, 29(4):1739–1747, Jul 2014.

[244] O. Alsac, J. Bright, M. Prais, and B. Stott. Further developments in lp-based optimal power flow. *IEEE Transactions on Power Systems*, 5(3):697–711, Aug 1990.

[245] Y.-C. Wu, A. S. Debs, and R. E. Marsten. A direct nonlinear predictor-corrector primal-dual interior point algorithm for optimal power flows. *IEEE Transactions on Power Systems*, 9(2):876–883, May 1994.

[246] G. L. Torres and V. H. Quintana. An interior-point method for nonlinear optimal power flow using voltage rectangular coordinates. *IEEE Transactions on Power Systems*, 13(4):1211–1218, Nov 1998.

[247] R. A. Jabr, A. H. Coonick, and B. J. Cory. A primal-dual interior point method for optimal power flow dispatching. *IEEE Transactions on Power Systems*, 17(3):654–662, Aug 2002.

[248] H. Wei, H. Sasaki, J. Kubokawa, and R. Yokoyama. An interior point nonlinear programming for optimal power flow problems with a novel data structure. *IEEE Transactions on Power Systems*, 13(3):870–877, Aug 1998.

[249] W. Yan, F. Liu, C. Y. Chung, and K. P. Wong. A hybrid genetic algorithm-interior point method for optimal reactive power flow. *IEEE Transactions on Power Systems*, 21(3):1163–1169, Aug 2006.

[250] A. A. Sousa, G. L. Torres, and C. A. Canizares. Robust optimal power flow solution using trust region and interior-point methods. *IEEE Transactions on Power Systems*, 26(2):487–499, May 2011.

[251] H. Wang, C. E. Murillo-Sanchez, R. D. Zimmerman, and R. J. Thomas. On computational issues of market-based optimal power flow. *IEEE Transactions on Power Systems*, 22(3):1185–1193, Aug 2007.

[252] A. Monticelli, M. V. F. Pereira, and S. Granville. Security-constrained optimal power flow with post-contingency corrective rescheduling. *IEEE Transactions on Power Systems*, 2(1):175–180, Feb 1987.

[253] Y. Fu, M. Shahidehpour, and Z. Li. Ac contingency dispatch based on security-constrained unit commitment. *IEEE Transactions on Power Systems*, 21(2):897–908, May 2006.

[254] P. E. O. Yumbla, J. M. Ramirez, and C. A. Coello Coello. Optimal power flow subject to security constraints solved with a particle swarm optimizer. *IEEE Transactions on Power Systems*, 23(1):33–40, Feb 2008.

[255] M. Dur. Copositive programming–a survey. In Moritz Diehl, Francois Glineur, Elias Jarlebring, and Wim Michiels, editors, *Recent Advances in Optimization and its Applications in Engineering*, pages 3–20. Springer, 2010.

[256] S. H. Low. Convex relaxation of optimal power flow–part i: Formulations and equivalence. *IEEE Transactions on Control of Network Systems*, 1(1):15–27, Mar 2014.

[257] S. H. Low. Convex relaxation of optimal power flow–part ii: Exactness. *IEEE Transactions on Control of Network Systems*, 1(2):177–189, Jun 2014.

[258] J. Lavaei. Zero duality gap for classical opf problem convexifies fundamental nonlinear power problems. In *Proceedings of the 2011 American Control Conference*, pages 4566–4573, Jun 2011.

[259] D. K. Molzahn, B. C. Lesieutre, and C. L. DeMarco. Investigation of non-zero duality gap solutions to a semidefinite relaxation of the optimal power flow problem. In *2014 47th Hawaii International Conference on System Sciences*, pages 2325–2334, Jan 2014.

[260] R. A. Jabr. Exploiting sparsity in sdp relaxations of the opf problem. *IEEE Transactions on Power Systems*, 27(2):1138–1139, May 2012.

[261] M. S. Andersen, A. Hansson, and L. Vandenberghe. Reduced-complexity semidefinite relaxations of optimal power flow problems. *IEEE Transactions on Power Systems*, 29(4):1855–1863, Jul 2014.

[262] J. Lavaei, D. Tse, and B. Zhang. Geometry of power flows and optimization in distribution networks. *IEEE Transactions on Power Systems*, 29(2):572–583, Mar 2014.

[263] G. Fazelnia, R. Madani, and J. Lavaei. Convex relaxation for optimal distributed control problem. In *53rd IEEE Conference on Decision and Control*, pages 896–903, Dec 2014.

[264] A. J. Conejo and J. A. Aguado. Multi-area coordinated decentralized dc optimal power flow. *IEEE Transactions on Power Systems*, 13(4):1272–1278, Nov 1998.

[265] P. N. Biskas, A. G. Bakirtzis, N. I. Macheras, and N. K. Pasialis. A decentralized implementation of dc optimal power flow on a network of computers. *IEEE Transactions on Power Systems*, 20(1):25–33, Feb 2005.

[266] L. Gan and S. H. Low. Optimal power flow in direct current networks. *IEEE Transactions on Power Systems*, 29(6):2892–2904, Nov 2014.

[267] H. Zhang and P. Li. Chance constrained programming for optimal power flow under uncertainty. *IEEE Transactions on Power Systems*, 26(4):2417–2424, Nov 2011.

[268] Y. Yuan, J. Kubokawa, and H. Sasaki. A solution of optimal power flow with multicontingency transient stability constraints. *IEEE Transactions on Power Systems*, 18(3):1094–1102, Aug 2003.

[269] R. Zarate-Minano, T. Van Cutsem, F. Milano, and A. J. Conejo. Securing transient stability using time-domain simulations within an optimal power flow. *IEEE Transactions on Power Systems*, 25(1):243–253, Feb 2010.

[270] R. Madani, M. Ashraphijuo, and J. Lavaei. Promises of conic relaxation for contingency-constrained optimal power flow problem. In *2014 52nd Annual Allerton Conference on Communication, Control, and Computing (Allerton)*, pages 1064–1071, Sep 2014.

[271] B. Zhang, A. Y. S. Lam, A. D. Domnguez-Garca, and D. Tse. An optimal and distributed method for voltage regulation in power distribution systems. *IEEE Transactions on Power Systems*, 30(4):1714–1726, Jul 2015.

[272] D. K. Molzahn, B. C. Lesieutre, and C. L. DeMarco. Approximate representation of zip loads in a semidefinite relaxation of the opf problem. *IEEE Transactions on Power Systems*, 29(4):1864–1865, Jul 2014.

[273] Y. Weng, Q. Li, R. Negi, and M. Ilic. Semidefinite programming for power system state estimation. In *2012 IEEE Power and Energy Society General Meeting*, pages 1–8, Jul 2012.

[274] S. Sastry and P. Varaiya. Hierarchical stability and alert state steering control of interconnected power systems. *IEEE Transactions on Circuits and Systems*, 27(11):1102–1112, Nov 1980.

[275] M. Crow. *Computational methods for electric power systems*. CRC Press, 2003.

[276] B. Bilir. *Bifurcation Analysis of Nonlinear Oscillations in Power Systems*. PhD thesis, University of Missouri-Columbia, 2000.

[277] A. R. Bergen and V. Vittal. *Power System Analysis*. Prentice Hall, 2000.

[278] H. Cai, Z. Qu, and J. F. Dorsey. Robust decentralized excitation control for large-scale power systems. *Central and Intelligent Systems*, 29(1):8–17, 2001.

[279] M. Gordon and D. J. Hill. Flexible nonlinear voltage control design for power systems. In *2007 IEEE International Conference on Control Applications*, pages 1097–1102, Oct 2007.

[280] H. Cai, Z. Qu, D. Gan, and J. F. Dorsey. A robust power system stabilizer design based on lyapunov's approach. In *Proceedings of the 1997 American Control Conference*, volume 3, pages 1958–1962, Jun 1997.

[281] A. I. Zecevic and D. D. Siljak. Robust control of large scale power systems via convex optimization. In Joe. H. Chow, Felix. F. Wu, and James. J. Mamoh, editors, *Applied Mathematics for Restructured Electric Power Systems*, chapter 7, pages 139–158. Springer, 2005.

[282] G. Fusco and M. Russo. *Adaptive Voltage Control in Power Systems*. Springer, 2007.

[283] A. Vaccaro, G. Velotto, and A. F. Zobaa. A decentralized and cooperative architecture for optimal voltage regulation in smart srids. *IEEE Transactions on Industrial Electronics*, 58(10):4593–4602, Oct 2011.

[284] M. Yilmaz and B. Bilir. Determination of power transfer capability by incremental changes. In *2013 IEEE Electrical Power Energy Conference*, pages 1–6, Aug 2013.

[285] A. Loria and E. Panteley. Stability, told by its developers. In Julio Antonio Loria Perez, Francoise Lamnabhi-Lagarrigue, and Elena Viatcheslavovna Panteley, editors, *Advanced Topics in Control Systems Theory*, chapter 6, pages 199–258. Springer, 2006.

[286] W. Hahn. *Theory and Application of Liapunov's Direct Method*. Prentice Hall, 1963.

[287] W. Hahn. *Stability of motion*. Springer, 1967.

[288] R. A. Freeman and P. V. Kokotovic. *Robust Nonlinear Control Design*. Birkhauser, 2008.

[289] B. D. O. Anderson and J. B. Moore. *Linear Optimal Control*. Prentice-Hall, 1990.

[290] G. Becker and A. Packard. Robust performance of linear parametrically varying systems using parametrically-dependent linear feedback. *Systems and Control Letters*, 23(1):205–215, Sep 1994.

[291] M. Chilali and P. Gahinet. h_∞ design with pole placement constraints: an lmi approach. *IEEE Transactions on Automatic Control*, 41(3):358–367, Mar 1996.

[292] M. Yilmaz, M. E. El-Hawary, and F. K. Bayat. Decentralized voltage control with linear parameter-varying. In *2016 IEEE 7th Annual Information Technology, Electronics and Mobile Communication Conference (IEMCON)*, pages 1–6, Oct 2016.

[293] R. D. Zimmerman, C. E. Murillo-Sanchez, and R. J. Thomas. Matpower: Steady-state operations, planning, and analysis tools for power systems research and education. *IEEE Transactions on Power Systems*, 26(1):12–19, Feb 2011.

[294] J. Lofberg. Yalmip : A toolbox for modeling and optimization in matlab. In *2004 IEEE International Conference on Robotics and Automation*, pages 284–289, Sep 2004.

[295] I. R. Manchester and J. J. E. Slotine. Control contraction metrics and universal stabilizability. {*IFAC*} *Proceedings Volumes*, 47(3):8223–8228, 2014.

[296] J. W. Simpson-Porco and Francesco Bullo. Contraction theory on riemannian manifolds. *Systems and Control Letters*, 65:74–80, Mar 2014.

[297] Peter Giesl. Converse theorems on contraction metrics for an equilibrium. *Journal of Mathematical Analysis and Applications*, 424(2):1380–1403, Apr 2015.

[298] M. F. Anjos and J. B. Lasserre. Introduction to semidefinite, conic and polynomial optimization. In Miguel F. Anjos and Jean B. Lasserre, editors, *Handbook on Semidefinite, Conic and Polynomial Optimization*, chapter 1, pages 1–22. Springer, 2012.

[299] H. W. Dommel and W. F. Tinney. Optimal power flow solutions. *IEEE Transactions on Power Apparatus and Systems*, PAS-87(10):1866–1876, Oct 1968.

[300] M. Laurent and P. Rostalski. The approach of moments for polynomial equations. In Miguel F. Anjos and Jean B. Lasserre, editors, *Handbook on Semidefinite, Conic and Polynomial Optimization*, chapter 2, pages 25–60. Springer, 2012.

[301] M. Fukuda, M.Kojima, K. Murota, and K. Nakata. Exploiting sparsity in semidefinite programming via matrix completion i: General framework. *SIAM Journal of Optimization*, 11(3):647–674, Mar 2000.

[302] K. Nakata, K. Fujisawa, M. Fukuda, M. Kojima, and K. Murota. Exploiting sparsity in semidefinite programming via matrix completion ii: Implementation and numerical results. *Math. Program*, 95(2):303–327, 2003.

[303] M. S. Andersen, A. Hansson, and L. Vandenberghe. Reduced-complexity semidefinite relaxations of optimal power flow problems. *IEEE Transactions on Power Systems*, 29(4):1855–1863, Jul 2014.

[304] Etienne de Klerk. *Aspects of Semidefinite Programming*. Kluwer Academic Publishers, 2002.

[305] B. Gartner and J. Matousek. *Approximation algorithms and semidefinite programming*. Springer, 2012.

[306] F. Glineur and T. Terlaky. Conic formulation for l_p-norm optimization. *Journal of Optimization Theory and Applications*, 122(2):285–307, Aug 2004.

[307] N. Amjady. Short-term hourly load forecasting using time-series modeling with peak load estimation capability. *IEEE Transactions on Power Systems*, 16(3):498–505, Aug 2001.

[308] G. A. N. Mbamalu and M. E. El-Hawary. Load forecasting via suboptimal seasonal autoregressive models and iteratively reweighted least squares estimation. *IEEE Transactions on Power Systems*, 8(1):343–348, Feb 1993.

[309] V. Knyazkin, C. A. Canizares, and L. H. Soder. On the parameter estimation and modeling of aggregate power system loads. *IEEE Transactions on Power Systems*, 19(2):1023–1031, May 2004.

[310] S. Boyd and L. Vandenberghe. *Convex Optimization*. Cambridge University Press, 2004.

[311] W. A. Bukhsh, A. Grothey, K. I. M. McKinnon, and P. A. Trodden. Local solutions of the optimal power flow problem. *IEEE Transactions on Power Systems*, 28(4):4780–4788, Nov 2013.